TREATMENT OF PER AND POLYFLUOROALKYL SUBSTANCES (PFAS) IN GROUNDWATER BY REACTIVE ACTIVATION OF SULFITE AND IODIDE THROUGH UV-NATURED TREATMENT (RADIANT) SYSTEM

TRAITEMENT DES SUBSTANCES POLY ET PERFLUOROALKYLEÉS (PFAS) DANS L'EAUX SOUTERRAINES PAR UN SYSTÈME SULFITE/IODURE ACTIVÉ PAR UV

A Thesis Submitted to the Division of Graduate Studies

Of the Royal Military College of Canada

by

Yang Xu, B.Sc. Chemistry

In Partial Fulfillment of the Requirements for the Degree of Master of Science

August, 2026

Acknowledgements

I would like to thank my supervisors, Dr. Iris Koch and Dr. Kela Weber, for consistently going above and beyond to support me throughout the past two years. Your time and patience is truly appreciated.

A special thank you to Dr. Adrian Pang for his assistance with analysis and overall good advice. Thank you to Matthew Banuelos, for spending two weeks collecting fluoride data, Isaac Timoffee-Maberly, for the good company, and everyone at the Environmental Sciences Group. And to Alex – thank you for keeping me happy, motivated, and consistently caffeinated.

Abstract

Per and polyfluoroalkyl substances (PFAS) are a large class of synthetic organofluorine compounds which demonstrate many desirable properties such as hydrophobicity, oleophobicity, tensioactivity, and exceptional stability. These properties have led to their widespread use in industry and commercial applications, and subsequently their ubiquity in the environment. Concerns surrounding environmental contamination of PFAS have mounted with increasing evidence of the toxicological effects associated with many of these PFAS compounds. While absorptive and filtration based technologies are successful at removing PFAS from the environment, the development of an effective destructive technology is required to address the issue of PFAS contamination. O'Connor et al. reported complete degradation of notoriously recalcitrant PFAS compounds in deionized (DI) water using a UV-sulfite/iodide system, which was further developed into the Reactive Activation of Sulfite and Iodide through UV-Natured Treatment (RADIANT) system. However, successful implementation of this technology in real-world applications requires further development to meet the challenges posed by more complex environmental matrices such as groundwater.

This thesis aimed to assess the feasibility of applying the RADIANT system in the treatment of PFAS-contaminated groundwater. A systematic study was conducted exploring the individual and combined effects of humic acid and nitrate, two common groundwater components identified as potential interferents to the RADIANT system. Experiments performed in DI water found the presence of humic acid to cause strong inhibitory effects on the degradation of PFOS, decreasing degradation efficiency from >99% to 86% with a 50 mM sulfite treatment. When humic acid was present, a delay in degradation was observed after the start of treatment, referred to as a "lag time" of 30 min. In contrast, nitrate did not cause a lag in treatment, and in certain experimental conditions was observed to increase the rate of degradation. The groundwater matrix appeared to mitigate the inhibitory effects of humic acid that were observed in DI water, eliminating the lag in degradation and increasing treatment efficiency to 99%. Groundwater also improved overall RADIANT system performance, and over 99% degradation of PFOS was achieved in all experiments performed in groundwater.

Treatment of short and ultra-short chain PFAS (PFPeA, TFA, PFPrS, and PFBS) was investigated under two treatment conditions (10 and 50 mM sulfite). PFPeA and TFA, both perfluorocarboxylic acids (PFCAs), were shown to degrade rapidly under both treatment conditions, reaching >99% degradation within 10 minutes of treatment. However, short and ultra-short chain perfluorosulfonic acids (PFSAs) were shown to be more recalcitrant. Greater than 99% degradation of PFBS was achieved after 8 hours through the application of an intermittent sulfite addition protocol, and the rate of reaction was shown to be increased when treatment was performed in synthetic hard water. Ultra-short chain PFPrS was shown to be the most recalcitrant form of PFAS studied in this work, with 95% degradation after 8 hours of treatment with the intermittent sulfite addition protocol.

Finally, RADIANT system performance at the cuvette (1 mL) scale was compared with the beaker (800 mL) set-up. Greater than 99% degradation of PFOS was achieved at both scales, but reaction rates at the beaker scale were up to three times higher than the reaction

rates observed at the cuvette scale. The addition of mixing and elevated temperatures during treatment were identified as parameters associated with the beaker apparatus that are likely to influence RADIANT system performance. In addition, the effect of changing experimental conditions was consistent across both experimental set-ups. Improved degradation in groundwater was observed at both scales, and it is suggested that the impact of factors such as DOC may be translated to the larger scale.

Résumé

Les substances perfluoroalkylées et polyfluoroalkylées (PFAS) constituent une vaste classe de composés organofluorés de synthèse présentant de nombreuses propriétés intéressantes telles que l'hydrophobie, l'oléophobie, la tensioactivité et une stabilité exceptionnelle. Ces propriétés ont conduit à leur utilisation généralisée dans l'industrie et le commerce, et par conséquent à leur présence omniprésente dans l'environnement. Les préoccupations liées à la contamination environnementale par les PFAS se sont accrues face aux preuves croissantes des effets toxiques associés à nombre de ces composés. Si les technologies d'absorption et de filtration permettent d'éliminer efficacement les PFAS de l'environnement, le développement d'une technologie de destruction efficace est nécessaire pour résoudre le problème de la contamination par les PFAS. O'Connor et al. ont rapporté la dégradation complète de composés PFAS particulièrement récalcitrants dans l'eau déminéralisée (DI) grâce à un système UV-sulfite/iodure, qui a ensuite été perfectionné pour donner naissance au système RADIANT (Reactive Activation of Sulfite and Iodide through UV-Natured Treatment). Cependant, la mise en œuvre réussie de cette technologie dans des applications concrètes nécessite des développements supplémentaires afin de relever les défis posés par des matrices environnementales plus complexes telles que les eaux souterraines.

Cette thèse visait à évaluer la faisabilité de l'application du système RADIANT au traitement des eaux souterraines contaminées par des PFAS. Une étude systématique a été menée afin d'explorer les effets individuels et combinés de l'acide humique et des nitrates, deux composants courants des eaux souterraines identifiés comme interférents potentiels avec le système RADIANT. Des expériences réalisées en eau désionisée ont révélé que la présence d'acide humique induit de forts effets inhibiteurs sur la dégradation du PFOS, diminuant l'efficacité de dégradation de plus de 99 % à 86 % avec un traitement au sulfite à 50 mM. En présence d'acide humique, un délai de dégradation a été observé après le début du traitement, appelé « temps de latence », de 30 minutes. En revanche, les nitrates n'ont pas induit de délai de traitement et, dans certaines conditions expérimentales, ont même accéléré la dégradation. Des expériences menées en eau souterraine ont montré que la matrice de l'eau souterraine semblait atténuer les effets inhibiteurs de l'acide humique observés dans l'eau désionisée, éliminant ainsi le délai de dégradation et portant l'efficacité du traitement à 99 %. L'eau souterraine a également amélioré les performances globales du système RADIANT, et une dégradation du PFOS supérieure à 99 % a été obtenue dans toutes les expériences réalisées en eau souterraine.

Le traitement des PFAS à chaîne courte et ultracourte (PFPeA, TFA, PFPrS et PFBS) a également été étudié dans deux conditions de traitement (10 et 50 mM de sulfite). Le PFPeA et le TFA se sont dégradés rapidement dans les deux conditions, atteignant une dégradation supérieure à 99 % en 10 minutes de traitement. Cependant, les PFAS à chaîne courte et ultracourte se sont révélés plus récalcitrants. Une dégradation du PFBS supérieure à 99 % a été obtenue grâce à l'application d'un protocole d'ajout intermittent de sulfite, et la vitesse de réaction s'est avérée accrue lors du traitement en eau dure synthétique. Il a été démontré que le PFPrS à chaîne ultra-courte était la forme de PFAS la plus récalcitrante étudiée dans ce travail, avec une dégradation de 95 % après 8 heures de traitement avec le protocole d'ajout intermittent de sulfite.

Enfin, les performances du système RADIANT à l'échelle de la cuvette (1 mL) ont été comparées à celles obtenues avec le bécher (800 mL). Une dégradation du PFOS supérieure à 99 % a été atteinte aux deux échelles, mais les vitesses de réaction à l'échelle du bécher étaient jusqu'à trois fois plus élevées qu'à l'échelle de la cuvette. L'agitation et l'élévation de la température pendant le traitement ont été identifiées comme des paramètres liés au dispositif en bécher susceptibles d'influencer les performances du système RADIANT. De plus, l'effet des modifications des conditions expérimentales était constant pour les deux dispositifs. Une dégradation améliorée dans les eaux souterraines a été observée aux deux échelles, ce qui suggère que l'impact de facteurs tels que le carbone organique dissous (COD) pourrait se confirmer à plus grande échelle.

Table of Contents

List of Tables

List of Figures

1. Introduction

1.1 Background

Per and polyfluoroalkyl substances (PFAS) are a large class of anthropogenic chemicals characterized by the presence of one or more carbon-fluorine moieties (-CF_2).[1] PFAS is used in a wide variety of commercial, industrial, and military applications due to its hydrophobicity, oleophobicity, and uniquely high stability.[2] Since its development in the early 1950s, widespread application of PFAS has led to its near ubiquity in the environment.[3] The persistence of PFAS in the environment has raised much concern in light of the growing body of evidence illuminating the negative human health impacts associated with this class of chemicals.[4–6] In response to this, the maximum level of PFAS in drinking water was set at 30 ng/L by Health Canada, calculated as the sum of 25 specific PFAS.[7] For PFOA and PFOS, two PFAS compounds commonly detected in groundwater, it has been noted by the U.S. Environmental Protection Agency (EPA) that there is no level of exposure at which there is no risk of health impacts.[8] As regulatory bodies place restrictions on specific forms of PFAS, such as PFOA and PFOS, companies have increasingly shifted towards short and ultra-short chain homologues that pose the potential of displaying similar toxic effects.

The presence of PFAS in groundwater[9] is a point of concern for communities that rely on groundwater as a source of drinking water. Filtration and sorption based treatment methods such as granular activated carbon (GAC), ion exchange resins (IXR), and nanofiltration (NF) are capable of achieving up to 100% removal of PFAS from water.[10] While effective, removal based treatment methods ultimately result in a contaminated waste stream that requires further treatment or disposal. As such, the development of destructive PFAS treatment methods capable of fully mineralizing PFAS in aqueous matrices has become the subject of much research. A number of destructive treatment methods have shown promise in degrading this highly recalcitrant class of compounds and include sonolysis,[11] electrochemical oxidation,[12] plasma treatment,[13] and photochemical treatment systems.[14–17] However, the aforementioned methods have not been developed past the pilot scale. At the full scale, thermal treatment in halogen-resistant incinerators is perhaps the most well-established technique that is commercially available.[18] Supercritical water oxidation, a technique employed by Battelle's PFAS Annihilator™, has also emerged as a very promising technique capable of >99% degradation of PFAS in aqueous matrices.[19–23]

Existing full-scale treatment methods are highly energy intensive. UV advanced reductive process (UV-ARP) systems hold the potential of fully destroying PFAS with lower energy requirements than the aforementioned techniques.[17] UV-ARP systems rely on photochemical reactions with electron donors to generate aqueous electrons, which have been demonstrated to be key reactive species in the destruction of PFAS.[24] O'Connor et al. reported >99% degradation and full defluorination of the highly recalcitrant PFBS using a UV-sulfite/iodide system that has been further developed into the Reactive Activation of Sulfite and Iodide through UV Natured Treatment (RADIANT) system.[25] While the RADIANT system has shown great promise under laboratory conditions, research demonstrating the RADIANT system's performance in more complex matrices has been limited.

Groundwater contains a variety of components that may interfere with PFAS degradation within the RADIANT system. Because the success of PFAS degradation is reliant on the generation of aqueous electrons, components that demonstrate a propensity to react with aqueous electrons have a high potential for inhibiting the destruction of PFAS. Dissolved organic matter (DOM) and nitrate are two common components of groundwater that are noted to have strong electron scavenging capacities,[26,27] and are immediately identifiable as potential interferents within the RADIANT system. Humic acid is commonly used to simulate DOM experimentally, and increasing concentrations have been reported to result in decreased defluorination in UV-ARP systems.[28] Similar effects have been reported for nitrate,[28] but the behaviour of these two groundwater components in UV-ARP is complicated by the series of transformations that arise after irradiation. Furthermore, the effect of these groundwater components has largely been examined in isolation, without consideration of how other groundwater parameters, such as water hardness, may influence their effects.

Further investigation is required to determine if the results reported in UV-ARP studies are transferable to the RADIANT system in complex matrices. Existing literature also largely focuses on long chain legacy PFAS, such as PFOS and PFOA, despite the detection of short and ultra-short chain PFAS in waters around the globe.[29] A pilot scale UV-sulfite treatment reported 50% degradation of PFPrS after 23 hours, indicating that ultra-short chain PFSAs such as PFPrS may be especially challenging to UV-ARP systems.[30] As the recalcitrance of specific PFAS is highly structurally dependent, further work is required to expand the capabilities of treatment systems to address short and ultra-short chain PFAS. Altogether, RADIANT system performance in more complex matrices, and for the degradation of ultra-short chain PFAS, remains relatively unexplored.

1.2 Objectives

This project aims to assess the feasibility of applying the RADIANT system to treat PFAS contamination in a real-life complex matrix such as groundwater. In order to do so, this project sought to accomplish the following objectives.

1) Investigate the individual and combined effects of humic acid and nitrate within the RADIANT system.
2) Assess RADIANT system performance in groundwater and the impact of increased matrix complexity.
3) Evaluate RADIANT treatment efficacy for short and ultra-short chain PFAS.
4) Compare RADIANT system performance at two different scales in order to inform future scale-up.

1.3 Thesis Organization

This thesis is presented in a manuscript style, consisting of 5 chapters and 2 appendices, as listed below.

Chapter 1 introduces the research topic and establishes thesis objectives.

Chapter 2 provides a literature review of existing PFAS treatment technologies and provides background information on the RADIANT system and potential interfering components of groundwater.

Chapter 3 details the application of the RADIANT system for treatment of short and ultra-short chain PFAS, and examines the impact of humic acid and nitrate on treatment efficacy.

Chapter 4 provides information relating to potential scale-up of the RADIANT system.

Chapter 5 summarizes key findings and provides recommendations for future work.

Appendix A contains supplemental information for Chapter 3.

Appendix B contains supplemental information for Chapter 4.

1.4 Co-authorship Statement

Chapter 3 was prepared for publication and co-authored by Adrian Pang, Iris Koch, and Kela Weber. Specifically, Adrian Pang assisted with analysis, and Iris Koch and Kela Weber provided resources and supervision.

Chapter 4 was written as a draft to be prepared for publication at a later date by co-authors. All data presented on the beaker set-up was collected and analyzed by Samuel Phillips. The draft presented in this thesis, as well as any data presented on the cuvette set-up, was produced by myself. Analysis of cuvette and beaker data was assisted by Adrian Pang, and Iris Koch and Kela Weber provided resources and supervision throughout.

1.5 References

(1) *Per and poly-fluorinated chemicals (PFAS)*. OECD. https://www.oecd.org/en/topics/sub-issues/risk-management-risk-reduction-and-sustainable-chemistry/per-and-poly-fluorinated-chemicals.html (accessed 2026-08-05).

(2) Glüge, J.; Scheringer, M.; Cousins, I. T.; DeWitt, J. C.; Goldenman, G.; Herzke, D.; Lohmann, R.; Ng, C. A.; Trier, X.; Wang, Z. An Overview of the Uses of Per- and Polyfluoroalkyl Substances (PFAS). *Environ. Sci.: Processes Impacts* **2020**, *22* (12), 2345–2373. https://doi.org/10.1039/D0EM00291G.

(3) Khan, B.; Burgess, R. M.; Cantwell, M. G. Occurrence and Bioaccumulation Patterns of Per- and Polyfluoroalkyl Substances (PFAS) in the Marine Environment. *ACS EST Water* **2023**, *3* (5), 1243–1259. https://doi.org/10.1021/acsestwater.2c00296.

(4) Du, X.; Wu, Y.; Tao, G.; Xu, J.; Du, Z.; Wu, M.; Gu, T.; Xiong, J.; Xiao, S.; Wei, X.; Ruan, Y.; Xiao, P.; Zhang, L.; Zheng, W. Association between PFAS Exposure and Thyroid Health: A Systematic Review and Meta-Analysis for Adolescents, Pregnant Women, Adults and Toxicological Evidence. *Science of The Total Environment* **2024**, *953*, 175958. https://doi.org/10.1016/j.scitotenv.2024.175958.

(5) Fang, S.; Sha, B.; Yin, H.; Bian, Y.; Yuan, B.; Cousins, I. T. Environment Occurrence of Perfluoroalkyl Acids and Associated Human Health Risks near a Major Fluorochemical Manufacturing Park in Southwest of China. *Journal of Hazardous Materials* **2020**, *396*, 122617. https://doi.org/10.1016/j.jhazmat.2020.122617.
(6) Fenton, S. E.; Ducatman, A.; Boobis, A.; DeWitt, J. C.; Lau, C.; Ng, C.; Smith, J. S.; Roberts, S. M. Per- and Polyfluoroalkyl Substance Toxicity and Human Health Review: Current State of Knowledge and Strategies for Informing Future Research. *Environ Toxicol Chem* **2021**, *40* (3), 606–630. https://doi.org/10.1002/etc.4890.
(7) Canada, H. *Objective for Canadian drinking water quality per- and polyfluoroalkyl substances*. https://www.canada.ca/en/health-canada/services/publications/healthy-living/objective-drinking-water-quality-per-polyfluoroalkyl-substances.html (accessed 2025-04-09).
(8) *PFAS National Primary Drinking Water Regulation*. Federal Register. https://www.federalregister.gov/documents/2024/04/26/2024-07773/pfas-national-primary-drinking-water-regulation (accessed 2026-08-05).
(9) Roy, J. W.; Weber, K. Per- and Polyfluoroalkyl Substances (PFASs) Contamination of Groundwater in Canada: A (Too) Short Review. *Canadian Water Resources Journal / Revue canadienne des ressources hydriques* **2025**, *50* (3), 236–249. https://doi.org/10.1080/07011784.2025.2519134.
(10) Merino, N.; Qu, Y.; Deeb, R. A.; Hawley, E. L.; Hoffmann, M. R.; Mahendra, S. Degradation and Removal Methods for Perfluoroalkyl and Polyfluoroalkyl Substances in Water. *Environmental Engineering Science* **2016**, *33* (9), 615–649. https://doi.org/10.1089/ees.2016.0233.
(11) Singh Kalra, S.; Cranmer, B.; Dooley, G.; Hanson, A. J.; Maraviov, S.; Mohanty, S. K.; Blotevogel, J.; Mahendra, S. Sonolytic Destruction of Per- and Polyfluoroalkyl Substances in Groundwater, Aqueous Film-Forming Foams, and Investigation Derived Waste. *Chemical Engineering Journal* **2021**, *425*, 131778. https://doi.org/10.1016/j.cej.2021.131778.
(12) Schaefer, C. E.; Choyke, S.; Ferguson, P. L.; Andaya, C.; Burant, A.; Maizel, A.; Strathmann, T. J.; Higgins, C. P. Electrochemical Transformations of Perfluoroalkyl Acid (PFAA) Precursors and PFAAs in Groundwater Impacted with Aqueous Film Forming Foams. *Environ. Sci. Technol.* **2018**, *52* (18), 10689–10697. https://doi.org/10.1021/acs.est.8b02726.
(13) Singh, R. K.; Multari, N.; Nau-Hix, C.; Anderson, R. H.; Richardson, S. D.; Holsen, T. M.; Mededovic Thagard, S. Rapid Removal of Poly- and Perfluorinated Compounds from Investigation-Derived Waste (IDW) in a Pilot-Scale Plasma Reactor.
(14) Gu, Y.; Liu, T.; Wang, H.; Han, H.; Dong, W. Hydrated Electron Based Decomposition of Perfluorooctane Sulfonate (PFOS) in the VUV/Sulfite System. *Sci Total Environ* **2017**, *607–608*, 541–548. https://doi.org/10.1016/j.scitotenv.2017.06.197.
(15) Li, A.; Zhang, Z.; Li, P.; Cai, L.; Zhang, L.; Gong, J. Nitrogen Dioxide Radicals Mediated Mineralization of Perfluorooctanoic Acid in Aqueous Nitrate Solution with UV Irradiation. *Chemosphere* **2017**, *188*, 367–374. https://doi.org/10.1016/j.chemosphere.2017.08.170.
(16) Banayan Esfahani, E.; Asadi Zeidabadi, F.; Jafarikojour, M.; Mohseni, M. Photo-Reductive Decomposition of Perfluorooctane Sulfonate (PFOS) and Its Common Alternatives by UV/VUV/Sulfite Process: Mechanism, Kinetic Modeling, and Water Matrix Effects. *Science of The Total Environment* **2024**, *951*, 175796. https://doi.org/10.1016/j.scitotenv.2024.175796.

(17) Fennell, B. D.; Mezyk, S. P.; McKay, G. Critical Review of UV-Advanced Reduction Processes for the Treatment of Chemical Contaminants in Water. *ACS Environ. Au* **2022**, *2* (3), 178–205. https://doi.org/10.1021/acsenvironau.1c00042.
(18) Blotevogel, J.; Giraud, R. J.; Rappé, A. K. Incinerability of PFOA and HFPO-DA: Mechanisms, Kinetics, and Thermal Stability Ranking. *Chemical Engineering Journal* **2023**, *457*, 141235. https://doi.org/10.1016/j.cej.2022.141235.
(19) Chiang, S.-Y. D.; Saba, M.; Leighton, M.; Ballenghien, D.; Hatler, D.; Gal, J.; Deshusses, M. A. Supercritical Water Oxidation for the Destruction of Spent Media Wastes Generated from PFAS Treatment. *Journal of Hazardous Materials* **2023**, *460*, 132264. https://doi.org/10.1016/j.jhazmat.2023.132264.
(20) Krause, M. J.; Thoma, E.; Sahle-Damesessie, E.; Crone, B.; Whitehill, A.; Shields, E.; Gullett, B. Supercritical Water Oxidation as an Innovative Technology for PFAS Destruction. *Journal of Environmental Engineering* **2022**, *148* (2), 05021006. https://doi.org/10.1061/(ASCE)EE.1943-7870.0001957.
(21) Rosansky, S.; Al-Dirani, S. M.; Scheitlin, C. G.; Dasu, K.; Dzurnak, M.; Xia, X.; Orth, C.; McCauley, M.; Mullins, L. Field Demonstration of PFAS Destruction in Various Alcohol-Resistant AFFFs Using Supercritical Water Oxidation (SCWO). *ACS EST Water* **2024**, *4* (10), 4486–4496. https://doi.org/10.1021/acsestwater.4c00499.
(22) Scheitlin, C. G.; Dasu, K.; Rosansky, S.; Dejarme, L. E.; Siriwardena, D.; Thorn, J.; Mullins, L.; Haggerty, I.; Shqau, K.; Stowe, J. Application of Supercritical Water Oxidation to Effectively Destroy Per- and Polyfluoroalkyl Substances in Aqueous Matrices. *ACS EST Water* **2023**, *3* (8), 2053–2062. https://doi.org/10.1021/acsestwater.2c00548.
(23) Webb, H.; Rosansky, S.; Al-Dirani, S. M.; Dasu, K.; Scheitlin, C. G.; Davis, J.; Chiques, L. PFAS Destruction Using Supercritical Water Oxidation (SCWO) at Peterson Space Force Base. *Journal of Hazardous Materials Letters* **2025**, *6*, 100156. https://doi.org/10.1016/j.hazl.2025.100156.
(24) Patch, D.; O'Connor, N.; Koch, I.; Cresswell, T.; Hughes, C.; Davies, J. B.; Scott, J.; O'Carroll, D.; Weber, K. Elucidating Degradation Mechanisms for a Range of Per- and Polyfluoroalkyl Substances (PFAS) via Controlled Irradiation Studies. *Science of The Total Environment* **2022**, *832*, 154941. https://doi.org/10.1016/j.scitotenv.2022.154941.
(25) O'Connor, N.; Patch, D.; Noble, D.; Scott, J.; Koch, I.; Mumford, K. G.; Weber, K. Forever No More: Complete Mineralization of per- and Polyfluoroalkyl Substances (PFAS) Using an Optimized UV/Sulfite/Iodide System. *Science of The Total Environment* **2023**, *888*, 164137. https://doi.org/10.1016/j.scitotenv.2023.164137.
(26) Fennell, B. D.; Odorisio, A.; McKay, G. Quantifying Hydrated Electron Transformation Kinetics in UV-Advanced Reduction Processes Using the $R_{e-,UV}$ Method. *Environ. Sci. Technol.* **2022**, *56* (14), 10329–10338. https://doi.org/10.1021/acs.est.2c02003.
(27) Fennell, B. D.; Fowler, D.; Mezyk, S. P.; McKay, G. Reactivity of Dissolved Organic Matter with the Hydrated Electron: Implications for Treatment of Chemical Contaminants in Water with Advanced Reduction Processes. *Environ. Sci. Technol.* **2023**, *57* (19), 7634–7643. https://doi.org/10.1021/acs.est.3c00909.
(28) Ren, Z.; Bergmann, U.; Leiviskä, T. Reductive Degradation of Perfluorooctanoic Acid in Complex Water Matrices by Using the UV/Sulfite Process. *Water Research* **2021**, *205*, 117676. https://doi.org/10.1016/j.watres.2021.117676.
(29) Ghorbani Gorji, S.; Mackie, R.; Prasad, P.; Knight, E. R.; Qu, X.; Vardy, S.; Bowles, K.; Higgins, C. P.; Thomas, K. V.; Kaserzon, S. L. Occurrence of Ultrashort-Chain PFASs

in Australian Environmental Water Samples. *Environ. Sci. Technol. Lett.* **2024**, *11* (12), 1362–1369. https://doi.org/10.1021/acs.estlett.4c00750.

(30) Liu, C. J.; McKay, G.; Jiang, D.; Tenorio, R.; Cath, J. T.; Amador, C.; Murray, C. C.; Brown, J. B.; Wright, H. B.; Schaefer, C.; Higgins, C. P.; Bellona, C.; Strathmann, T. J. Pilot-Scale Field Demonstration of a Hybrid Nanofiltration and UV-Sulfite Treatment Train for Groundwater Contaminated by per- and Polyfluoroalkyl Substances (PFASs). *Water Research* **2021**, *205*, 117677. https://doi.org/10.1016/j.watres.2021.117677.

2. Literature Review

2.1 Per- and Polyfluoroalkyl Substances (PFAS)

Per- and polyfluoroalkyl substances (PFAS) constitute a large and growing class of anthropogenic chemicals, distinguished by their characteristic fluorinated carbon chains. The general structure of a PFAS molecule consists of a hydrophobic fluorinated carbon chain attached to a hydrophilic head group. Because of the presence of both polar and nonpolar regions on the molecule, PFAS can demonstrate both hydrophobicity and oleophobicity depending on its orientation.[1] This surfactant-like property has led to extensive use of PFAS in industrial and commercial applications.[2] However, PFAS is perhaps most widely known for its exceptional resistance to degradation.[3] This high stability can be attributed to the carbon fluorine bonds characteristic of PFAS compounds. As the most electronegative element, when fluorine interacts with carbon the resulting bond is considered to be one of the strongest in organic chemistry.[4] The high energy requirement of cleaving a C-F bond gives PFAS its characteristic thermal resistivity.[3] Its chemical resistivity is a result of fluorine's influence on the PFAS molecule's geometry, as the carbon chain twists to minimize repulsion between highly charged fluorine substituents.[5] This results in a compact helical structure. The electronegative fluorine substituents draw away electron density from the carbon chain, creating an electron-dense fluorine shell that effectively shields the carbon chain from attack.

PFAS refers to a broad class of fluorinated organic compounds, encompassing over 14,000 distinct structures.[6] This diversity arises from the many possible configurations of their fluorinated carbon backbone and variable functional groups. The properties of individual PFAS molecules are influenced by structural factors such as the functional group, the length of its carbon chain, and the degree of fluorination of that carbon chain. Due to the vast number of PFAS compounds and their unique properties, these substances are extensively used in a variety of applications. They are an integral component of aqueous film forming foams (AFFF), where its thermal resistivity and surfactant like properties make the molecule incredibly effective at extinguishing hydrocarbon fires.[7] Because of PFAS' hydrophobic and oleophobic behaviour, its presence in AFFF creates a film that smothers fire by cutting off access to oxygen. PFAS has undoubtedly provided incredible benefits through its application in life-saving technologies. However, PFAS is also extensively used in the production of commercial goods. PFAS is an integral component of waterproof clothing, makeup, food packaging, and much more.[8]

PFAS compounds can be broadly grouped into polymeric and non-polymeric types. Teflon, a polymeric PFAS, has become widely known for its application in non-stick cookware.[9] Polymeric PFAS such as Teflon have not historically been considered as a cause for concern due to their larger size, which inhibits their uptake by biological receptors. However, issues arise when polymeric PFAS compounds degrade into their smaller non-polymeric constituents.[9] In particular, ionic short-chain forms of PFAS are more soluble in water and thus highly mobile.[10] Application of AFFF and the widespread application of PFAS in consumer goods provide multiple avenues for PFAS to enter the environment, where they persist due to their exceptional stability and potentially cause deleterious health effects to

plants, animals, and humans.[11,12] PFAS has been linked with cancers, altered hormone and metabolic function, and an increasing amount of alarming health effects.[13,14] Human exposure to PFAS is effectively unavoidable due to its ubiquity in the environment.[2,15] PFAS has often been detected in the human body,[16,17] likely enabled by the ability of PFAS to bind to proteins such as human serum albumin.[18] This demonstrates PFAS' potential for bioaccumulation[19,20] and emphasizes the importance of developing effective PFAS treatment technology to address the issue of PFAS contamination in the environment.

2.1.1 PFAS Contamination in Groundwater

Groundwater serves as a primary source of drinking water for nearly one third of the national population, acting as the sole water supply for 80% of Canada's rural population.[21] PFAS contamination in groundwater[22] is a point of concern for these communities, in addition to being a piece in the larger issue of PFAS contamination in the environment. High volumes of PFAS production and their resistance to degradation mean that PFAS is now ubiquitous in the environment, measurable in every possible matrix.[23] However, most forms of PFAS are thought to ultimately make their way into water.[23] For example, military bases, commercial airports, and fire-training facilities have seen significant environmental PFAS contamination due to the use of AFFF.[24] The individual composition of each PFAS molecule influences its physicochemical properties, and in turn its behavior in the environment. Short (4-7 C) and ultra-short (<2 C) chain PFAS exhibit high mobility in the environment due to their solubility in water and minimal affinity for organic matter.[25] PFPrS is one of the more commonly detected forms of ultra-short chain PFAS, and one study found PFPrS in 83% of surface, groundwater, and wastewater samples, ranging from <0.2-8106 ng/L.[25] In another study, PFPrS was detected in all groundwater samples (19-63000 ng/L) sampled in the proximity of U.S. military bases.[26] While soluble forms of PFAS, such as the aforementioned short and ultra-short chain PFAS, may enter the groundwater directly, longer chain PFAS readily adsorb onto the soil.[27] This PFAS contaminated soil in the unsaturated zone then functions as a long term source of PFAS for underlying groundwater systems,[28] as precipitation infiltrates the soil and carries adsorbed PFAS into the saturated zone. Conventional water and wastewater treatment plants often struggle to remove PFAS, and PFAS effluent concentrations can even be higher than the influent due to the degradation of PFAS-like precursor compounds.[29] As such, storm water runoff, landfill leachate, and effluent from waste water treatment plants can also serve as sources of PFAS contamination in groundwater. [30]

Groundwater concentrations of PFAS are largely dependent on proximity to a PFAS source. McMahon et al. found in a 2019 study of five US aquifer systems that the distance to the nearest fire-training area and percentage of urban land use were strong predictors of PFAS detection in groundwater samples.[31] The presence of other contaminants associated with human activity – such as VOCs, pharmaceuticals, and personal care products – has also been linked to a higher likelihood of PFAS detection.[31] The occurrence of PFAS in groundwater is also dictated by hydrologic and geochemical factors relating to its fate and transport. Because PFAS originates from land-surface sources, the depth and age of a groundwater sample as dictated by its position in the groundwater flow system are factors that may predict the occurrence of PFAS in groundwater. The likelihood of PFAS detection

decreases with increasing well depth.[31] Mixed age groundwater, which includes water recharged prior to the widespread use of PFAS, is also less likely to have PFAS.[31] PFBS, PFHxS, PFOS, PFHpA, PFOA, PFNA, and various 4-9 carbon PFSA and PFCA compounds are some of the most commonly detected forms of PFAS in groundwater, but PFOA and PFOS are by far the most widely studied.

Groundwater chemistry can also play a role in determining the presence of PFAS in water by influencing its sorption and mobility. Low pH, higher concentrations of divalent cations, or lower concentrations of DOC and Cl can increase PFAS sorption to aquifer solids. Divalent cations can increase PFAS sorption by reducing the negative charge on soil surfaces, mitigating the repulsion between aquifer solids and negatively charged PFAS.[32,33] In contrast, anoxic conditions in groundwater can lead to reductive dissolution of minerals (Mn and Fe oxides), which then decreases PFAS sorption or mobilizes previously adsorbed PFAS.[31] Elevated DOC concentrations are thought to increase PFAS mobility through electrostatic/hydrophobic interactions or by competing with PFAS for sorption sites.[10,34] Because of this, PFAS detection in groundwater is typically associated with elevated DOC concentrations and high concentrations of inorganic anions, such as Cl and SO_4, which can also compete for sorption sites.[33] In essence, the occurrence of PFAS in groundwater is affected by the properties of both the PFAS compound itself and the chemistry of the surrounding water.

PFAS contamination in water can manifest as large, low-concentration plumes which appear to be fed by multiple sources.[35] This can be attributed in part to the sorption of PFAS onto sediment, as driven by groundwater chemistry and matrix diffusion effects, which adds further complexity to the management PFAS contamination due to the ability of these aquifer solids to act as non-point sources of contamination. Early understandings of contamination made the assumption that source zones were confined to the unsaturated zone.[35] The in-situ treatment approach typically consisted of the excavation of the source mass, with a pump and treat system for dissolved phase contaminants. However, matrix diffusion and other source processes can sustain plumes for long periods of time – significantly extending the duration of treatment. Due to this and the current state of PFAS treatment technology, complete restoration of PFAS sites in the near term may be unlikely. Given the persistence and mobility of PFAS in groundwater systems, strategies such as long term source and/or plume containment, coupled with point of use drinking water treatment where necessary, may be more feasible and practical approaches to the management of PFAS contamination.[35]

2.2 Treatment of PFAS Contaminated Water

Mounting evidence of the adverse environmental and human health impacts associated with PFAS have triggered scrutiny from the scientific and regulatory communities. The guidelines surrounding PFAS reflect the evolving nature of our understanding of this class of chemicals. In 2024, the objective set for the maximum level of PFAS in drinking water was set at 30 ng/L by Health Canada, calculated as the sum of 25 specific PFAS.[36] The low concentration of this objective underscores the severity of the issue, and may be at odds with existing PFAS treatment capabilities. With consideration of the current state of PFAS treatment technology,

the concentration of PFAS in drinking water is recommended to be maintained as low as reasonably achievable (ALARA).[36]

Generally, treatment of PFAS contamination in water can be categorized as removal or destruction based. Removal technologies, which focus only on the displacement of contamination, include filtration and sorption based methods like granular activated carbon (GAC), ion exchange resins (IXR), nanofiltration (NF), and reverse osmosis (RO).[37–39] These technologies have demonstrated the ability to achieve up to 100% removal of PFAS from water, although removal efficiencies decrease with use.[29,40] In practice, GAC and IXR are the most common treatment technologies used for the removal of PFAS from groundwater and drinking water.[29] IXR systems in particular can be more expensive than GAC, but benefit from the capability of on-site regeneration that enables repeated use. Although effective, removal technologies like GAC ultimately result in contaminated solid waste, which must then be remediated through solid state destructive technologies such as ball milling[40] or smouldering.[29,41] Similarly, IXR regeneration produces an effluent that is high in concentrations of PFAS, salt, and residual organic compounds.[29] As such, the development of destructive PFAS treatment technology is a necessary part of a comprehensive solution to the issue of environmental PFAS contamination, and offers the potential of in-situ treatment of contamination in aqueous matrices such as groundwater.

2.2.1 PFAS Destruction

The unique stability of this highly recalcitrant class of chemicals has made the development of effective destructive treatment methods particularly challenging. For a long time, the most widely available full-scale destructive technique was incineration in halogen-resistant incinerators.[42] Although incineration requires high energy input and transportation for off-site treatment, capital costs are likely to be lower due to the well-established nature of the technique. Incomplete degradation, resulting in the formation of short and ultra-short chain PFAS, as well as the emission of volatile transformation products has become a significant point of concern surrounding this technique.[43] As such, efforts have been made to expand the range of destructive treatment methods available. Promising non-thermal treatment methods include electrochemical oxidation, plasma, photocatalysis, sonolysis, supercritical water oxidation, and hydrothermal alkaline treatment. Table 1 provides a brief summary of the aforementioned treatment methods.

Table 1: Selected Studies in PFAS Destructive Treatment Methods

Paper	Treatment Method	Type of PFAS	Matrix	Analytical Methods	PFAS Degradation/ Fluoride Recovery	Notes
Singh Kalra et al.[44] (2021) 10.1016/j.cej.2021.131778	Sonolysis	24 native PFAS mix	Deionized water Dilute AFFF Low total dissolved solids (TDS) groundwater (388 mg/L) High-TDS groundwater (10.2 g/L)	LC-MS/MS (PFAS analysis)	98% degradation of most PFAS in 120 min	Uses high-energy ultrasound (>29 kHz) to produce nanoscale/microscale cavities with high temperatures and pressures capable of destroying PFAS through pyrolysis
Singh et al.[45] (2019) 10.1021/acs.est.9b02964	Plasma	2.7-1440 µg/L total PFAA PFOS PFHpS PFOA PFHxS PFHpA PFBS PFPeA PFBA	Investigation-derived waste (development and purge water from groundwater monitoring wells)	UPLC-QToF-HRMS & UPLC-MS-MS (PFAS analysis) ISE meter (fluoride recovery)	>93% degradation of PFOA and PFOS 56 ± 38% degradation of PFBS 33 ± 14% fluoride recovery	Pilot scale plasma reactor (4 L) Highly reactive oxidative and reductive species formed in response to electrical discharge Mechanisms reported to be unknown, posited to be bulk liquid redox reactions No effect on degradation efficiency reported from co-contaminants

Schaefer et al.[46] (2018) 10.1021/acs.est.8b02726	Electro-chemical oxidation	PFOA spike (20 mg/L) PFOS PFHpS PFHxS PFBS PFOA PFHpA PFHxA PFPeA PFBA	AFFF impacted/ spiked groundwater	LC-MS/MS (PFAS analysis)	91% degradation of PFOS 78% degradation of PFBS 71% fluoride recovery	Direct oxidation of PFAS through electron transfer from PFAS to anode Increase in short-chain PFAAs (PFHxA, PFPeA, PFBA) noted due to transformation of precursors High effectiveness for long-chain PFAS, lower effectiveness for short-chain PFAS
Li et al.[47] (2020) 10.1016/j.watres.2020.116219	Photocatalytic	PFOA (100 µg/L)	Deionized water	LC-MS/MS (PFAS analysis)	>90% degradation in 4 h 62% fluoride recovery	Fe/TNTs@AC adsorptive photocatalyst based on activated carbon and TiO_2 PFOA degradation initiated by direct hole oxidation, followed by decarboxylation, C-F bond cleavage, and chain shortening reactions
Hao et al.[48] (2022)	Hydrothermal alkaline treatment (HALT)	148 PFAS mix	Aqueous Film Forming Foam (AFFF) impacted	LC-QToF-MS (PFAS analysis)	>99% for most PFAS within 90 min	Degradation was function of reaction temp, NaOH concentration,

10.1021/acs.est.2c00654			groundwater and soil Groundwater contained nitrate (5.7 and 9.5 mg/L), high total organic carbon (TOC) (28 and 59 mg/L) and hardness (120 mg/L)	pH/ISE meter (fluoride recovery)	132% fluoride recovery	and reaction time General nucleophile OH- substitution mechanism thought to be responsible for defluorination of PFAS Short chain (3-5 C) PFSAs found to be most recalcitrant, and degradation was limited
Scheitlin et al.[49] (2023) 10.1021/acsestwater.2c00548	Supercritical water oxidation (PFAS Annihilator)	22.8 mg/L total PFAS PFOA PFOS PFBA PFPeA PFHxA PFHpA PFDA,PFUnDA PFDoDA 8:2FTS N-MeFOSAA N-EtFOSAA L-PFBS and PFBS	Laboratory prepared feed with VOC and diesel fuel added as co-contaminants	LC/MS/MS (PFAS analysis) LC-QToF-MS (analysis of transformation products)	>99% for total PFAS 77.6% fluoride recovery	PFAS destruction reported to be largely unaffected by addition of organic co-contaminants Total concentration of co-contaminant also decreased All final PFAS concentrations <70 ng/L

Many treatment methods are implemented as part of a treatment chain, with a pre-treatment concentrating step to increase treatment efficiency. Hydrothermal alkaline treatment, for example, has been used in conjunction with foam fractionation to concentrate PFAS.[50] Although less efficient for short-chain sulfonic acids, HALT systems have achieved >99% destruction and near-complete defluorination of total PFAS.[50] The treatment involves the reaction of PFAS with NaOH in subcritical hydrothermal water, and as a result requires high energy input and careful selection of materials to offset the corrosive solutions used in treatment. While the aforementioned treatment methods have emerged as promising alternatives to thermal treatment, few have progressed past the pilot scale. Supercritical water oxidation (SCWO) is notable in that it is one of the few non-thermal treatment methods that has reached commercial availability.[51] Due to its extreme operating conditions, SCWO has been reported to currently not be economical for large volumes of dilute streams.[52] Despite this, SCWO has been reported to be highly effective (>99% total PFAS destruction) and minimally affected by variable groundwater components. [49] However, more energy efficient techniques under investigation include UV advanced oxidative processes (UV-AOP) and advanced reductive processes (UV-ARP).

In contrast to many other AOP/ARP treatment methods, photochemical techniques are particularly attractive due to their lower energy requirement. While UV based treatment is a standard step in many wastewater treatment facilities, direct photolysis has been shown to be ineffective at breaking down PFAS compounds.[53] UV-AOP use highly reactive oxygen species (ROS) to oxidatively degrade PFAS, destroying the C-F and C-C bonds in PFAS. Reactive oxidant species include hydroxyl and sulfate radicals, which can be generated through UV activation of oxidizing reagents such as hydrogen peroxide, sodium persulfate, ozone, or halogens.[54] UV-H_2O_2 systems are one of the most commonly used UV-AOP systems, but have shown limited efficacy with PFAS.[55] Hydroxyl typically oxidizes saturated organic compounds through hydrogen atom abstraction (removal of a hydrogen by a radical) or radical addition with unsaturated organic compounds.[56] Because perfluorinated compounds like PFOA and PFOS have no hydrogen available for abstraction, the hydroxyl radical can only undergo direct electron transfer. This would result in the formation of the hydroxide ion, which is thermodynamically unfavoured.[56] Another UV-AOP system, the UV activated persulfate anion, can generate sulfate radicals that are capable of oxidizing short chain PFCAs to form CO_2 and fluoride.[57] Fluorotelomers can be converted to PFCAs through oxidation by hydroxyl radicals,[58] while sulfate radicals have been shown to successfully degrade PFCAs.[57] However, different PFAS compounds will exhibit varying degrees of susceptibility to oxidation. Oxidative degradation is generally considered to be less effective for PFSAs.[55]

2.2.1.1 Ultraviolet Advanced Reductive Processes (UV-ARP)

While UV-AOP systems oxidize PFAS via reactive oxygen species, UV-ARP systems use aqueous electrons (e^-_{aq}) as the key reactive species to initiate the degradation of PFAS. There are several developing PFAS destruction techniques that involve the capture of aqueous electrons. The term aqueous electron refers to the arrangement of molecules resulting from the presence of a free electron in water. The generally accepted model of an aqueous electron in bulk water depicts an electron in a solvent-free void, surrounded by a 4-6 molecule

solvation shell.[59] The aqueous electron is a highly reducing species, with a reduction potential of -2.9 V.[53] Aqueous electrons may be directly generated by pulse radiolysis, released during the ionization of water molecules by x-rays or gamma-rays, or generated through photochemical interactions with electron donors – as is the case in UV-ARP.[4,59] In the latter, UV activation triggers photosensitizers to generate aqueous electrons.

In UV-ARP, photosensitizers are the electron donating reagents used to generate the aqueous electrons that create a reductive environment. Photosensitizers such as sulfite, iodide, and phenol undergo UV photolysis to produce aqueous electrons, as described in Eq (1-3).

Elementary Reaction	Quantum Yield (Φ)	ε ($M^{-1}cm^{-1}$)	
$SO_3^{2-} + UV \rightarrow SO_3^{\cdot -} + e^-_{aq}$	0.116	18-20	(1)
$I^- + H_2O + UV \rightarrow I^{\cdot} + H_2O + e^-_{aq}$	0.170-0.286	162-220	(2)
$C_6H_5OH + UV \rightarrow C_6H_5O^{\cdot} + H^+ + e^-_{aq}$	0.230-0.240	942	(3)

The quantum yield of a photosensitizer describes the number of aqueous electrons generated for every photon absorbed, while the molar absorptivity describes how strongly a particular chemical attenuates photons at a given wavelength (e.g. 248 nm).[61] High quantum yields increase a system's capacity to generate aqueous electrons, thereby increasing degradation. High molar absorptivity may decrease the amount of photons available for aqueous electron generation and inhibit system performance. As such, photosensitizers may be selected for high quantum yield and low molar absorptivity. Aqueous electrons reduce the PFAS compound to form a radical anion as described in eq (4) and (5).

$PFOA + e^-_{aq} \rightarrow PFOA^{\cdot}$	$k = 1.7 \times 10^7\ M^{-1}s^{-1} – 7.1 \times 10^8\ M^{-1}s^{-1}$	(4)
$PFOS + e^-_{aq} \rightarrow PFOS^{\cdot}$	$k = 2.4 \times 10^9\ M^{-1}s^{-1}$	(5)

McTaggart et al. (2023) used density functional theory (DFT) simulation to demonstrate the stretching of C-C bonds in PFAS upon electron capture, causing the helix to unwind into a metastable state before irreversibly reverting back to its helical structure.[5] The PFAS molecule's return to helicity is what triggers defluorination, as the additional electron is ejected with a fluoride ion.[5] Spontaneous bond stretching from the addition of the "extra" electron can also result in the ejection of the functional group.[60] For example, C-S bond stretching in PFOS causes the ejection of the sulfonate group, and the formation of PFOA.[60] Following aqueous electron attack, the resulting products then undergo electron recombination with different radical species to produce a variety of substituted products, such as –F/+H and $-CF_3$/+H exchanged PFAS.[60] Electron recombination with a hydroxyl radical may result in the formation of the –F/+OH exchanged PFAS, which has been observed experimentally with PFCAs.[60]

Because the degradation of PFAS is largely initiated by aqueous electrons, the effectiveness of UV-ARP is inhibited by the presence of electron-deficient species. These electrophiles are referred to as electron scavengers, and eq (6) and (7) describe two common electron scavenging reactions,

$$e^-_{aq} + H^+ \rightarrow H^\cdot \qquad k = 2.3 \times 10^{10}\ M^{-1}s^{-1} \qquad (6)$$

$$e^-_{aq} + O_2 \rightarrow O_2^{\cdot -} \qquad k = 1.9 \times 10^{10}\ M^{-1}s^{-1} \qquad (7)$$

wherein protons or dissolved oxygen react with the generated electrons. The concentration of aqueous electrons available to react with PFAS is decreased by electron scavenging reactions, thereby inhibiting PFAS degradation. Because of the electron scavenging effects associated with protons and dissolved oxygen, UV-ARP systems are ideally performed under anaerobic and alkaline conditions. It is also worth noting that photosensitizers themselves are able to act as electron scavengers,

$$e^-_{aq} + SO_3^{2-} \rightarrow \text{products} \qquad k = <1.5 \times 10^{6}\ M^{-1}s^{-1} \qquad (8)$$

$$e^-_{aq} + I^- \rightarrow \text{products} \qquad k = <2.4 \times 10^{5}\ M^{-1}s^{-1} \qquad (9)$$

although this effect is thought to be minimized at lower photosensitizer concentrations. The impact of electron scavengers on PFAS degradation can be represented by eq (10),

$$k'_{S,t} = \sum_i k_{S_i,e^-_{aq}}[S_i]_t \qquad (10)$$

wherein $k_{S_i,e^-_{aq}}$ is the bimolecular e^-_{aq} scavenging rate constant for any electron scavenger S, and $[S_i]_t$ is the concentration of electron scavenger S at any point in time. The sum product is used to determine the first-order scavenging capacity $k'_{S,t}$ of the background water matrix.

2.2.1.1.1 UV-Sulfite/Iodide

The selection of photosensitizer is a significant factor in the design of an effective PFAS treatment system. Although quantum yield is a measure of a photosensitizer's electron-producing ability, higher quantum yields are not necessarily indicative of greater PFAS degradation. Photosensitizers react to generate electrons, but their resulting products, in addition to the photosensitizer itself, can participate in electron-scavenging reactions that

inhibit PFAS degradation. This is shown to be the case with UV-iodide systems, which experience electron scavenging effects from the reactive iodine species (RIS) generated,

$$I^{\cdot} + I^{-} \rightarrow I_2^{\cdot -} \qquad k = 1.2 \times 10^{4}\ M^{-1}s^{-1} \qquad (11)$$

$$I^{\cdot} + I^{\cdot} \rightarrow I_2 \qquad k = 1.0 \times 10^{10}\ M^{-1}s^{-1} \qquad (12)$$

$$I^{\cdot} + I_2^{\cdot -} \rightarrow I_3^{-} \qquad k = >6.4 \times 10^{9}\ M^{-1}s^{-1} \qquad (13)$$

$$I_2^{\cdot -} + I_2^{\cdot -} \leftrightarrow I_3^{-} + I^{-} \qquad k = 3.2 \times 10^{9}\ M^{-1}s^{-1} \qquad (14)$$

$$I^{-} + I_2 \rightarrow I_3^{-} \qquad k = 7.2 \times 10^{2}\ M^{-1}s^{-1} \qquad (15)$$

which are shown to scavenge initial iodide concentrations in addition to participating in the electron scavenging reactions described below by eq (16-18).

$$e^{-}_{aq} + I_2 \rightarrow I_2^{\cdot -} \qquad k = 5.3 \times 10^{10}\ M^{-1}s^{-1} \qquad (16)$$

$$e^{-}_{aq} + I_2^{\cdot -} \rightarrow 2I^{-} \qquad k = 9.0 \times 10^{10}\ M^{-1}s^{-1} \qquad (17)$$

$$e^{-}_{aq} + I_3^{-} \rightarrow I^{-} + I_2^{\cdot -} \qquad k = 3.5 \times 10^{10}\ M^{-1}s^{-1} \qquad (18)$$

Although RIS are reported to have higher electron scavenging capacities than phenol, the several competing rate constants prevent electron scavenging reactions from dominating UV-iodide systems.[61] The iodide radical has also been hypothesized to participate in PFOS degradation,[62] with UV-iodide systems being reported to reach 67% degradation of PFOS in comparison to the 41% degradation achieved by phenol.[61]

UV-sulfite systems benefit from the generation of the anionic radical sulfite, which reacts with oxygen to limit its electron scavenging capacity.

$$SO_3^{\cdot -} + O_2 \rightarrow SO_5^{\cdot -} \qquad k = 1.5 \times 10^{9}\ M^{-1}s^{-1} \qquad (19)$$

Because of this, UV-sulfite systems are generally more effective than UV-iodide and UV-phenol systems - achieving 91% degradation of PFOS.[61] However, the degradation of PFOS can be further improved up to 98% in UV-sulfite/iodide systems.[61] When used in conjunction sulfite and iodide undergo a series of synergistic reactions,

$$I^{\cdot} + SO_3^{2-} \rightarrow I^{-} + SO_3^{\cdot -} \qquad k = 1.4 \times 10^{9}\ M^{-1}s^{-1} \qquad (20)$$

$I_2^{\bullet-} + SO_3^{2-} \rightarrow 2I^- + SO_3^{\bullet-}$ $k = 1.5 \times 10^9\ M^{-1}s^{-1}$ (21)

$I_3^- + SO_3^{2-} \rightarrow 2I^- + ISO_3^-$ $k = 1.5 \times 10^9\ M^{-1}s^{-1}$ (22)

$I_2 + SO_3^{2-} \rightarrow ISO_3^- + I^-$ $k = 1.5 \times 10^9\ M^{-1}s^{-1}$ (23)

$ISO_3^- + H_2O \rightarrow SO_4^{2-} + I^- + 2H^+$ $k = 1.5 \times 10^9\ M^{-1}s^{-1}$ (24)

wherein sulfite is able to undergo spontaneous redox reactions with reactive iodine species to regenerate iodide. This mitigates the electron scavenging effect associated with reactive iodine species, while increasing the system's capacity to generate aqueous electrons.

Liu et al. demonstrated that the combination of both sulfite and iodide in UV activated systems significantly accelerated the reductive degradation of PFAS. At pH 12.0, the UV-sulfite/iodide system achieved >99.7% destruction of most PFAS and >90% overall defluorination.[63] The degradation of highly recalcitrant PFBS was improved from 86% in a UV-sulfite system to >99% through the addition of 2 mM KI to the initial 10 mM Na_2SO_3 mixture.[63] The overall defluorination after 24 h was also improved from 69% in UV-sulfite to 78% in a UV-sulfite/iodide system.[63] O'Connor et al. was able to further increase the defluorination of PFBS through the continuous addition of sulfite, reporting >99.9% degradation and 106 ± 4% defluorination.[61] Treatment with this optimized system began with 20 mM sulfite and 10 mM iodide, with 10 mM sulfite additions every 2 h over the course of an 11 h treatment, achieving final reagent concentrations of 60 mM sulfite and 10 mM iodide. Continuous sulfite addition was thought to enhance PFBS degradation by sustaining the regeneration of iodide. This, combined with a higher sulfite/iodide ratio (2:1 in O'Connor et al. vs 5:1 in Liu et al.) resulted in improved defluorination.

The initial concentration of sulfite is also of significance. O'Connor et al. report that the degradation of PFBS was increased from 81 ± 6% to 93 ± 2% and then 97.9 ± 0.4% for initial sulfite concentrations of 10 mM, 20 mM, and 50 mM respectively.[61] Although degradation was improved at 50 mM sulfite, large initial concentrations of sulfite have historically been avoided due to the electron scavenging effect of sulfite at higher concentrations. Alternatively, it has also been postulated that high sulfite concentrations reduce the electrostatic repulsion between negatively charged headgroups, enhancing surfactant characteristics and promoting the formation of micelles.[64] The aggregation and micellization of PFBS would decrease its reactivity with e^-_{aq}, thereby inhibiting degradation. In contrast to the aforementioned studies, Jiang et al. suggests that high concentrations of sulfite may improve PFAS degradation through mechanisms beyond the generation of aqueous electrons. A downward shift in NMR signals associated with distinct F positions on the PFBS structure was observed with increasing concentrations of sulfite, ranging from 0-0.5 M.[64] This was interpreted as a reduction in electron density around the F atoms in response to increasing sulfite concentrations, attributed to the influence of the sulfur atom's lone pair electrons. DFT calculations modelling PFBS-sulfite interactions further illustrated this effect, reporting a decrease in bond dissociation energy (BDE) in the presence of sulfite.[64] Notably, the reduction in BDE was largest in the C-F bonds of the terminal $–CF_3$ group, which is typically thought to have the highest C-F BDE of the molecule. This was supported

experimentally, as defluorination showed significant improvement with increasing sulfite concentrations up to 0.2 M.[64] Given this, it may be worthwhile to explore increasing sulfite concentrations beyond those used in prior studies.

The work reported by O'Connor et al. forms the foundation for the UV-sulfite/iodide system that will henceforth be referred to as the Reactive Activation of Sulfite and Iodide through UV Natured Treatment (RADIANT) system.

2.3 Application of UV Sulfite/Iodide Systems for Treatment of PFAS Contaminated Groundwater

Although UV-sulfite/iodide systems have shown great success in the treatment of PFAS-contaminated water, experiments thus far have been conducted in laboratory settings under optimal conditions. Generally, UV-ARP systems require high pH, anoxic conditions, and reagent concentrations that allow for sufficient PFAS-e^-_{aq} interaction. These conditions do not necessarily align with operational environments. Environmentally relevant concentrations of PFAS are typically orders of magnitude below the initial concentrations used in experiments. Reported concentrations of PFAS in real-world waters range from the ng/L to µg/L scale.[65] In contrast, starting concentrations of PFAS used in experimental UV-sulfite/iodide trials are rarely lower than mg/L. Work by O'Connor et al. with the RADIANT system investigated concentrations of PFAS ranging from 1-30 mg/L,[66] while other UV-ARP systems have been investigated with starting concentrations ranging from 70 µg/L[67] to 2-12 mg/L[4].

When initial PFAS concentrations are low, such as those typically found in groundwater, the challenge is then to maximize the interaction between PFAS and e^-_{aq}. This can be accomplished by increasing the concentration of PFAS through a pre-treatment step, or by increasing the concentration of aqueous electrons. Aqueous electron concentrations may be enhanced by increasing photosensitizer concentrations or by minimizing electron scavenging reactions. As such, this study is particularly concerned with components of groundwater that are expected to exhibit an electron scavenging effect. In complex matrices such as groundwater, the presence of co-contaminants with the natural components of groundwater introduce an additional layer of complexity. Electron scavenging by groundwater matrix components is by far one of the greatest limiting factors, but groundwater components may also influence the degradation of PFAS beyond their interaction with aqueous electrons. The following sections aim to summarize the basic processes that influence groundwater chemistry, with a focus on groundwater compositions characteristic of Ontario to meet the study interests of the project.

2.3.1 Composition of Groundwater

Groundwater is largely replenished by precipitation, which travels downwards through soil until it reaches a dense rock layer. This creates a zone where the ground is fully saturated with water. Groundwater is defined as the water that exists in this saturated zone, filling all available spaces between particles of soil and rock. At times, this rock may become fractured and create areas of void space where groundwater accumulates. The water pooled in the more

porous layers of rock moves slowly across pressure gradients, eventually discharging into bodies of surface water.

Regional variations in the composition of the earth play a major role in determining the composition of groundwater. Groundwater chemistry is determined by a variety of processes, including the type of rock it interacts with, and the duration of this interaction.[68] Some regions have soil or rock types that are more permeable, allowing water to easily flow through and join the existing groundwater supply. In these regions, the residence time of groundwater is decreased due to this increased permeability, and the composition of groundwater will differ from regions where water is more stagnant. Often in areas of higher elevation, recharge zones are regions of permeable earth where the groundwater supply is replenished. Conversely, discharge zones are areas where groundwater is released into surface water bodies. These discharge zones are typically found at lower elevations, where the water table intersects with the Earth's surface. Recharge zones have been characterized by relatively low pH, low total dissolved solids (TDS), high tritium, and elevated oxidation-reduction potential.[69] As rainwater dissolves CO_2, carbonic acid is produced, resulting in a lower pH and increased mineral dissolution in recharge zones.[69] Discharge zones tend to have higher concentrations of magnesium, sodium, potassium, chloride and bicarbonate than recharge zones.[69] The trend is reversed for calcium, which tends to be more concentrated in recharge zones.[69]

Groundwater mineral components enter the groundwater through weathering reactions, described as water-rock interactions. Major components include Na^+, Ca^{2+}, Mg^{2+}, Cl^-, SO_4^{2-}, and HCO_3^-, while minor components may include K^+, Fe^{2+}, Al^{3+}, CO_3^{2-}, SiO_3^{2-}, NO_2^-, NO_3^-, and NH_4^+.[68] Other variables in groundwater chemistry include pH and redox state, which control the composition of groundwater through redox and acid-base reactions. The oxic/anoxic conditions of groundwater, represented by the concentration of dissolved oxygen (DO), can also influence the types of reactions that may occur. These variables are relevant because they influence the parameters that impact UV-sulfite/iodide systems. Water hardness is a factor relevant to UV-sulfite/iodide systems due to its association with ionic strength, and parameters like the concentration of tritium may indicate regions that are more vulnerable to contamination.[69] In all, there are a variety of processes that influence the composition of groundwater. The most significant processes are thought to be recharge, ion exchange, salinization, and organic degradation.[69]

2.3.1.1 Groundwater Composition in Ontario

Groundwater classifications have evolved over time. Early methods of classification simply categorized waters by taste – subdividing water into fresh, brackish, salt, sour, bitter, and sweet water.[68] Modern methods of categorization will classify groundwater by composition, differentiating categories by their dominating cations and anions. However, groundwater properties can also be greatly affected by their minor constituents. In response to this, many different systems of chemical classification have emerged, some of which include as many as 625 types of water.[68] For ease of discussion, this study uses the classification method of Cloutier et al., in which there are seven geochemically distinct types of water named by the dominant major cation (Ca, Mg, Na, or K) and anion (HCO_3, Cl^-, or SO_4^{2-}), as determined by

the highest meq/L concentrations.[70] Mx is used to denote water where each ion is less than 20% meq. The frequencies of each water type in eastern Ontario are represented in Table 2.[69]

Table 2: Water Type Frequency in Eastern Ontario

Water Type	Frequency (%)
Ca-Cl	3
Ca-HCO_3	55
Ca-SO_4	1
Mg-Cl	1
Mg-HCO_3	6
Mx-Cl	2
Mx-HCO_3	8
Na-Cl	10
Na-HCO_3	15
Na-SO_4	1

The most common water type by far is Ca-HCO_3, followed by the Na-HCO_3 water type. Ca-HCO_3 type water is typically associated with fresh, modern, and meteoric water.[69] As such, Ca-HCO_3 water type tends to dominate unconfined recharge areas.[71,72]

The Ca-HCO_3 water type is commonly referred to as "hard" water. Water hardness is a particularly significant variable in UV-sulfite/iodide systems, defined as the sum of dissolved calcium and magnesium in a solution.[73] One of its regulatory processes is ion exchange, which can be responsible for water softening.[69] Natural water softening describes the process by which divalent and trivalent cations are replaced by monovalent species. In Eastern Ontario, this commonly occurs through the following ion exchange,

$$Ca^{2+} + 2Na_{ad} \rightarrow Ca_{ad} + 2Na^{+} \quad (25)$$

wherein Na^+ adsorbed onto a negatively charged surface is replaced by dissolved Ca^{2+}, causing the sodium to enter solution. Divalent and trivalent cations have a higher affinity for adsorption than monovalent species, and as a result Ca-HCO_3 and Mg-HCO_3 water types can naturally evolve into the Na-HCO_3 water type.[71] As such, water hardness is thought to

naturally decreases in the presence of a Na^+ source. In Ontario, the Champlain Sea incursion is one such Na^+ source.[69]

The Na-HCO_3 water type is the second most common water type in the region and the most alkaline among measured water types with an average pH of 7.94, reflecting sodium's effect on the carbonate system that regulates pH in natural waters.[74] The increase of pH can occur via the following reaction,

$$CaCO_3 + 2Na_{ad} + CO_2 + H_2O \rightarrow 2HCO_3^- + Ca_{ad} + 2Na^+ \quad (26)$$

wherein the bicarbonate anion, a weak base, is formed through the dissolution of calcite. The solubility of calcite is increased at higher pH,[69] leading to further bicarbonate anion formation. However, it is important to note that the major source of HCO_3 in eastern Ontario is not carbonate dissolution but the build-up of organic decomposition products caused by regional bedrock depressions.[69] Bicarbonate can be produced by microorganisms through their metabolic respiration, and is correlated with other products of organic decomposition such as DOC, NH_4^+, and NH_3.[69] Hard water is associated with lower F^- concentrations, due to the increase in fluorite CaF_2 dissolution caused by softening reactions.[69] Fluoride retention on charged surfaces is decreased at elevated pH due to displacement by OH^-.[75] As a result, Na-HCO_3 water exhibits the highest average F^- (1.2 mg/L) concentration of all water types.[69] Na-HCO_3 type water is found in regions on Ontario with glaciomarine deposits, thick drift, and bedrock depression.[69] From a physical perspective, confinement and restricted flow are driving factors in these regional ion exchange processes.[69] Concentrations of tritium are also low in Na-HCO_3 dominant regions,[69] indicating a lack of recharge since the 1950s, which has significant implications on the likelihood of PFAS detection in these waters.

2.3.2 Groundwater Matrix Effects

Effective PFAS degradation in a UV-sulfite/iodide system depends on the exposure of PFAS to aqueous electrons. Therefore, discussion of groundwater matrix effects on PFAS degradation is largely centered around how these groundwater constituents interact with aqueous electrons and influence their availability for PFAS reduction. The electron scavenging capacities for selected groundwater constituents are presented below in Table 3.

Table 3: Electron Scavenging Capacities of Groundwater Components

Electron Scavenger (S)	$k_{S,e^-_{aq}}$ ($M^{-1}s^{-1}$)	Source
DOM	1.2×10^8	Fennell et al. (2023)
NO_3^-	1.0×10^{10}	Cui et al. (2020)
NO_2^-	3.5×10^9	Fennell et al. (2022)
HCO_3^-	$<1 \times 10^6$	Fennell et al. (2022)

However, the reduction of PFAS by e^-_{aq} can be influenced not only by their concentrations, but the electrostatic conditions that influence their interactions in solution. In water, most forms of PFAS will deprotonate and exist as their conjugate base – carrying a negative charge as an anion.[5] The influence of ionic strength is described by the Brønsted-Bjerrum equation,

$$\log\left(\frac{k_{2,I}}{k_{2,I=0}}\right) = 1.02 Z_A Z_B \frac{\sqrt{I}}{1+\sqrt{I}} \tag{27}$$

wherein $k_{2,I}$ represents the bimolecular rate constant at ionic strength I, $k_{2,I=0}$ represents the bimolecular rate constant at infinite dilution, and $Z_A Z_B$ is the product of the charges of reactants. Eq (27) states that the rate constant for two like-charged reactants increases with ionic strength. The increased ionic strength provides a shielding effect between the two like-charged reactants, PFAS and e^-_{aq}, increasing their reactivity by decreasing their repulsion. Because of this, increasing water hardness is expected to promote PFAS degradation.[33]

Although the constituents presented in Table 3 are anticipated to be problematic due to their propensity to engage in electron scavenging reactions, the reality is that these components undergo a series of complex reactions influenced by both environmental and systemic parameters. The following sections will discuss two selected components in depth, and attempt to explore their anticipated behavior and impact in a UV-sulfite/iodide system.

2.3.2.1 Dissolved Organic Matter (DOM)

Dissolved organic matter (DOM) is a naturally occurring complex heterogenous mixture of organic compounds. These compounds exhibit a high degree of reactivity with oxidizing radicals, and are well known for their interference in UV-AOP systems due to their affinity for key reactive species such as $^{\cdot}OH$ and $Cl^{\cdot}$.[76] However, their reactivity with aqueous electrons, and therefore their impact on contaminant degradation in UV-ARP, is currently less well understood. There are two primary mechanisms by which DOM may inhibit e^-_{aq} initiated PFAS degradation. The first is by preventing the generation of aqueous electrons by photosensitizers. The chromophores in DOM act like a barrier between photosensitizers and UV light, intercepting incoming UV radiation and interfering with aqueous electron

generation by competing with sulfite/iodide for photons.[77] The impact of UV absorption by DOM chromophores has been referred to in literature as a "screening" effect, and can be estimated based on absorbance measurements that differ depending on the specific isolate.

It is worth noting that this screening effect will change as UV-ARP treatment progresses due to structural modifications resulting from UV irradiation and aqueous electron exposure.[77] A 24 h UV-sulfite experiment run by Fennell et al. in the presence of 10 mg/L natural organic matter (NOM) reported that the fraction of light absorbed by sulfite increased from 38% at 0 h to nearly 100% after 4 h.[77] Additionally, the measured scavenging capacity ($k'_{S,t}$) at 4 h suggested no e^-_{aq} scavenging activity from NOM.[77] These results were interpreted to mean that the reaction between NOM and e^-_{aq} results in a product that does not act as an electron scavenger and is not chromophoric – due to the fact that the degradation inhibiting effects exhibited by DOM are attenuated after 4 hours.[77] Ren et al. reported similar results, demonstrating that the presence of 10 mg/L humic acid (HA) inhibited PFOA degradation in a UV-sulfite system during the first 2 h, but ultimately resulted in enhanced degradation and defluorination when compared with a control after 24 h.[78] The possibility of HA's positive effect on PFOA degradation has been previously proposed for UV-iodide systems. Guo et al. posited that low concentrations of HA could promote PFOA degradation by facilitating the regeneration of iodide. The aromatic rings in HA are thought to form a π-complex with I_2, which would then be reduced to I^- by electron-donating groups in HA.[79] This would not only accelerate the regeneration of iodide, but prevent I_2 from participating in electron scavenging reactions. Similarly, Sun et al. reported enhanced PFOS degradation by a UV-iodide system in the presence of 1.0 mg/L HA, proposing that HA could assist in PFOS degradation through the formation of I^--HA-PFOS adducts.[80] The large surface area and diverse aliphatic and aromatic moieties of HA allow for the formation of these adducts, and could enhance degradation by enabling the production of e^-_{aq} in close proximity to PFOS.[80] However, any positive effects associated with DOM are confined to low concentrations. Sun et al. reported decreasing defluorination with increasing concentrations of HA, as defluorination was reduced from 55.6% with 1.0 mg/L HA to 12.0% when the HA concentration was increased to 30.0 mg/L.[80] Ren et al. demonstrated similar effects on PFOA, as increasing concentrations of HA reduced defluorination from 93% in the presence of 10 mg/L HA, to 75% and 20% in the presence of 25 mg/L HA and 50 mg/L HA respectively. At 0 h, increasing concentrations of HA correspond with higher UV absorbance.[78] The measured UV absorbance at 10 mg/L HA was shown to decrease steadily over time to near 0 after 24 h.[78] In contrast, the decrease in UV absorbance at 25 and 50 mg/L HA was minimal, with a respective 53% and 16% reduction after 24 h.[78] As such, Ren et al. attributes the reduced PFOA degradation to the screening effect of HA at higher concentrations.[78]

The second mechanism by which DOM inhibits PFAS degradation is through its role as an electron scavenger. The various electron-withdrawing groups on DOM (such as –F, -Cl, -COOH, -CHO and etc) are reported to be highly reactive with aqueous electrons.[81] The reactivity of any particular DOM isolate with aqueous electrons can be expressed through its bimolecular rate constant ($k_{DOM,e^-_{aq}}$), which is recommended as 1.2 x 10^8 $M_C^{-1}s^{-1}$ based on an average of $k_{DOM,e^-_{aq}}$ measured from humic substance and NOM isolates.[77] This translates to an electron scavenging capacity of 1.0 x 10^5 s^{-1} at a [DOC] of 10 mg/L. Notably, Fennell et al.

reports that measured $k_{DOM,e^-_{aq}}$ were on average comparable to literature values of bimolecular rate constants between DOM and oxidizing radicals, and were exceeded only by $k_{DOM,HO^\cdot}$ and $k_{DOM,Cl^\cdot}$.[77] Understanding of the structure-reactivity relationships that govern DOM electron scavenging capacities is still underdeveloped, but Fennell et al. reports a strong positive correlation between $k_{DOM,e^-_{aq}}$ and % carbonyl carbon.[77] This is consistent with the high e^-_{aq} reactivity exhibited by other carbonyl compounds.[82] Overall, the impact of DOM in the UV-sulfite/iodide system is highly concentration dependent. Fennel et al. demonstrates that at low concentrations, DOM has the potential to be transformed by e^-_{aq} into more benign structures that do not exhibit the original UV absorption or electron scavenging effects.[77] At this point, DOM may even enhance PFAS degradation by facilitating the regeneration of photosensitizers. However, the DOM screening effect dominates at high concentrations, and PFAS degradation is significantly inhibited. DOM absolutely has the potential to exhibit long-lasting electron scavenging effects that influence PFAS degradation in UV-ARP.

2.3.2.2 Nitrate

Nitrate is a common component of groundwater, present as a natural constituent and as a result of anthropogenic activity. Without nutrient pollution, environmental concentrations of nitrate in groundwater are typically below 3 mg/L,[83] but contaminated groundwater can reach up to 70 mg/L.[84] The role of nitrate as an electron scavenger is widely recognized, and the presence of nitrate in UV-ARP is generally thought to inhibit PFAS degradation through nitrate's strong electron scavenging capacity.

$$e^-_{aq} + NO_3^- \rightarrow (NO_3)^{\cdot 2-} \qquad k = 1.0 \times 10^{10}\ M^{-1}s^{-1} \qquad (28)$$

This anticipated effect has been well documented in the literature. Ren et al. reported an increasing reduction in PFAS degradation with rising nitrate concentrations, investigating concentrations ranging from 62-775 mg/L.[78] At 10 mM sulfite and 62 mg/L nitrate, 89% defluorination and complete PFOA degradation was achieved after 24 h.[78] Although significant inhibition occurred within the first 2 h, PFOA degradation reached 99% by 4 h.[78] At 62 mg/L nitrate, the initial lag in degradation observed in the first 2 h can likely be attributed to nitrate's electron scavenging effects. Once nitrate was consumed, system performance appeared to rapidly recover. However, nitrate concentrations above 124 mg/L resulted in marked reductions in both degradation and defluorination.[78] This effect appeared to be overcome by increasing sulfite concentrations from 10 to 20 mM. This increase in initial sulfite concentration restored system performance despite high nitrate levels, resulting in 99% defluorination and complete degradation after 24 h.[78] These results suggest that the electron scavenging effects of nitrate may be offset by initial photosensitizer concentrations. O'Connor et al examined the effects of 0-3100 mg/L nitrate on the degradation of PFOS and 6:2 FTS in the RADIANT system, and found that the degradation of both compounds through a 20 mM sulfite treatment was inhibited when nitrate concentrations were greater than 62 mg/L.[66] However, it is reasonable to note that the range of concentrations at which the inhibiting effects of nitrate have been observed are often far above the concentrations

expected in the environment. The concentration of nitrate in eastern Ontario ranges from <0.027 to 50.9 mg/L, with a median value of <0.058 mg/L.[69]

Despite nitrate's noted inhibitory effects, Li et al. demonstrated the oxidative degradation of PFOA by nitrogen dioxide radicals $^{\cdot}NO_2$ generated through the photolysis of nitrate in a UV-nitrate system.[84] The initial reduction of nitrate by e^-_{aq} as described in eq (29-33) is followed by the formation of reactive nitrogen species (RNS),

$(NO_3)^{2\cdot-} + H_2O \rightarrow 2OH^- + {}^{\cdot}NO_2$	$k = 2.3 \times 10^5\ M^{-1}s^{-1}$	(29)
${}^{\cdot}NO_2 + e^-_{aq} \rightarrow NO_2^-$	$k = 4.1 \times 10^9\ M^{-1}s^{-1}$	(30)
$NO_2^- + e^-_{aq} \rightarrow (NO_3)^{2\cdot-}$	$k = 6 \times 10^9\ M^{-1}s^{-1}$	(31)
$(NO_3)^{2\cdot-} + H_3O^+ \leftrightarrow NO_2H^{\cdot-} + H_2O$	$pK_a = 3.3$	(32)
$(NO_3)^{2\cdot-} + H_2O \rightarrow {}^{\cdot}NO + 2OH^-$	$k = 9 \times 10^4\ M^{-1}s^{-1}$	(33)

which include the generation of oxidizing species such as the $(NO_3)^{2\cdot-}$, $^{\cdot}NO_2$, and $^{\cdot}NO$ radicals. Yuan et al. proposes that the use of nitrate in UV-sulfite systems creates a synergistic effect wherein e^-_{aq} initiated reductive defluorination is paired with RNS mediated electrophilic oxidation.[84] Enhanced defluorination was reported for nitrate concentrations ranging from 5-30 mg/L, with complete PFOA defluorination achieved at 20 mg/L.[84] An initial lag in defluorination was observed, consistent with the findings of previous studies, and was shown to increase with nitrate concentration – ranging from 10, 30, and 60 min for nitrate concentrations of 5, 20, and 30 mg/L respectively.[84] This lag time is attributed to the removal of nitrate via e^-_{aq} induced reduction, which is then followed by the oxidative defluorination of PFOA prompted by the generated RNS. The proposed mechanism involves electrophilic RNS attack of the H-rich moieties of FTCAs.[84] Acknowledging this, there is evidence that the presence of nitrate within a specific range of concentrations may be beneficial due to the generation of RNS. Further work is required to determine the boundaries in which this positive effect occurs.

2.4 References

(1) Naidu, R.; Nadebaum, P.; Fang, C.; Cousins, I.; Pennell, K.; Conder, J.; Newell, C. J.; Longpré, D.; Warner, S.; Crosbie, N. D.; Surapaneni, A.; Bekele, D.; Spiese, R.; Bradshaw, T.; Slee, D.; Liu, Y.; Qi, F.; Mallavarapu, M.; Duan, L.; McLeod, L.; Bowman, M.; Richmond, B.; Srivastava, P.; Chadalavada, S.; Umeh, A.; Biswas, B.; Barclay, A.; Simon, J.; Nathanail, P. Per- and Poly-Fluoroalkyl Substances (PFAS): Current Status and Research Needs. *Environmental Technology & Innovation* **2020**, *19*, 100915. https://doi.org/10.1016/j.eti.2020.100915.

(2) De Silva, A. O.; Armitage, J. M.; Bruton, T. A.; Dassuncao, C.; Heiger-Bernays, W.; Hu, X. C.; Kärrman, A.; Kelly, B.; Ng, C.; Robuck, A.; Sun, M.; Webster, T. F.; Sunderland, E. M. PFAS Exposure Pathways for Humans and Wildlife: A Synthesis of Current

Knowledge and Key Gaps in Understanding. *Environ Toxicol Chem* **2021**, *40* (3), 631–657. https://doi.org/10.1002/etc.4935.

(3) Buck, R. C.; Franklin, J.; Berger, U.; Conder, J. M.; Cousins, I. T.; de Voogt, P.; Jensen, A. A.; Kannan, K.; Mabury, S. A.; van Leeuwen, S. P. Perfluoroalkyl and Polyfluoroalkyl Substances in the Environment: Terminology, Classification, and Origins. *Integrated Environmental Assessment and Management* **2011**, *7* (4), 513–541. https://doi.org/10.1002/ieam.258.

(4) Bentel, M. J.; Yu, Y.; Xu, L.; Li, Z.; Wong, B. M.; Men, Y.; Liu, J. Defluorination of Per- and Polyfluoroalkyl Substances (PFASs) with Hydrated Electrons: Structural Dependence and Implications to PFAS Remediation and Management. *Environ. Sci. Technol.* **2019**, *53* (7), 3718–3728. https://doi.org/10.1021/acs.est.8b06648.

(5) McTaggart, M.; Malardier-Jugroot, C. The Role of Helicity in PFAS Resistance to Degradation: DFT Simulation of Electron Capture and Defluorination. October 16, 2023. https://doi.org/10.26434/chemrxiv-2023-lvj76.

(6) *CompTox Chemicals Dashboard*. https://comptox.epa.gov/dashboard/chemical-lists/PFASSTRUCTV5 (accessed 2025-04-15).

(7) Reinikainen, J.; Perkola, N.; Äystö, L.; Sorvari, J. The Occurrence, Distribution, and Risks of PFAS at AFFF-Impacted Sites in Finland. *Science of The Total Environment* **2022**, *829*, 154237. https://doi.org/10.1016/j.scitotenv.2022.154237.

(8) Glüge, J.; Scheringer, M.; Cousins, I. T.; DeWitt, J. C.; Goldenman, G.; Herzke, D.; Lohmann, R.; Ng, C. A.; Trier, X.; Wang, Z. An Overview of the Uses of Per- and Polyfluoroalkyl Substances (PFAS). *Environ. Sci.: Processes Impacts* **2020**, *22* (12), 2345–2373. https://doi.org/10.1039/D0EM00291G.

(9) Sajid, M.; Ilyas, M. PTFE-Coated Non-Stick Cookware and Toxicity Concerns: A Perspective. *Environ Sci Pollut Res* **2017**, *24* (30), 23436–23440. https://doi.org/10.1007/s11356-017-0095-y.

(10) Du, Z.; Deng, S.; Bei, Y.; Huang, Q.; Wang, B.; Huang, J.; Yu, G. Adsorption Behavior and Mechanism of Perfluorinated Compounds on Various Adsorbents—A Review. *Journal of Hazardous Materials* **2014**, *274*, 443–454. https://doi.org/10.1016/j.jhazmat.2014.04.038.

(11) Fang, S.; Sha, B.; Yin, H.; Bian, Y.; Yuan, B.; Cousins, I. T. Environment Occurrence of Perfluoroalkyl Acids and Associated Human Health Risks near a Major Fluorochemical Manufacturing Park in Southwest of China. *Journal of Hazardous Materials* **2020**, *396*, 122617. https://doi.org/10.1016/j.jhazmat.2020.122617.

(12) Wang, S.; Huang, J.; Yang, Y.; Hui, Y.; Ge, Y.; Larssen, T.; Yu, G.; Deng, S.; Wang, B.; Harman, C. First Report of a Chinese PFOS Alternative Overlooked for 30 Years: Its Toxicity, Persistence, and Presence in the Environment. *Environ. Sci. Technol.* **2013**, *47* (18), 10163–10170. https://doi.org/10.1021/es401525n.

(13) Rudzanová, B.; Thon, V.; Vespalcová, H.; Martyniuk, C. J.; Piler, P.; Zvonař, M.; Klánová, J.; Bláha, L.; Adamovsky, O. Altered Transcriptome Response in PBMCs of Czech Adults Linked to Multiple PFAS Exposure: B Cell Development as a Target of PFAS Immunotoxicity. *Environ. Sci. Technol.* **2024**, *58* (1), 90–98. https://doi.org/10.1021/acs.est.3c05109.

(14) Fenton, S. E.; Ducatman, A.; Boobis, A.; DeWitt, J. C.; Lau, C.; Ng, C.; Smith, J. S.; Roberts, S. M. Per- and Polyfluoroalkyl Substance Toxicity and Human Health Review: Current State of Knowledge and Strategies for Informing Future Research. *Environ Toxicol Chem* **2021**, *40* (3), 606–630. https://doi.org/10.1002/etc.4890.

(15) Khan, B.; Burgess, R. M.; Cantwell, M. G. Occurrence and Bioaccumulation Patterns of Per- and Polyfluoroalkyl Substances (PFAS) in the Marine Environment. *ACS EST Water* **2023**, *3* (5), 1243–1259. https://doi.org/10.1021/acsestwater.2c00296.
(16) Zheng, G.; Schreder, E.; Dempsey, J. C.; Uding, N.; Chu, V.; Andres, G.; Sathyanarayana, S.; Salamova, A. Per- and Polyfluoroalkyl Substances (PFAS) in Breast Milk: Concerning Trends for Current-Use PFAS. *Environ. Sci. Technol.* **2021**, *55* (11), 7510–7520. https://doi.org/10.1021/acs.est.0c06978.
(17) Calafat, A. M.; Wong, L.-Y.; Kuklenyik, Z.; Reidy, J. A.; Needham, L. L. Polyfluoroalkyl Chemicals in the U.S. Population: Data from the National Health and Nutrition Examination Survey (NHANES) 2003–2004 and Comparisons with NHANES 1999–2000. *Environ Health Perspect* **2007**, *115* (11), 1596–1602. https://doi.org/10.1289/ehp.10598.
(18) *Rapid Characterization of Human Serum Albumin Binding for Per- and Polyfluoroalkyl Substances Using Differential Scanning Fluorimetry - PMC*. https://pmc.ncbi.nlm.nih.gov/articles/PMC8651256/ (accessed 2024-12-23).
(19) Shi, Y.; Vestergren, R.; Zhou, Z.; Song, X.; Xu, L.; Liang, Y.; Cai, Y. Tissue Distribution and Whole Body Burden of the Chlorinated Polyfluoroalkyl Ether Sulfonic Acid F-53B in Crucian Carp (Carassius Carassius): Evidence for a Highly Bioaccumulative Contaminant of Emerging Concern. *Environ. Sci. Technol.* **2015**, *49* (24), 14156–14165. https://doi.org/10.1021/acs.est.5b04299.
(20) Qian, S.; Lu, H.; Xiong, T.; Zhi, Y.; Munoz, G.; Zhang, C.; Li, Z.; Liu, C.; Li, W.; Wang, X.; He, Q. Bioaccumulation of Per- and Polyfluoroalkyl Substances (PFAS) in Ferns: Effect of PFAS Molecular Structure and Plant Root Characteristics. *Environ. Sci. Technol.* **2023**, *57* (11), 4443–4453. https://doi.org/10.1021/acs.est.2c06883.
(21) *The Sustainable Management of Groundwater in Canada*; Council of Canadian Academies, Ed.; Council of Canadian Academies: Ottawa, 2009.
(22) Roy, J. W.; Weber, K. Per- and Polyfluoroalkyl Substances (PFASs) Contamination of Groundwater in Canada: A (Too) Short Review. *Canadian Water Resources Journal / Revue canadienne des ressources hydriques* **2025**, *50* (3), 236–249. https://doi.org/10.1080/07011784.2025.2519134.
(23) Zhi, Y.; Lu, X.; Munoz, G.; Yeung, L. W. Y.; De Silva, A. O.; Hao, S.; He, H.; Jia, Y.; Higgins, C. P.; Zhang, C. Environmental Occurrence and Biotic Concentrations of Ultrashort-Chain Perfluoroalkyl Acids: Overlooked Global Organofluorine Contaminants. *Environ. Sci. Technol.* **2024**, *58* (49), 21393–21410. https://doi.org/10.1021/acs.est.4c04453.
(24) Hu, X. C.; Andrews, D. Q.; Lindstrom, A. B.; Bruton, T. A.; Schaider, L. A.; Grandjean, P.; Lohmann, R.; Carignan, C. C.; Blum, A.; Balan, S. A.; Higgins, C. P.; Sunderland, E. M. Detection of Poly- and Perfluoroalkyl Substances (PFASs) in U.S. Drinking Water Linked to Industrial Sites, Military Fire Training Areas, and Wastewater Treatment Plants. *Environ. Sci. Technol. Lett.* **2016**, *3* (10), 344–350. https://doi.org/10.1021/acs.estlett.6b00260.
(25) Ghorbani Gorji, S.; Mackie, R.; Prasad, P.; Knight, E. R.; Qu, X.; Vardy, S.; Bowles, K.; Higgins, C. P.; Thomas, K. V.; Kaserzon, S. L. Occurrence of Ultrashort-Chain PFASs in Australian Environmental Water Samples. *Environ. Sci. Technol. Lett.* **2024**, *11* (12), 1362–1369. https://doi.org/10.1021/acs.estlett.4c00750.
(26) Barzen-Hanson, K. A.; Field, J. A. Discovery and Implications of C_2 and C_3 Perfluoroalkyl Sulfonates in Aqueous Film-Forming Foams and Groundwater.

Environ. Sci. Technol. Lett. **2015**, *2* (4), 95–99. https://doi.org/10.1021/acs.estlett.5b00049.
(27) Mejia-Avendaño, S.; Zhi, Y.; Yan, B.; Liu, J. Sorption of Polyfluoroalkyl Surfactants on Surface Soils: Effect of Molecular Structures, Soil Properties, and Solution Chemistry. *Environ. Sci. Technol.* **2020**, *54* (3), 1513–1521. https://doi.org/10.1021/acs.est.9b04989.
(28) Guo, B.; Zeng, J.; Brusseau, M. L. A Mathematical Model for the Release, Transport, and Retention of Per- and Polyfluoroalkyl Substances (PFAS) in the Vadose Zone. *Water Resour Res* **2020**, *56* (2), e2019WR026667. https://doi.org/10.1029/2019wr026667.
(29) Meegoda, J. N.; Bezerra De Souza, B.; Casarini, M. M.; Kewalramani, J. A. A Review of PFAS Destruction Technologies. *IJERPH* **2022**, *19* (24), 16397. https://doi.org/10.3390/ijerph192416397.
(30) Zhang, H.; Xu, H.; Qin, B.; Fu, Y.; Yao, Y.; Zhao, Y.; Qin, C. Review on the Sources, Distribution and Treatment of per- and Polyfluoroalkyl Substances in Global Groundwater. *Environ Res* **2025**, *275*, 121387. https://doi.org/10.1016/j.envres.2025.121387.
(31) McMahon, P. B.; Tokranov, A. K.; Bexfield, L. M.; Lindsey, B. D.; Johnson, T. D.; Lombard, M. A.; Watson, E. Perfluoroalkyl and Polyfluoroalkyl Substances in Groundwater Used as a Source of Drinking Water in the Eastern United States. *Environ. Sci. Technol.* **2022**, *56* (4), 2279–2288. https://doi.org/10.1021/acs.est.1c04795.
(32) Higgins, C. P.; Luthy, R. G. Sorption of Perfluorinated Surfactants on Sediments. *Environ. Sci. Technol.* **2006**, *40* (23), 7251–7256. https://doi.org/10.1021/es061000n.
(33) Lyu, X.; Liu, X.; Sun, Y.; Ji, R.; Gao, B.; Wu, J. Transport and Retention of Perfluorooctanoic Acid (PFOA) in Natural Soils: Importance of Soil Organic Matter and Mineral Contents, and Solution Ionic Strength. *Journal of Contaminant Hydrology* **2019**, *225*, 103477. https://doi.org/10.1016/j.jconhyd.2019.03.009.
(34) Kothawala, D. N.; Köhler, S. J.; Östlund, A.; Wiberg, K.; Ahrens, L. Influence of Dissolved Organic Matter Concentration and Composition on the Removal Efficiency of Perfluoroalkyl Substances (PFASs) during Drinking Water Treatment. *Water Research* **2017**, *121*, 320–328. https://doi.org/10.1016/j.watres.2017.05.047.
(35) Newell, C. J.; Adamson, D. T.; Kulkarni, P. R.; Nzeribe, B. N.; Stroo, H. Comparing PFAS to Other Groundwater Contaminants: Implications for Remediation. *Remediation Journal* **2020**, *30* (3), 7–26. https://doi.org/10.1002/rem.21645.
(36) Canada, H. *Objective for Canadian drinking water quality per- and polyfluoroalkyl substances*. https://www.canada.ca/en/health-canada/services/publications/healthy-living/objective-drinking-water-quality-per-polyfluoroalkyl-substances.html (accessed 2025-04-09).
(37) Rahman, M. F.; Peldszus, S.; Anderson, W. B. Behaviour and Fate of Perfluoroalkyl and Polyfluoroalkyl Substances (PFASs) in Drinking Water Treatment: A Review. *Water Research* **2014**, *50*, 318–340. https://doi.org/10.1016/j.watres.2013.10.045.
(38) Xiao, X.; Ulrich, B. A.; Chen, B.; Higgins, C. P. Sorption of Poly- and Perfluoroalkyl Substances (PFASs) Relevant to Aqueous Film-Forming Foam (AFFF)-Impacted Groundwater by Biochars and Activated Carbon. *Environ. Sci. Technol.* **2017**, *51* (11), 6342–6351. https://doi.org/10.1021/acs.est.7b00970.
(39) Boo, C.; Wang, Y.; Zucker, I.; Choo, Y.; Osuji, C. O.; Elimelech, M. High Performance Nanofiltration Membrane for Effective Removal of Perfluoroalkyl Substances at High Water Recovery. *Environ. Sci. Technol.* **2018**, *52* (13), 7279–7288. https://doi.org/10.1021/acs.est.8b01040.

(40) Merino, N.; Qu, Y.; Deeb, R. A.; Hawley, E. L.; Hoffmann, M. R.; Mahendra, S. Degradation and Removal Methods for Perfluoroalkyl and Polyfluoroalkyl Substances in Water. *Environmental Engineering Science* **2016**, *33* (9), 615–649. https://doi.org/10.1089/ees.2016.0233.
(41) Duchesne, A. L.; Brown, J. K.; Patch, D. J.; Major, D.; Weber, K. P.; Gerhard, J. I. Remediation of PFAS-Contaminated Soil and Granular Activated Carbon by Smoldering Combustion. *Environ. Sci. Technol.* **2020**, *54* (19), 12631–12640. https://doi.org/10.1021/acs.est.0c03058.
(42) Blotevogel, J.; Giraud, R. J.; Rappé, A. K. Incinerability of PFOA and HFPO-DA: Mechanisms, Kinetics, and Thermal Stability Ranking. *Chemical Engineering Journal* **2023**, *457*, 141235. https://doi.org/10.1016/j.cej.2022.141235.
(43) Wang, B.; Yao, Y.; Chen, H.; Chang, S.; Tian, Y.; Sun, H. Per- and Polyfluoroalkyl Substances and the Contribution of Unknown Precursors and Short-Chain (C2-C3) Perfluoroalkyl Carboxylic Acids at Solid Waste Disposal Facilities. *Sci Total Environ* **2020**, *705*, 135832. https://doi.org/10.1016/j.scitotenv.2019.135832.
(44) Singh Kalra, S.; Cranmer, B.; Dooley, G.; Hanson, A. J.; Maraviov, S.; Mohanty, S. K.; Blotevogel, J.; Mahendra, S. Sonolytic Destruction of Per- and Polyfluoroalkyl Substances in Groundwater, Aqueous Film-Forming Foams, and Investigation Derived Waste. *Chemical Engineering Journal* **2021**, *425*, 131778. https://doi.org/10.1016/j.cej.2021.131778.
(45) Singh, R. K.; Multari, N.; Nau-Hix, C.; Anderson, R. H.; Richardson, S. D.; Holsen, T. M.; Mededovic Thagard, S. Rapid Removal of Poly- and Perfluorinated Compounds from Investigation-Derived Waste (IDW) in a Pilot-Scale Plasma Reactor.
(46) Schaefer, C. E.; Choyke, S.; Ferguson, P. L.; Andaya, C.; Burant, A.; Maizel, A.; Strathmann, T. J.; Higgins, C. P. Electrochemical Transformations of Perfluoroalkyl Acid (PFAA) Precursors and PFAAs in Groundwater Impacted with Aqueous Film Forming Foams. *Environ. Sci. Technol.* **2018**, *52* (18), 10689–10697. https://doi.org/10.1021/acs.est.8b02726.
(47) Li, F.; Wei, Z.; He, K.; Blaney, L.; Cheng, X.; Xu, T.; Liu, W.; Zhao, D. A Concentrate-and-Destroy Technique for Degradation of Perfluorooctanoic Acid in Water Using a New Adsorptive Photocatalyst. *Water Research* **2020**, *185*, 116219. https://doi.org/10.1016/j.watres.2020.116219.
(48) Hao, S.; Choi, Y. J.; Deeb, R. A.; Strathmann, T. J.; Higgins, C. P. Application of Hydrothermal Alkaline Treatment for Destruction of Per- and Polyfluoroalkyl Substances in Contaminated Groundwater and Soil. *Environ. Sci. Technol.* **2022**, *56* (10), 6647–6657. https://doi.org/10.1021/acs.est.2c00654.
(49) Scheitlin, C. G.; Dasu, K.; Rosansky, S.; Dejarme, L. E.; Siriwardena, D.; Thorn, J.; Mullins, L.; Haggerty, I.; Shqau, K.; Stowe, J. Application of Supercritical Water Oxidation to Effectively Destroy Per- and Polyfluoroalkyl Substances in Aqueous Matrices. *ACS EST Water* **2023**, *3* (8), 2053–2062. https://doi.org/10.1021/acsestwater.2c00548.
(50) Hao, S.; Reardon, P. N.; Choi, Y. J.; Zhang, C.; Sanchez, J. M.; Higgins, C. P.; Strathmann, T. J. Hydrothermal Alkaline Treatment (HALT) of Foam Fractionation Concentrate Derived from PFAS-Contaminated Groundwater. *Environ. Sci. Technol.* **2023**, *57* (44), 17154–17165. https://doi.org/10.1021/acs.est.3c05140.
(51) *PFAS ANNIHILATOR® Destruction Technology | Battelle Product Solution*. Battelle. https://www.battelle.org/markets/environment/pfas-and-emerging-chemicals/pfas-

destruction-and-remediation/pfas-annihilator-destruction-technology (accessed 2026-07-31).
(52) Chiang, S.-Y. D.; Saba, M.; Leighton, M.; Ballenghien, D.; Hatler, D.; Gal, J.; Deshusses, M. A. Supercritical Water Oxidation for the Destruction of Spent Media Wastes Generated from PFAS Treatment. *Journal of Hazardous Materials* **2023**, *460*, 132264. https://doi.org/10.1016/j.jhazmat.2023.132264.
(53) Fennell, B. D.; Mezyk, S. P.; McKay, G. Critical Review of UV-Advanced Reduction Processes for the Treatment of Chemical Contaminants in Water. *ACS Environ. Au* **2022**, *2* (3), 178–205. https://doi.org/10.1021/acsenvironau.1c00042.
(54) Ersan, M. S.; Wang, B.; Wong, M. S.; Westerhoff, P. Advanced Oxidation Processes May Transform Unknown PFAS in Groundwater into Known Products. *Chemosphere* **2024**, *349*, 140865. https://doi.org/10.1016/j.chemosphere.2023.140865.
(55) Venkatesan, A. K.; Lee, C.-S.; Gobler, C. J. Hydroxyl-Radical Based Advanced Oxidation Processes Can Increase Perfluoroalkyl Substances beyond Drinking Water Standards: Results from a Pilot Study. *Science of The Total Environment* **2022**, *847*, 157577. https://doi.org/10.1016/j.scitotenv.2022.157577.
(56) Umar, M. Reductive and Oxidative UV Degradation of PFAS—Status, Needs and Future Perspectives. *Water* **2021**, *13* (22), 3185. https://doi.org/10.3390/w13223185.
(57) Hori, H.; Yamamoto, A.; Hayakawa, E.; Taniyasu, S.; Yamashita, N.; Kutsuna, S.; Kiatagawa, H.; Arakawa, R. Efficient Decomposition of Environmentally Persistent Perfluorocarboxylic Acids by Use of Persulfate as a Photochemical Oxidant. *Environ. Sci. Technol.* **2005**, *39* (7), 2383–2388. https://doi.org/10.1021/es0484754.
(58) Houtz, E. F.; Sedlak, D. L. Oxidative Conversion as a Means of Detecting Precursors to Perfluoroalkyl Acids in Urban Runoff. *Environ. Sci. Technol.* **2012**, *46* (17), 9342–9349. https://doi.org/10.1021/es302274g.
(59) Ahmadi, S. Hydrated Electrons and Cluster Science. *Journal of Molecular Structure* **2022**, *1250*, 131898. https://doi.org/10.1016/j.molstruc.2021.131898.
(60) Patch, D.; O'Connor, N.; Koch, I.; Cresswell, T.; Hughes, C.; Davies, J. B.; Scott, J.; O'Carroll, D.; Weber, K. Elucidating Degradation Mechanisms for a Range of Per- and Polyfluoroalkyl Substances (PFAS) via Controlled Irradiation Studies. *Science of The Total Environment* **2022**, *832*, 154941. https://doi.org/10.1016/j.scitotenv.2022.154941.
(61) O'Connor, N.; Patch, D.; Noble, D.; Scott, J.; Koch, I.; Mumford, K. G.; Weber, K. Forever No More: Complete Mineralization of per- and Polyfluoroalkyl Substances (PFAS) Using an Optimized UV/Sulfite/Iodide System. *Science of The Total Environment* **2023**, *888*, 164137. https://doi.org/10.1016/j.scitotenv.2023.164137.
(62) Park, H.; Vecitis, C. D.; Cheng, J.; Dalleska, N. F.; Mader, B. T.; Hoffmann, M. R. Reductive Degradation of Perfluoroalkyl Compounds with Aquated Electrons Generated from Iodide Photolysis at 254 Nm. *Photochem Photobiol Sci* **2011**, *10* (12), 1945–1953. https://doi.org/10.1039/c1pp05270e.
(63) Liu, Z.; Chen, Z.; Gao, J.; Yu, Y.; Men, Y.; Gu, C.; Liu, J. Accelerated Degradation of Perfluorosulfonates and Perfluorocarboxylates by UV/Sulfite + Iodide: Reaction Mechanisms and System Efficiencies. *Environ. Sci. Technol.* **2022**, *56* (6), 3699–3709. https://doi.org/10.1021/acs.est.1c07608.
(64) Jiang, Z.; Denisov, S.; Adjei, D.; Mostafavi, M.; Ma, J. Overlooked Activation Role of Sulfite in Accelerating Hydrated Electron Treatment of Perfluorosulfonates. *Environ. Sci. Technol.* **2024**, *58* (21), 9427–9435. https://doi.org/10.1021/acs.est.4c01444.

(65) Ateia, M.; Maroli, A.; Tharayil, N.; Karanfil, T. The Overlooked Short- and Ultrashort-Chain Poly- and Perfluorinated Substances: A Review. *Chemosphere* **2019**, *220*, 866–882. https://doi.org/10.1016/j.chemosphere.2018.12.186.
(66) O'Connor, N. M.; Biology, B. A Thesis Submitted to the Division of Graduate Studies of the Royal Military College of Canada.
(67) Tenorio, R.; Liu, J.; Xiao, X.; Maizel, A.; Higgins, C. P.; Schaefer, C. E.; Strathmann, T. J. Destruction of Per- and Polyfluoroalkyl Substances (PFASs) in Aqueous Film-Forming Foam (AFFF) with UV-Sulfite Photoreductive Treatment. *Environ. Sci. Technol.* **2020**, *54* (11), 6957–6967. https://doi.org/10.1021/acs.est.0c00961.
(68) Tikhomirov, V. V. *Hydrogeochemistry Fundamentals and Advances, Groundwater Composition and Chemistry*, Volume 1 edition.; Wiley-Scrivener: Hoboken, 2016.
(69) Colgrove, L. M. A Regional Chemical Characterization and Analysis of Groundwater in Eastern Ontario.
(70) Cloutier, V.; Lefebvre, R.; Therrien, R.; Savard, M. M. Multivariate Statistical Analysis of Geochemical Data as Indicative of the Hydrogeochemical Evolution of Groundwater in a Sedimentary Rock Aquifer System. *Journal of Hydrology* **2008**, *353* (3–4), 294–313. https://doi.org/10.1016/j.jhydrol.2008.02.015.
(71) Cloutier, V.; Lefebvre, R.; Savard, M. M.; Therrien, R. Desalination of a Sedimentary Rock Aquifer System Invaded by Pleistocene Champlain Sea Water and Processes Controlling Groundwater Geochemistry. *Environ Earth Sci* **2010**, *59* (5), 977–994. https://doi.org/10.1007/s12665-009-0091-8.
(72) Blanchette, D.; Lefebvre ,René; Nastev ,Miroslav; and Cloutier, V. Groundwater Quality, Geochemical Processes and Groundwater Evolution in the Chateauguay River Watershed, Quebec, Canada. *Canadian Water Resources Journal / Revue canadienne des ressources hydriques* **2010**, *35* (4), 503–526. https://doi.org/10.4296/cwrj3504503.
(73) Canada, H. *Guidelines for Canadian Drinking Water Quality: Operational Parameters*. https://www.canada.ca/en/health-canada/programs/guidelines-canadian-drinking-water-quality-operational-parameters.html (accessed 2025-04-15).
(74) Drever, J. I. *The Geochemistry of Natural Waters*, 2nd ed.; Prentice Hall: Englewood Cliffs, N.J, 1988.
(75) Cronin, S. J.; Manoharan ,V.; Hedley ,M. J.; and Loganathan, P. Fluoride: A Review of Its Fate, Bioavailability, and Risks of Fluorosis in Grazed-pasture Systems in New Zealand. *New Zealand Journal of Agricultural Research* **2000**, *43* (3), 295–321. https://doi.org/10.1080/00288233.2000.9513430.
(76) Gar Alalm, M.; Boffito, D. C. Mechanisms and Pathways of PFAS Degradation by Advanced Oxidation and Reduction Processes: A Critical Review. *Chemical Engineering Journal* **2022**, *450*, 138352. https://doi.org/10.1016/j.cej.2022.138352.
(77) Fennell, B. D.; Fowler, D.; Mezyk, S. P.; McKay, G. Reactivity of Dissolved Organic Matter with the Hydrated Electron: Implications for Treatment of Chemical Contaminants in Water with Advanced Reduction Processes. *Environ. Sci. Technol.* **2023**, *57* (19), 7634–7643. https://doi.org/10.1021/acs.est.3c00909.
(78) Ren, Z.; Bergmann, U.; Leiviskä, T. Reductive Degradation of Perfluorooctanoic Acid in Complex Water Matrices by Using the UV/Sulfite Process. *Water Research* **2021**, *205*, 117676. https://doi.org/10.1016/j.watres.2021.117676.
(79) Guo, C.; Zhang, C.; Sun, Z.; Zhao, X.; Zhou, Q.; Hoffmann, M. R. Synergistic Impact of Humic Acid on the Photo-Reductive Decomposition of Perfluorooctanoic Acid. *Chemical Engineering Journal* **2019**, *360*, 1101–1110. https://doi.org/10.1016/j.cej.2018.10.204.

(80) Sun, Z.; Zhang, C.; Chen, P.; Zhou, Q.; Hoffmann, M. R. Impact of Humic Acid on the Photoreductive Degradation of Perfluorooctane Sulfonate (PFOS) by UV/Iodide Process. *Water Research* **2017**, *127*, 50–58. https://doi.org/10.1016/j.watres.2017.10.010.
(81) Li, C.; Zheng, S.; Li, T.; Chen, J.; Zhou, J.; Su, L.; Zhang, Y.-N.; Crittenden, J. C.; Zhu, S.; Zhao, Y. Quantitative Structure-Activity Relationship Models for Predicting Reaction Rate Constants of Organic Contaminants with Hydrated Electrons and Their Mechanistic Pathways. *Water Res* **2019**, *151*, 468–477. https://doi.org/10.1016/j.watres.2018.12.010.
(82) Buxton, G. V.; Greenstock, C. L.; Helman, W. P.; Ross, A. B. Critical Review of Rate Constants for Reactions of Hydrated Electrons, Hydrogen Atoms and Hydroxyl Radicals (·OH/·O− in Aqueous Solution. *Journal of Physical and Chemical Reference Data* **1988**, *17* (2), 513–886. https://doi.org/10.1063/1.555805.
(83) Cui, J.; Gao, P.; Deng, Y. Destruction of Per- and Polyfluoroalkyl Substances (PFAS) with Advanced Reduction Processes (ARPs): A Critical Review. *Environ Sci Technol* **2020**, *54* (7), 3752–3766. https://doi.org/10.1021/acs.est.9b05565.
(84) Yuan, Y.; Feng, L.; He, X.; Wu, M.; Ai, Z.; Zhang, L.; Gong, J. Nitrate Promoted Defluorination of Perfluorooctanoic Acid in UV/Sulfite System: Coupling Hydrated Electron/Reactive Nitrogen Species-Mediated Reduction and Oxidation. *Environmental Pollution* **2022**, *313*, 120172. https://doi.org/10.1016/j.envpol.2022.120172.

3. Reactive Activation of Iodide and Sulfite through UV-Natured Treatment (RADIANT) System for the Destruction of Per- and Polyfluoroalkyl Substances in Complex Aqueous Matrices

3.1 Abstract

The Reactive Activation of Iodide and Sulfite through UV-Natured Treatment (RADIANT) is a UV advanced reductive process that has been demonstrated to be capable of degrading the highly recalcitrant class of per- and polyfluoroalkyl substances (PFAS). Application of RADIANT in deionized (DI) water resulted in >99% degradation of TFA, PFPeA, and PFOS following a two-hour treatment. To assess the feasibility of RADIANT in the treatment of complex matrices such as groundwater, the individual and combined effects of humic acid and nitrate on PFOS degradation in the RADIANT system were studied in deionized (DI) water and groundwater. Humic acid was found to be a strong inhibitor of PFOS degradation, but groundwater conditions appeared to mitigate the inhibitory effects of humic acid observed in DI water. Greater than 99% degradation of PFOS was achieved in groundwater of varying complexities, and 95% degradation of ultra-short chain PFPrS was observed in DI water after an 8-hour treatment period.

3.2 Introduction

Per- and polyfluoroalkyl substances (PFAS) are a class of anthropogenic organofluorine chemicals widely used for their unique properties, which include oleophobicity, hydrophobicity, and high physicochemical stability. This exceptional stability is often attributed to the high electronegativity of the fluorine atom, which results in the high bond dissociation energy of the C-F bond and the formation of an electron-dense shell surrounding the helical carbon chain.[1] Widespread use of PFAS across a variety of commercial, industrial, and military applications has resulted in their near ubiquity in the environment.[2] This has become a point of significant concern in light of the growing body of evidence linking the class as a whole to a variety of adverse human health effects.[3–5]

PFAS contamination in groundwater is especially concerning as a direct line of exposure for communities who rely on groundwater as a primary source of drinking water. In 2024, the maximum level of PFAS in drinking water was set at 30 ng/L by Health Canada, with recommendations that concentrations be as low as reasonable achievable (ALARA).[6] Filtration and sorption based technologies such as granular activated carbon (GAC),[7,8] ion exchange (IX) resins,[9] and nanofiltration (NF)[10] are capable of removing up to 100% of PFAS in aqueous matrices. While effective, these treatment methods produce a contaminated waste stream that requires further treatment. As such, there are strong incentives to develop destructive treatment methods capable of fully mineralizing PFAS in aqueous matrices. Supercritical water oxidation (SCWO) and hydrothermal alkaline treatment (HALT) have emerged as two particularly well-developed treatment methods, capable of degrading 80.9%[11] and >90%[12] of total PFAS respectively. However, SCWO and HALT utilize extreme operating

conditions that are inherently energy intensive and costly, posing challenges to the adaptability of these systems at different scales.[13] The high temperature, pressure, and pH of these systems during operation also lead to corrosion and salt plugging, requiring consistent upkeep and careful selection of materials. Alternatively, PFAS destruction through advanced reductive processes (ARP) has been reported to be especially promising. ARP systems utilize the strong reducing potential of aqueous electrons to initiate the destruction of PFAS. These aqueous electrons may be generated through a variety of means, including the use of plasma,[14] electrodes,[15] and photochemical interactions with electron donors.[16–23] The aforementioned ultraviolet advanced reductive processes (UV-ARP) vary in their selection of electron donors, which are commonly referred to as photosensitizers. The combination of sulfite and iodide as photosensitizers in a UV-ARP system was shown to be highly effective by O'Connor et al, who demonstrated >99.9% degradation and full defluorination of the highly recalcitrant PFBS.[21]

The work communicated by O'Connor et al. (2023) forms the foundation of the Reactive Activation of Sulfite and Iodide through UV-Natured Treatment (RADIANT) system that this study reports on.[21] While there is evidence that the RADIANT system is effective under laboratory conditions, it has been reported that more complex matrices introduce additional challenges by way of competing reactions and/or issues with transmission.[23,24] Previous work by O'Connor examined the inhibitory effects of butyl carbitol, methanol, isopropanol, and nitrate on RADIANT system performance.[25] These potential interferents were selected due to their role as electron scavengers, but are specific to legacy and modern AFFF formulations.

The present study seeks to assess the feasibility of applying the RADIANT system to a real-life matrix such as groundwater. In order to do this, the effect of common groundwater components was investigated. Humic acid, as a DOM simulant, and nitrate were selected due to their prevalence in groundwater and their high propensity to react with aqueous electrons.[16,26] In addition, while RADIANT has been applied successfully to several specific PFAS, there has been little attention to the more challenging short and ultra-short chain homologues despite their detection in waters worldwide.[27] Overall, this study seeks to investigate the effect of complex matrices on the RADIANT system with consideration of how these findings translate to short and ultra-short chain PFAS.

3.3 Materials and Methods

3.3.1 Chemicals and Reagents

All PFAS analytical standards and chemicals were purchased from the sources listed in section A.2 of Appendix A. Details of all other chemical reagents and their sources are provided in Table A6.

3.3.2 Experimental Setup and Procedures

Reagents were combined in the quantities listed in Table A7 to make 15 mL of treatment solution. To simulate a complex matrix such as contaminated groundwater, 30 mL of

deionized (DI) water or clean groundwater was prepared with varying levels of interferents (humic acid, nitrate) and spiked with PFAS (individual compounds separately). The treatment solution was then combined with the prepared matrix to create an initial PFAS concentration of approximately 3 mg/L of a single PFAS compound prior to treatment. 1 mL of the untreated solution was pipetted into 27 BRAND cuvettes (purchased from Sigma Aldrich), and placed into a rotating rack during treatment with a 36 W lamp, purchased from Coospider. Three cuvettes were removed from the treatment rack at each time point. Following removal from the treatment rack, the reaction was quenched with 9 µL of glacial acetic acid. Details including reagent concentrations and treatment times for each trial are listed in Table A7.

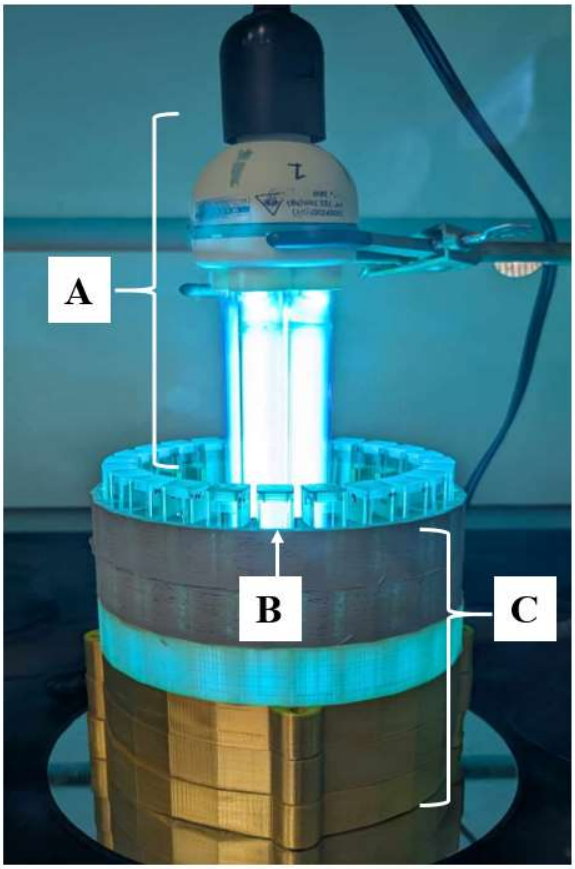

Figure 1. RADIANT cuvette set-up, featuring (A) UV lamp (36 W, 254 nm), (B) cuvette (1 mL), and (C) rotating treatment rack.

The clean groundwater was sampled directly (bypassing any treatment systems) from a domestic drinking water well in Ontario, from an unimpacted residential site. The collected clean groundwater was analyzed for total metals and general chemistry by the Analytical Services Unit (ASU) at Queens University. Collected groundwater was measured to contain 2.3 mg/L dissolved organic carbon (DOC), with a pH of 7.0 and hardness of 199 mg/L. Nitrate was found to be < 0.20 mg/L. Other basic water quality parameters of the clean groundwater can be found in Table A8.

Synthetic AOAC hard water was prepared using the protocol outlined by the U.S. EPA (SOP No. MB-30-02). Two synthetic hard water solutions were prepared at 160 mg/L and 1300 mg/L, using the materials listed in Table A7. When combined with reagents, the pH of the PFAS-spiked synthetic hard water solutions was found to be comparable to other treatment solutions. Addition of 150 mM hydroxide and 10 mM bicarbonate buffer resulted in an approximate pH of 13, consistent across all matrices.

3.3.3 Analytical Methods

Target PFAS analysis was performed using the Agilent Triple Quadrupole LC/MS using methods adapted from U.S. EPA Method 1633a. Analytical information is tabulated and presented in section A.2 of Appendix A. To prepare samples for PFAS analysis, samples were diluted with a mixture of methanol and DI water combined in a 1:1 ratio. Dilution factors were varied across time points to accommodate for changing expected PFAS concentrations. PFAS concentrations are reported as a percentage of the initial PFAS concentration measured at 0 h.

For fluoride analysis, 850 µL of solution was sampled from each cuvette and combined with total ionic strength adjustment buffer (TISAB) in a 1:1 ratio. The pH of the resulting solution was adjusted to approximately 5.5 pH with 10 µL of glacial acetic acid. Measurement of free fluoride ions was then performed with the ThermoFisher Orion Fluoride Ion Selective Electrode (FISE) probe, using a six-point matrix matched calibration curve ($R^2 > 0.99$). Fluoride recovery was calculated by expressing the measured free fluoride concentrations in treated samples as a percentage of the total fluorine contained in parent PFAS compounds.

3.4 Results and Discussion

3.4.1 PFAS Destruction in Deionized (DI) Water

Two treatment conditions were investigated throughout this study. A series of experiments performed in DI water investigated the degradation of selected PFAS (PFOS, PFPrS, PFPeA, and TFA) in the presence of high (50 mM) and low (10 mM) sulfite concentrations, with remaining reagent concentrations held constant (10 mM iodide, 10 mM bicarbonate, 150 mM sodium hydroxide). Figure 2 shows the change in PFAS concentration and fluoride recovery throughout the course of treatment.

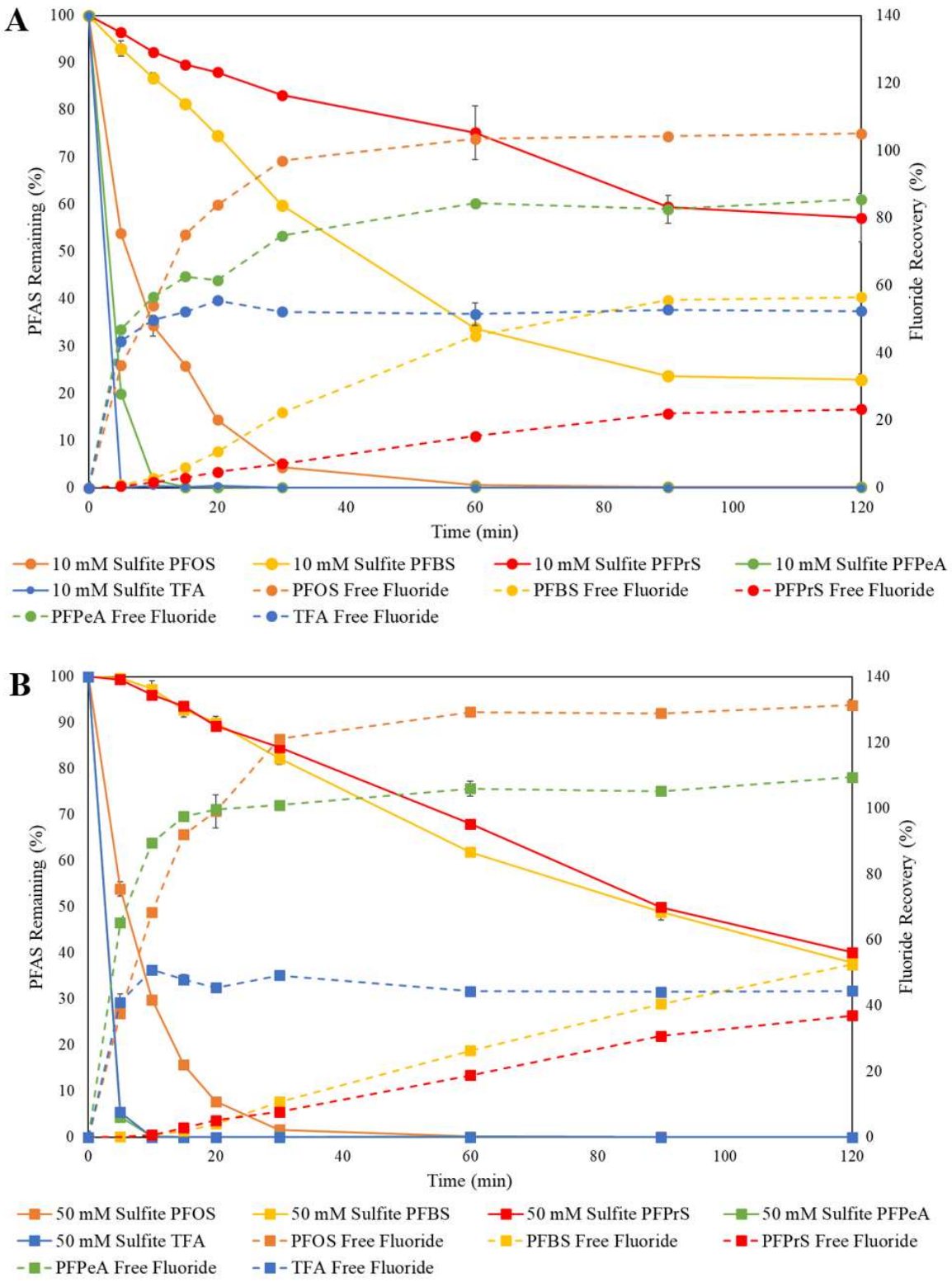

Figure 2. Degradation of (A) PFOS, PFBS, PFPrS, PFPeA, and TFA in DI water with 10 mM sulfite, (B) PFOS, PFBS, PFPrS, PFPeA, and TFA in DI water with 50 mM sulfite. Error bars are the standard deviation of triplicates and may be obscured by markers. Remaining reagent concentrations are held constant (10 mM iodide, 10 mM bicarbonate, 150 mM hydroxide).

Degradation of a range of PFAS compounds by the RADIANT system was investigated. Panels (A) and (B) in Figure 2 demonstrate the disappearance of PFAS compounds and generation of fluoride ions over time, where PFAS compounds were selected for different chain length (C3, C4, C5, and C8) and functional groups (sulfonates, PFSAs, and carboxylates, PFCAs). The degradation of PFOS is shown to be much slower than the degradation of PFCAs, with PFOS concentrations reaching 12 μg/L after two hours with 10 mM sulfite and 0.18 μg/L with 50 mM sulfite. PFSAs are reported in the literature to be more recalcitrant in comparison to their PFCA counterparts, a difference widely attributed to the protective nature of the sulfonate head group.[28] Chain length is generally reported to be inversely proportional to PFSA degradation, and this was found to be true for the PFSAs investigated in this study. PFBS was found to be more recalcitrant than PFOS, achieving 62% and 77% degradation for the 10 and 50 mM sulfite treatments respectively, in contrast to the >99% degradation of PFOS seen in both treatment conditions. PFPrS, an ultra-short chain sulfonic acid, is notably shown to be the most resistant to degradation. Two hours of treatment with 10 mM sulfite resulted in 1500 μg/L PFPrS remaining, and the 50 mM sulfite treatment was shown to yield only slightly better results, with 1000 μg/L PFPrS remaining. Final degradation efficiencies for PFPrS were 43% and 60% for the 10 and 50 mM sulfite treatments respectively, indicating the requirement for an adapted treatment protocol to address the short and ultra-short chain PFSAs.

While shorter chain lengths were found to correspond with higher recalcitrance in PFSAs, short chain PFCAs were not shown to be significantly more recalcitrant than long chain PFCAs in the RADIANT system. O'Connor et al. reported degradation of PFOA to non-detect levels by the 15-minute mark of a 10 mM sulfite treatment in the RADIANT system.[21] The short and ultra-short chain PFCAs investigated in this study, PFPeA and TFA, were shown to degrade rapidly within the first 10 minutes. TFA concentrations were below the limit of detection (0.05 μg/L) after 10 minutes across both treatment conditions, while PFPeA final concentrations were 1.3 and 0.36 μg/L for the 10 mM and 50 mM sulfite treatment conditions respectively. However, the low fluoride recovery from TFA trials suggests that although degradation of the parent compound was achieved, full defluorination may require additional or modified treatment. Greater than 100% fluoride recovery was observed for PFOS and PFPeA following a 50 mM sulfite treatment, and for PFOS following the 10 mM sulfite treatment. This excess fluoride recovery may be attributed to the presence of impurities within PFAS stock solutions, as target PFAS analysis of PFOS stock solutions revealed the presence of PFHxS and PFHpS in concentrations ranging from 60-100 μg/L. Trace amounts of various sulfonic acids were also detected. Concentrations of PFHxS and PFHpS were shown to decrease alongside PFOS concentrations throughout treatment, indicating that these additional PFAS compounds may be contributing to the generation of fluoride. The presence of other PFAS compounds, some of which may not be detected, provides a possible source of additional fluoride which may result in greater than 100% fluoride recovery.

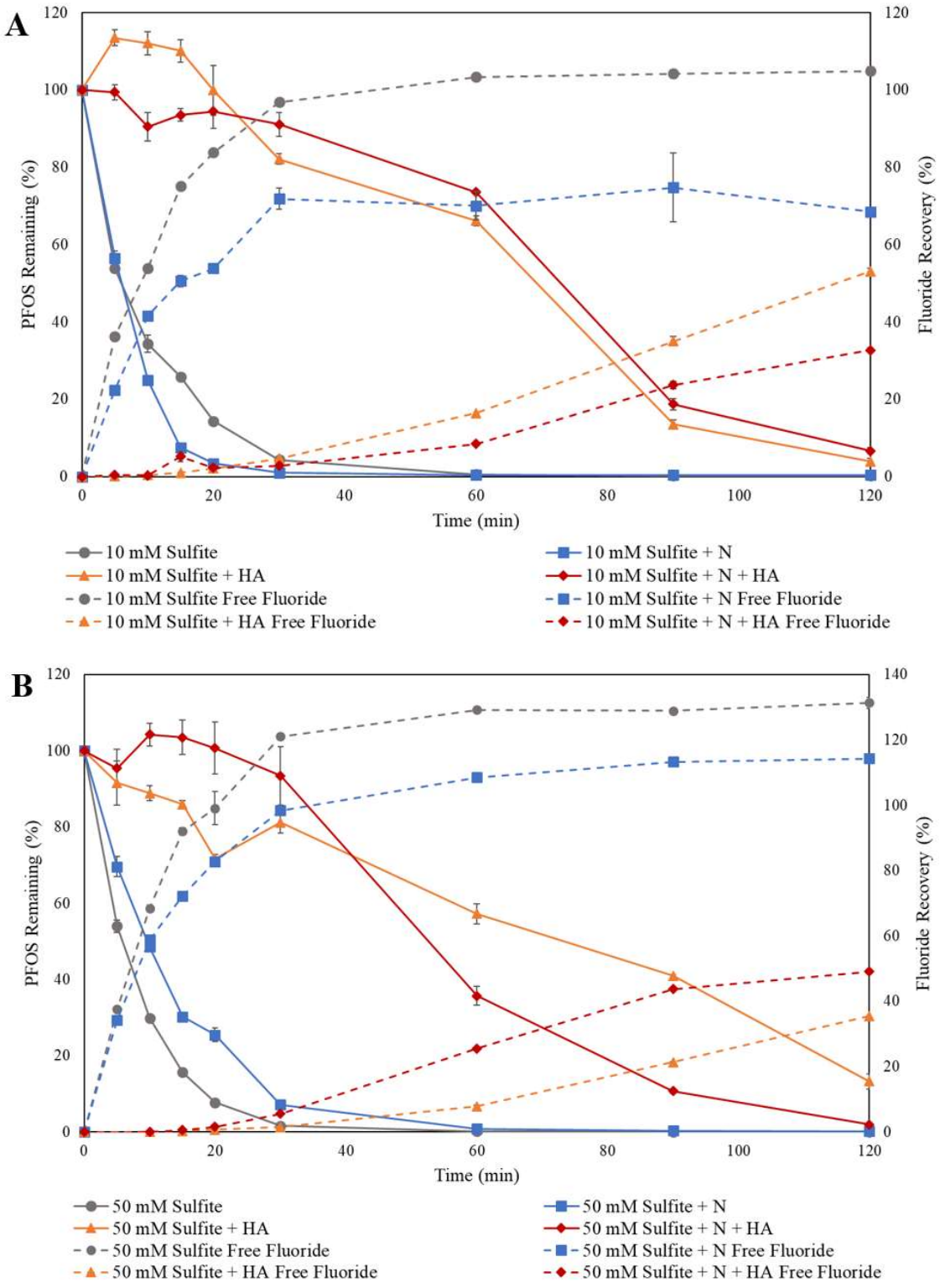

Figure 3. PFOS degradation in DI water with nitrate (N) and humic acid (HA), treated with (A) 10 mM sulfite, and (B) 50 mM sulfite. Interfering parameter concentrations are 10 mg/L nitrate (blue), 20 mg/L HA (orange), and the two combined (red). Error bars are the standard deviation of triplicates and may be hidden by markers. Remaining reagent concentrations are held constant (10 mM iodide, 10 mM bicarbonate, 150 mM hydroxide).

Humic acid and nitrate were identified as two common groundwater components that posed a high potential for interference within the RADIANT system. To investigate their effects, PFOS was selected as a probe compound. Their effect on the degradation of PFOS throughout the course of a two-hour treatment was observed, and is represented in Figure 3. Nitrate was initially identified as a potential interferent due to its strong capacity to scavenge aqueous electrons. However, the results presented in Figure 3 show that the presence of nitrate did not seem to be a strong inhibitor of PFOS degradation for both treatment conditions. The degradation of PFOS without the presence of any interferents is represented in grey in Figure 3, and can be used as a point of comparison. The 10 mM sulfite nitrate spiked trial achieved a final concentration lower than that of the uninhibited trial, reaching 6.4 μg/L in comparison to the 12 μg/L remaining when the 10 mM sulfite treatment was conducted without interferents. This may be attributed to the production of reactive nitrogen species (RNS) that are generated following the photolysis or reduction of nitrate in the RADIANT system. The resulting oxidizing species, such as the $(NO_3)^{2\cdot-}$, $^{\cdot}NO_2$, and $^{\cdot}NO$ radicals, are theorized to participate in the degradation of PFAS through the oxidation of PFAS transformation products following the initial aqueous electron initiated reductive defluorination.[22] The potential positive effects of nitrate in the RADIANT system are suggested by the 10 mM trials, but experiments conducted with the 50 mM sulfite treatment condition showed that the presence of nitrate resulted in moderate inhibition of PFOS degradation. The experiment conducted at 50 mM sulfite without the presence of any interferents resulted in a final concentration of 0.17 μg/L PFOS, while the nitrate-spiked 50 mM trial resulted in a final concentration of 3.72 μg/L PFOS. Overall, >99% degradation of PFOS was achieved across both treatment conditions even in the presence of nitrate.

In contrast, humic acid was shown to be a stronger inhibitor of PFOS degradation. Degradation of PFOS was decreased from >99% to 86% when humic acid was present. Humic acid is used in this study to simulate dissolved organic matter (DOM), which is known to exhibit a high degree of reactivity with aqueous electrons due to their inclusion of various electron-withdrawing groups. In addition, these organic compounds may include chromophores that are thought to compete with sulfite and iodide for photons, thereby inhibiting the RADIANT system's capacity to generate aqueous electrons. The presence of humic acid is shown in Figure 3 to have a visible effect on the progression of treatment. When humic acid is not present, a significant reduction in PFOS concentration is observed within the first five minutes of treatment. Experiments performed with a humic acid spike show a "lag" in treatment, wherein the concentration of PFOS remains high for the first 20 minutes of treatment before slowly starting to decrease after the 30-minute mark. The aforementioned "lag" is used to describe the period of time between the start of treatment and the beginning of degradation. The photodegradation of humic acid may occur during this initial lag time, and suggests that PFOS degradation is minimal until humic acid concentrations have been sufficiently reduced. Fluoride recovery was also significantly inhibited by the presence of humic acid, and may be attributed to the high degree of reactivity between humic acid and the oxidizing radicals that are thought to participate in the full degradation of PFOS.

Although increasing initial concentrations of sulfite should theoretically increase the generation of aqueous electrons, sulfite's ability to act as an electron scavenger in itself has

been reported to become prominent at concentrations greater than 10 mM.[16] As such, previous work has reported that increasing sulfite concentrations does not necessarily lead to proportional improvements in PFAS degradation.[29] Despite this, the results depicted in Figure 2 show that the 50 mM sulfite treatment achieved lower final concentrations when treatment was performed in DI water without the presence of potential interferents. However, this improved performance was not observed as the complexity of the matrix was increased by the presence of nitrate and humic acid, as depicted in Figure 3. This is particularly evident in the humic acid trials, where 130 µg/L PFOS remained after the 50 mM sulfite treatment in comparison to the 30 µg/L remaining after the 10 mM trial. Altogether, the results depicted in Figure 2 demonstrate that the susceptibility of specific PFAS to degradation is highly influenced by individual characteristics such as chain length and functional groups. Chain length was found to be an especially important indicator of recalcitrance for PFSAs. Ultra-short chain PFPrS (the PFSA with the shortest chain length included in the present study) was found to be the most recalcitrant form of PFAS investigated in this study, showing greater resistance to degradation than the highly challenging PFBS. Figure 3 highlights the inhibitory effect of humic acid on PFOS degradation, and suggests that these inhibitory effects cannot be overcome by simply increasing the concentration of sulfite. Alternatively, the RADIANT system may benefit from integration into a treatment train approach, with pre-treatment steps that could serve to remove organics and other inhibitory co-contaminants.

3.4.2 PFAS Destruction in Groundwater

Despite the inhibitory effects discussed in the previous section, there is evidence that UV-S/I systems such as RADIANT are capable of degrading PFAS in more complex matrices. However, O'Connor's work showed that the introduction of AFFF components, such as butyl carbitol, has been shown to inhibit the degradation of PFOS and 6:2 FTS.[25] To further increase the complexity of the matrix, a series of experiments was conducted assessing the individual and combined effects of nitrate and humic acid on the degradation of PFOS in groundwater. The groundwater used in this study was sampled from an unimpacted residential site, and spiked with PFOS and varying conditions of interferents.

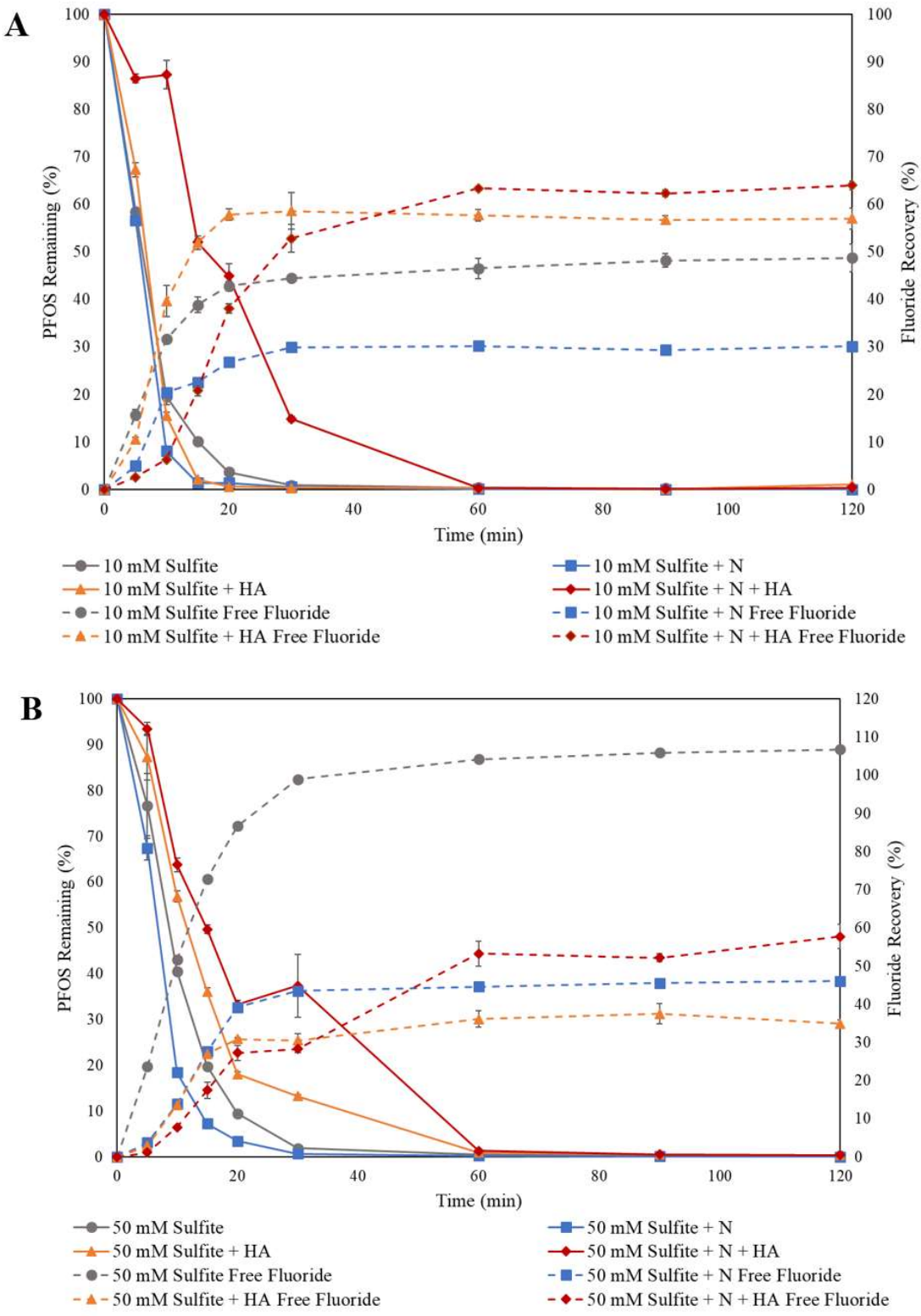

Figure 4. Degradation of PFOS in groundwater with (A) 10 mM sulfite, in the presence of nitrate (N) (10 mg/L) and humic acid (HA) (20 mg/L), (B) 50 mM sulfite, in the presence of nitrate (N) (10 mg/L) and humic acid (HA) (20 mg/L). Remaining reagent concentrations are held constant (10 mM iodide, 10 mM bicarbonate, 150 mM hydroxide). Error bars are the standard deviation of triplicates.

Humic acid and nitrate trials conducted in groundwater showed the same general trends as the DI water trials discussed in the previous section, in that humic acid was found to be a stronger inhibitor than nitrate. However, Figure 4 shows that the inhibitory effects of both humic acid and nitrate appear to be far less pronounced when experiments were conducted in groundwater. This is particularly apparent in the humic acid trials, which, when performed in DI water, resulted in 96% and 86% degradation of PFOS for the 10 and 50 mM sulfite treatment conditions respectively. Humic acid trials conducted in groundwater achieved 99% degradation for both treatment conditions, and the lag in degradation observed in the DI water humic acid trials was not present in groundwater. This may be attributed to the hardness of the groundwater. Because humic acid tends to have a net negative charge in groundwater, it may be neutralized by nonspecific binding of cations such as Na^+, K^+, Ca^{2+}, and Mg^{2+}. The presence of cations in groundwater may result in competition for binding sites on humic acid, mitigating its electron scavenging effects and reactivity with other radical species. Overall, >99% degradation of PFOS was achieved across all experiments conducted in groundwater, and final concentrations were altogether lower in groundwater than in DI water. Despite the enhanced PFOS degradation observed in groundwater, fluoride recoveries were measured to be much lower than the recoveries seen in DI water trials. This is theorized to be due to the cations (Mg^{2+}, Ca^{2+}) present in hard water, which may lead to the formation of precipitates such as MgF_2 and CaF_2.

In addition to the potential mitigation of humic acid by hardness cations, the increased ionic strength of groundwater may also assist in directly promoting the interaction between aqueous electron and PFAS. Higher ionic strength is theorized to minimize the repulsion between aqueous electrons and anionic PFAS, thereby promoting PFAS degradation.[16,30] To investigate the effect of water hardness within the RADIANT system, synthetic hard water was prepared according to AOAC protocol. Two levels of water hardness were investigated, 160 and 1300 mg/L, and PFBS was treated using an adapted protocol developed by O'Connor et al.[25]

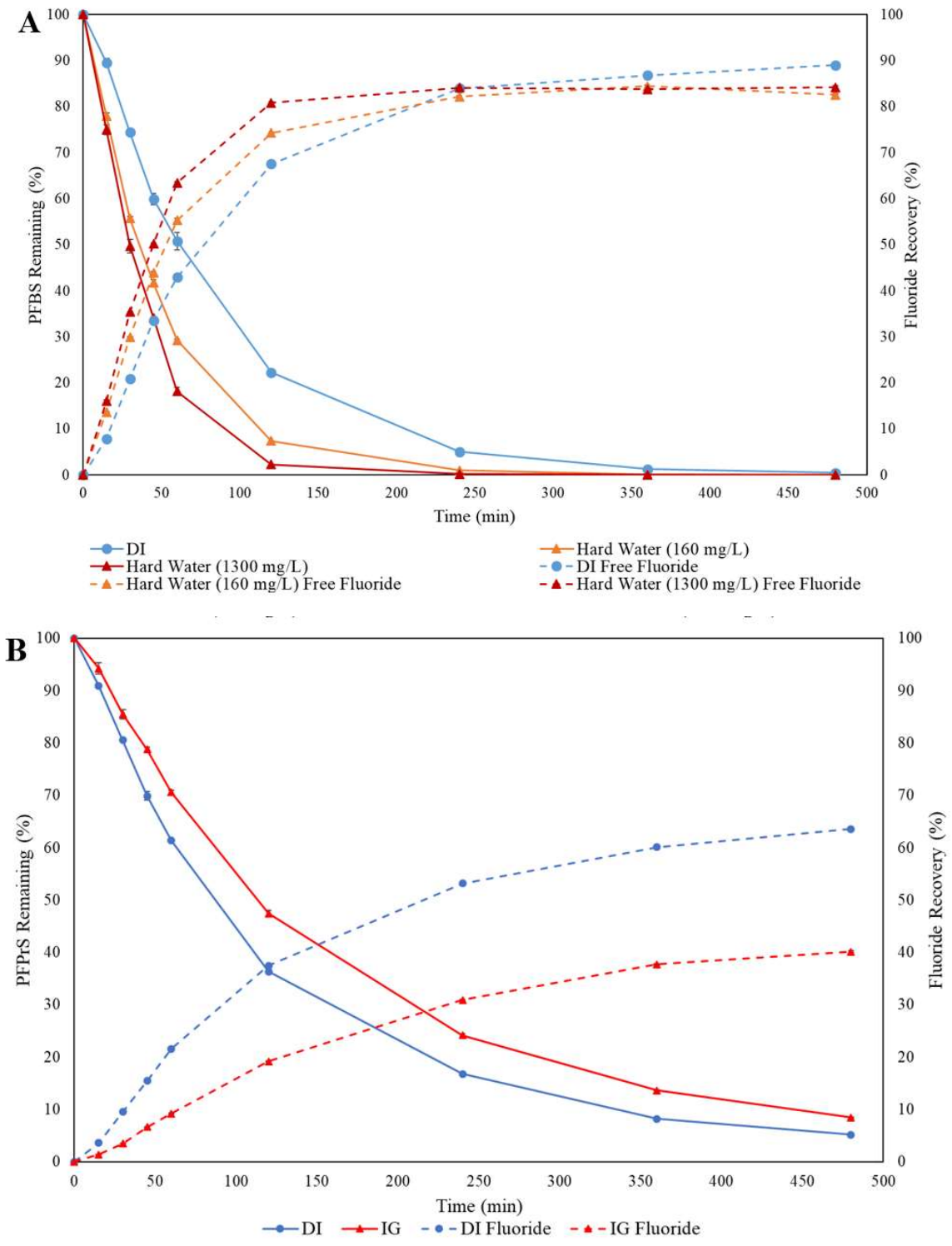

Figure 5. Application of intermittent sulfite addition protocol (20 mM sulfite, with 10 mM sulfite additions every two hours) for the degradation of (A) PFBS in DI water (blue) and synthetic hard water prepared at varying levels of hardness (160 mg/L in orange, 1300 mg/L in red), (B) PFPrS in DI water (blue) and groundwater (red). Remaining reagent concentrations are held constant (10 mM iodide, 10 mM bicarbonate, 150 mM hydroxide). Error bars are the standard deviation of triplicates and may be obscured by markers.

The adapted 8-hour treatment was performed with 20 mM sulfite and amended with 10 mM sulfite additions every two hours. The intermittent addition of sulfite is thought to provide the RADIANT system with the capacity to regenerate iodide,[21] and the results from this treatment are demonstrated in of Figure 5, achieving >99% degradation of PFBS. PFBS degradation was shown to follow a pseudo-first order reaction for the entire 8-hour treatment period in DI water. In synthetic hard water, PFBS degradation was found to follow a pseudo-first order reaction for the first 6 hours in the 160 mg/L synthetic hard water, and 2 hours in the 1300 mg/L. The pseudo-first order rate of reaction was found to be 1.2×10^{-2} min^{-1} in DI water. Rate of reaction was shown to increase to 1.9×10^{-2} min^{-1} and 3.2×10^{-2} min^{-1} for the 160 mg/L and 1300 mg/L levels of water hardness respectively. The increased rate of PFBS degradation with increasing water hardness is also evident in observing the extent of degradation, as 99% degradation is achieved in hard water by the 4-hour time point, in comparison to the 95% degradation observed in DI water at 4 hours.

Panel (B) of Figure 5 depicts the application of the adapted protocol to PFPrS in DI water and groundwater. After 8 hours of treatment, 95% degradation of PFPrS was achieved in DI water, and 92% degradation was observed in groundwater. Like PFBS, PFPrS degradation in both DI water and groundwater was shown to follow a pseudo-first order reaction for the entire 8-hour treatment period. Rate of reaction decreased from 6.4×10^{-3} min^{-1} in DI water to 5.3×10^{-3} min^{-1} in groundwater. As such, positive effects from increasing water hardness were not observed when the adapted protocol was applied to PFPrS.

3.5 Conclusions and Future Work

This study found humic acid to be a strong inhibitor of PFOS degradation within the RADIANT system. An initial lag in PFOS degradation was observed in the presence of humic acid, and it was theorized that the degradation of PFOS is minimal until the photodegradation of humic acid is complete. Further work would benefit from total organic carbon (TOC) analysis to monitor changing concentrations of humic acid throughout the progression of treatment for a more comprehensive understanding of this relationship. Groundwater was found to mitigate the inhibitory effects of humic acid, but low fluoride recoveries suggest that fluoride recovery cannot be accurately measured in groundwater using the current methodology, possibly because of the precipitation of the fluoride ion with matrix components.

Ultra-short chain PFPrS was found to be the most recalcitrant of the PFAS compounds investigated in this study. A maximum of 95% degradation of PFPrS was reported in DI water following an 8-hour treatment, and defluorination was confirmed with 64% fluoride recovery. Further work is required to adapt the RADIANT system to achieve full defluorination of highly recalcitrant ultra-short chain PFAS. Future work will also investigate the scale-up potential of RADIANT, as well as the application of RADIANT to a wider suite of PFAS.

3.5 References

(1) Simons, J. H. Fluorocarbons: The Marriage of Carbon and the Reactive Gas Fluorine Has Resulted in a Whole New Family of Stable and Promising Compounds. *SCIENTIFIC AMERICAN* **1949**.

(2) Evich, M. G.; Davis, M. J. B.; McCord, J. P.; Acrey, B.; Awkerman, J. A.; Knappe, D. R. U.; Lindstrom, A. B.; Speth, T. F.; Tebes-Stevens, C.; Strynar, M. J.; Wang, Z.; Weber, E. J.; Henderson, W. M.; Washington, J. W. Per- and Polyfluoroalkyl Substances in the Environment. *Science* **2022**, *375* (6580), eabg9065. https://doi.org/10.1126/science.abg9065.

(3) Du, X.; Wu, Y.; Tao, G.; Xu, J.; Du, Z.; Wu, M.; Gu, T.; Xiong, J.; Xiao, S.; Wei, X.; Ruan, Y.; Xiao, P.; Zhang, L.; Zheng, W. Association between PFAS Exposure and Thyroid Health: A Systematic Review and Meta-Analysis for Adolescents, Pregnant Women, Adults and Toxicological Evidence. *Science of The Total Environment* **2024**, *953*, 175958. https://doi.org/10.1016/j.scitotenv.2024.175958.

(4) Fang, S.; Sha, B.; Yin, H.; Bian, Y.; Yuan, B.; Cousins, I. T. Environment Occurrence of Perfluoroalkyl Acids and Associated Human Health Risks near a Major Fluorochemical Manufacturing Park in Southwest of China. *Journal of Hazardous Materials* **2020**, *396*, 122617. https://doi.org/10.1016/j.jhazmat.2020.122617.

(5) Fenton, S. E.; Ducatman, A.; Boobis, A.; DeWitt, J. C.; Lau, C.; Ng, C.; Smith, J. S.; Roberts, S. M. Per- and Polyfluoroalkyl Substance Toxicity and Human Health Review: Current State of Knowledge and Strategies for Informing Future Research. *Environ Toxicol Chem* **2021**, *40* (3), 606–630. https://doi.org/10.1002/etc.4890.

(6) Canada, H. *Objective for Canadian drinking water quality per- and polyfluoroalkyl substances*. https://www.canada.ca/en/health-canada/services/publications/healthy-living/objective-drinking-water-quality-per-polyfluoroalkyl-substances.html (accessed 2025-04-09).

(7) Belkouteb, N.; Franke, V.; McCleaf, P.; Köhler, S.; Ahrens, L. Removal of Per- and Polyfluoroalkyl Substances (PFASs) in a Full-Scale Drinking Water Treatment Plant: Long-Term Performance of Granular Activated Carbon (GAC) and Influence of Flow-Rate. *Water Research* **2020**, *182*, 115913. https://doi.org/10.1016/j.watres.2020.115913.

(8) Riegel, M.; Haist-Gulde, B.; Sacher, F. Sorptive Removal of Short-Chain Perfluoroalkyl Substances (PFAS) during Drinking Water Treatment Using Activated Carbon and Anion Exchanger. *Environmental Sciences Europe* **2023**, *35* (1), 12. https://doi.org/10.1186/s12302-023-00716-5.

(9) Merino, N.; Qu, Y.; Deeb, R. A.; Hawley, E. L.; Hoffmann, M. R.; Mahendra, S. Degradation and Removal Methods for Perfluoroalkyl and Polyfluoroalkyl Substances in Water. *Environmental Engineering Science* **2016**, *33* (9), 615–649. https://doi.org/10.1089/ees.2016.0233.

(10) Boo, C.; Wang, Y.; Zucker, I.; Choo, Y.; Osuji, C. O.; Elimelech, M. High Performance Nanofiltration Membrane for Effective Removal of Perfluoroalkyl Substances at High Water Recovery. *Environ. Sci. Technol.* **2018**, *52* (13), 7279–7288. https://doi.org/10.1021/acs.est.8b01040.

(11) Scheitlin, C. G.; Dasu, K.; Rosansky, S.; Dejarme, L. E.; Siriwardena, D.; Thorn, J.; Mullins, L.; Haggerty, I.; Shqau, K.; Stowe, J. Application of Supercritical Water Oxidation to Effectively Destroy Per- and Polyfluoroalkyl Substances in Aqueous Matrices. *ACS EST Water* **2023**, *3* (8), 2053–2062. https://doi.org/10.1021/acsestwater.2c00548.

(12) Hao, S.; Reardon, P. N.; Choi, Y. J.; Zhang, C.; Sanchez, J. M.; Higgins, C. P.; Strathmann, T. J. Hydrothermal Alkaline Treatment (HALT) of Foam Fractionation Concentrate Derived from PFAS-Contaminated Groundwater. *Environ. Sci. Technol.* **2023**, *57* (44), 17154–17165. https://doi.org/10.1021/acs.est.3c05140.
(13) Meegoda, J. N.; Bezerra De Souza, B.; Casarini, M. M.; Kewalramani, J. A. A Review of PFAS Destruction Technologies. *IJERPH* **2022**, *19* (24), 16397. https://doi.org/10.3390/ijerph192416397.
(14) *Enhancing Interface Reactions by Introducing Microbubbles into a Plasma Treatment Process for Efficient Decomposition of PFOA | Environmental Science & Technology*. https://pubs.acs.org/doi/10.1021/acs.est.1c01724 (accessed 2026-07-18).
(15) Yin, S.; Calvillo Solís, J. J.; Sandoval-Pauker, C.; Puerto-Diaz, D.; Villagrán, D. Advances in PFAS Electrochemical Reduction: Mechanisms, Materials, and Future Perspectives. *Journal of Hazardous Materials* **2025**, *491*, 137943. https://doi.org/10.1016/j.jhazmat.2025.137943.
(16) Fennell, B. D.; Mezyk, S. P.; McKay, G. Critical Review of UV-Advanced Reduction Processes for the Treatment of Chemical Contaminants in Water. *ACS Environ. Au* **2022**, *2* (3), 178–205. https://doi.org/10.1021/acsenvironau.1c00042.
(17) Gu, Y.; Liu, T.; Wang, H.; Han, H.; Dong, W. Hydrated Electron Based Decomposition of Perfluorooctane Sulfonate (PFOS) in the VUV/Sulfite System. *Sci Total Environ* **2017**, *607–608*, 541–548. https://doi.org/10.1016/j.scitotenv.2017.06.197.
(18) Li, A.; Zhang, Z.; Li, P.; Cai, L.; Zhang, L.; Gong, J. Nitrogen Dioxide Radicals Mediated Mineralization of Perfluorooctanoic Acid in Aqueous Nitrate Solution with UV Irradiation. *Chemosphere* **2017**, *188*, 367–374. https://doi.org/10.1016/j.chemosphere.2017.08.170.
(19) Liu, Z.; Chen, Z.; Gao, J.; Yu, Y.; Men, Y.; Gu, C.; Liu, J. Accelerated Degradation of Perfluorosulfonates and Perfluorocarboxylates by UV/Sulfite + Iodide: Reaction Mechanisms and System Efficiencies. *Environ. Sci. Technol.* **2022**, *56* (6), 3699–3709. https://doi.org/10.1021/acs.est.1c07608.
(20) Mirzaei, M.; Asgarpour Khansary, M.; Mohseni, M. Degradation of PFOS in Concentrated Saline Waste Streams Using UV/ Sulfite Process: Critical Impact of Aggregation. *Journal of Hazardous Materials* **2025**, *496*, 139477. https://doi.org/10.1016/j.jhazmat.2025.139477.
(21) O'Connor, N.; Patch, D.; Noble, D.; Scott, J.; Koch, I.; Mumford, K. G.; Weber, K. Forever No More: Complete Mineralization of per- and Polyfluoroalkyl Substances (PFAS) Using an Optimized UV/Sulfite/Iodide System. *Science of The Total Environment* **2023**, *888*, 164137. https://doi.org/10.1016/j.scitotenv.2023.164137.
(22) Ren, Z.; Bergmann, U.; Leiviskä, T. Reductive Degradation of Perfluorooctanoic Acid in Complex Water Matrices by Using the UV/Sulfite Process. *Water Research* **2021**, *205*, 117676. https://doi.org/10.1016/j.watres.2021.117676.
(23) Sun, Z.; Zhang, C.; Chen, P.; Zhou, Q.; Hoffmann, M. R. Impact of Humic Acid on the Photoreductive Degradation of Perfluorooctane Sulfonate (PFOS) by UV/Iodide Process. *Water Research* **2017**, *127*, 50–58. https://doi.org/10.1016/j.watres.2017.10.010.
(24) Guo, C.; Zhang, C.; Sun, Z.; Zhao, X.; Zhou, Q.; Hoffmann, M. R. Synergistic Impact of Humic Acid on the Photo-Reductive Decomposition of Perfluorooctanoic Acid. *Chemical Engineering Journal* **2019**, *360*, 1101–1110. https://doi.org/10.1016/j.cej.2018.10.204.
(25) O'Connor, N. M.; Biology, B. A Thesis Submitted to the Division of Graduate Studies of the Royal Military College of Canada.

(26) Fennell, B. D.; Fowler, D.; Mezyk, S. P.; McKay, G. Reactivity of Dissolved Organic Matter with the Hydrated Electron: Implications for Treatment of Chemical Contaminants in Water with Advanced Reduction Processes. *Environ. Sci. Technol.* **2023**, *57* (19), 7634–7643. https://doi.org/10.1021/acs.est.3c00909.
(27) Ghorbani Gorji, S.; Mackie, R.; Prasad, P.; Knight, E. R.; Qu, X.; Vardy, S.; Bowles, K.; Higgins, C. P.; Thomas, K. V.; Kaserzon, S. L. Occurrence of Ultrashort-Chain PFASs in Australian Environmental Water Samples. *Environ. Sci. Technol. Lett.* **2024**, *11* (12), 1362–1369. https://doi.org/10.1021/acs.estlett.4c00750.
(28) Bentel, M. J.; Yu, Y.; Xu, L.; Li, Z.; Wong, B. M.; Men, Y.; Liu, J. Defluorination of Per- and Polyfluoroalkyl Substances (PFASs) with Hydrated Electrons: Structural Dependence and Implications to PFAS Remediation and Management. *Environ. Sci. Technol.* **2019**, *53* (7), 3718–3728. https://doi.org/10.1021/acs.est.8b06648.
(29) Bentel, M. J.; Liu, Z.; Yu, Y.; Gao, J.; Men, Y.; Liu, J. Enhanced Degradation of Perfluorocarboxylic Acids (PFCAs) by UV/Sulfite Treatment: Reaction Mechanisms and System Efficiencies at pH 12. *Environ. Sci. Technol. Lett.* **2020**, *7* (5), 351–357. https://doi.org/10.1021/acs.estlett.0c00236.
(30) Lyu, X.-J.; Li, W.-W.; Lam, P. K. S.; Yu, H.-Q. Photodegradation of Perfluorooctane Sulfonate in Environmental Matrices. *Separation and Purification Technology* **2015**, *151*, 172–176. https://doi.org/10.1016/j.seppur.2015.07.049.

4. Comparison of Reactive Activation of Sulfite and Iodide Through UV-Natured Treatment (RADIANT) System for Treatment of PFAS Contaminated Groundwater at the Cuvette and Beaker Scale

4.1 Abstract

The Reactive Activation of Sulfite and Iodide through UV-Natured Treatment (RADIANT) System is a UV advanced reductive process (UV-ARP) that has been demonstrated to be capable of degrading highly recalcitrant PFAS compounds. However, the majority of work has been performed at the 1 mL scale using a cuvette set-up. This paper offers a comparison of two bench-scale set-ups by examining the performance of both the 1 mL cuvette and 800 mL beaker set-ups in the degradation of PFOS and PFBS. Greater than 99% degradation of PFOS was achieved at both scales, but reaction rate and extent of degradation was considerably improved at the beaker scale. The rate of reaction at the beaker scale was approximately two times greater than the rate of reaction at the cuvette scale, and the beaker set-up was shown to consistently achieve lower final concentrations. Improved degradation was observed in groundwater at both scales, and the impact of factors such as DOC concentrations observed at the cuvette scale is likely transferrable to the beaker apparatus.

4.2 Introduction

Per- and polyfluoralkyl substances (PFAS) are a large class of anthropogenic chemicals known for their surfactant-like properties and exceptional stability. Widespread use of PFAS since their development in the 1950s has resulted in their near ubiquity in the environment. A wide range of PFAS has been detected in surface waters and groundwater worldwide.[1,2] This has become a point of concern due to the growing body of evidence linking this highly recalcitrant class of chemicals to a range of human health effects.[3] The U.S. Environmental Protection Agency (EPA) has stated that for PFOA and PFOS, two PFAS compounds commonly detected in groundwater, there is no level of exposure at which there is no risk of health impacts. Due to this, the maximum contaminant level (MCLs) set by the U.S. EPA are 4.0 ng/L for PFOA and PFOS, and 10 ng/L for PFNA, PFHxS, and HFPO-DA.[4] Canadian guidelines are similarly low, with a federal objective of 30 ng/L for a sum of 25 PFAS, and the Ontario provincial guidance value of 70 ng/L for 11 PFAS.[5] Sorption and filtration based technologies such as granular activated carbon, ion exchange resins, and nanofiltration have been demonstrated to be effective at removing PFAS from aqueous matrices and are commercially available.[6] However, the aforementioned removal-based techniques result in the production of a contaminated waste stream that requires further treatment.[7] As a result, significant efforts have been made to develop water treatment technologies capable of fully destroying this highly recalcitrant class of chemicals.

Destructive treatment of PFAS is especially challenging due to its exceptional stability. Thermal decomposition in halogen-resistant incinerators is one of the most well-

established full-scale destructive techniques capable of destroying PFAS on a commercial scale.[8] However, operation is inherently energy intensive and requires transport for ex-situ treatment. On-site thermal treatment is possible through mobile smouldering units, which have been shown to be effective for the remediation of PFAS-contaminated soils and granular activated carbon.[7,9] For aqueous matrices, Battelle's PFAS Annihilator™ is a supercritical water oxidation (SCWO) based technique that is now available on a commercial scale, and has been demonstrated to effectively treat highly contaminated and complex streams such as aqueous film forming foams (AFFF),[10] and AFFF-impacted waters in the presence of co-contaminants such as VOCs and diesel fuel.[11] An emerging destructive technique, hydrothermal alkaline treatment (HALT) has shown promising results at a pilot scale, and is similar to SCWO in that it leverages PFAS' increased susceptibility to degradation under extreme conditions in combination with a pre-treatment concentrating step.[12] The energy intensive nature of these extreme operating conditions means that techniques like SCWO are only economical for the treatment of large, highly concentrated volumes of water, and pose potential challenges for the adaptability of these systems at different scales.[13] Electrochemical oxidation, plasma, sonolysis, and photocatalytic techniques are other destructive treatment methods in development that have progressed to pilot-scale operation.[8] The latter is often referred to ultraviolet advanced reductive processes (UV-ARP), and rely on photochemical interactions with electron donors (photosensitizers) to produce aqueous electrons, which have been demonstrated to initiate the destruction of PFAS.[14] The use of sulfite and iodide as photosensitizers in a UV-sulfite/iodide system was shown to be effective in PFAS degradation by O'Connor et al, who achieved >99% degradation and full defluorination of the highly recalcitrant PFBS.[15] The work reported by O'Connor et al. was developed into the Reactive Activation of Sulfite and Iodide through UV-Natured Treatment (RADIANT) system, and has shown great promise at the bench top scale in degrading highly recalcitrant forms of PFAS at a relatively low energy cost. However, more work is required to guide the scale-up of this treatment technology. A recent pilot-scale study showed the efficacy of UV-ARP at a larger scale.[16] While comparative studies have been conducted on PFAS removal and destructive technologies at different scales,[9,17–20] the impact of scale on RADIANT system performance has yet to be assessed.

The objectives of this paper are to 1) evaluate RADIANT system performance at two different volumes of water (1 mL and 800 mL), 2) determine if findings at the cuvette scale can be applied at the beaker scale, 3) guide future scale-up operations by identifying parameters that would benefit from optimization.

4.3 Materials and Methods

4.3.1 Chemicals and Reagents

All PFAS analytical standards and chemicals were purchased from the sources listed in section A.2 of Appendix A. Details of all other chemicals reagents and their sources are provided in Table A6.

4.3.2 Experimental Set-Up and Procedure

The experimental conditions of the trials discussed in this study are listed in the table below.

Table 4: List of Experimental Conditions

Trial Name	PFAS	Matrix	Reagent Concentrations	Initial PFAS Concentration	Scale	
					Cuvette	Beaker
PFOS-0.5C	PFOS	DI water	10 mM Na_2SO_3	0.4 mg/L	X	
PFOS-1C	PFOS	DI water	10 mM KI	1 mg/L	X	
PFOS-3C	PFOS	DI water	10 mM $NaHCO_3$	3 mg/L	X	
PFOS-1B	PFOS	DI water	150 mM NaOH	1 mg/L		X
PFOS-GW	PFOS	Groundwater		2 mg/L	X	
PFOS-GW	PFOS	Groundwater		0.7 mg/L		X
PFBS-DI	PFBS	DI water		3 mg/L	X	
PFBS-DI	PFBS	DI water		0.8 mg/L		X

The potable groundwater used in this study was sampled directly from a domestic drinking water well in Ontario, bypassing any treatment systems. More information on the collected groundwater can be found in Chapter 3, and basic water quality parameters can be found in Table A8.

4.3.2.1 Cuvette Set-Up (1 mL)

Treatment was carried out using the protocol outlined in Chapter 3. Reagent concentrations specific to the results discussed in this chapter are listed in Table 4.

4.3.2.2 Beaker Set-Up (800 mL)

Treatment was performed in a 1 L Berzelius tall form beaker. A 36 W 120 V ozone-free UV lamp (Coospider) was submerged into 800 mL of PFAS-spiked solution. PFAS spiked solutions were created by combining the reagents in the quantities listed in Table 4, and mixed in deionized (DI) water or groundwater for a minimum of 30 min prior to treatment. The beaker and lamp were placed on a magnetic stir plate (Corning, PC-400), and stirred continuously with a stir bar at 360 rpm throughout treatment. The treatment was considered to start when the UV lamp was turned on.

Table 5: Cuvette and Beaker Experimental Set-Up

Parameter	Cuvette	Beaker
Volume	1 mL	800 mL
Mixing	N/A	360 rpm
Lamp position	~7.25 cm from cuvette	Submerged in solution
Highest measured temperature	38 °C	45 °C

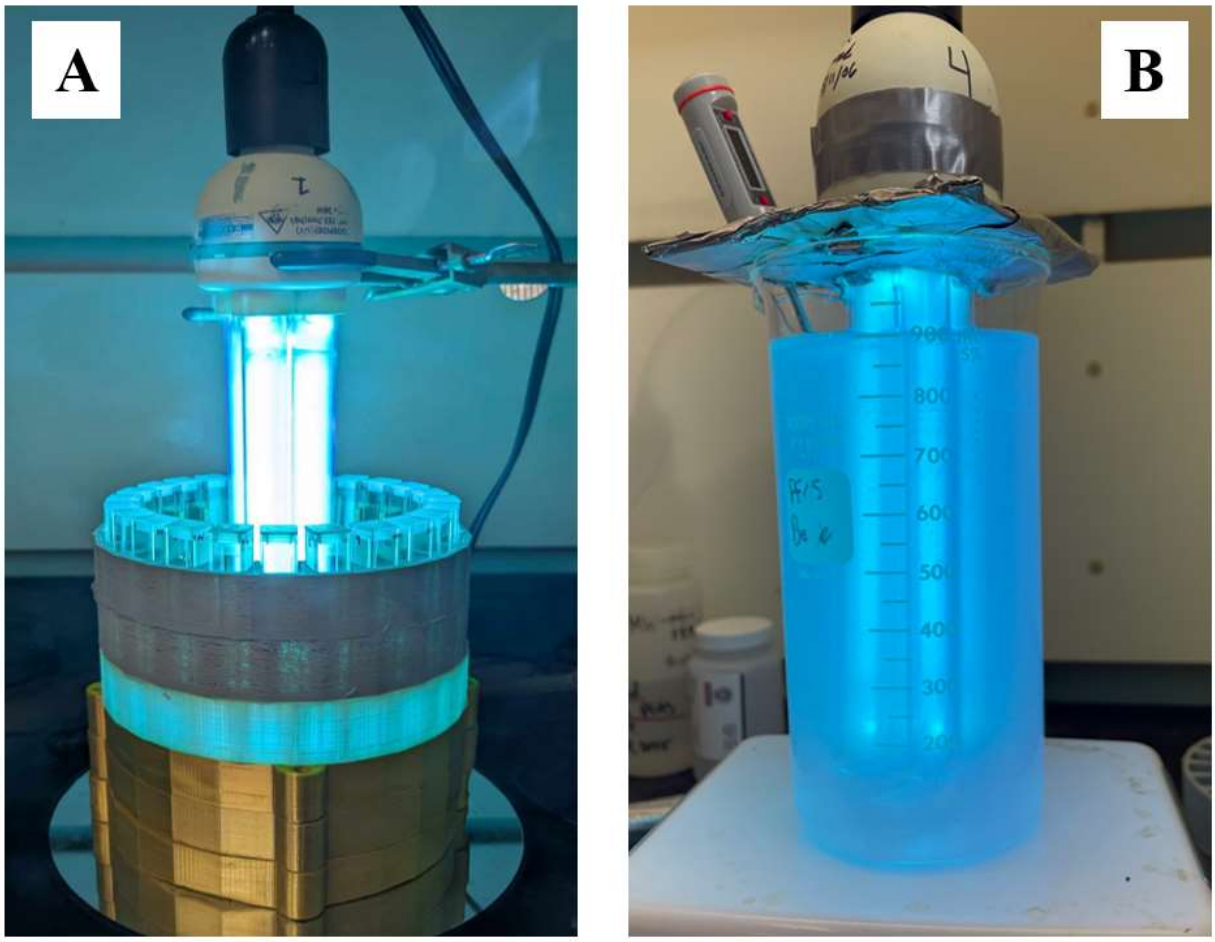

Figure 6. 1 mL cuvette set-up (A) and 800 mL beaker set-up (B).

4.3.3 Analytical Methods

PFAS and fluoride analysis were carried out following the methods described in Chapter 3.

4.4 Results and Discussion

4.4.1 Effect of Initial Concentration

In preliminary experiments at the cuvette scale, the impact of initial concentration on the rate of PFOS degradation was investigated. A two hour 10 mM sulfite treatment was performed with three different initial concentrations of PFOS in deionized (DI) water.

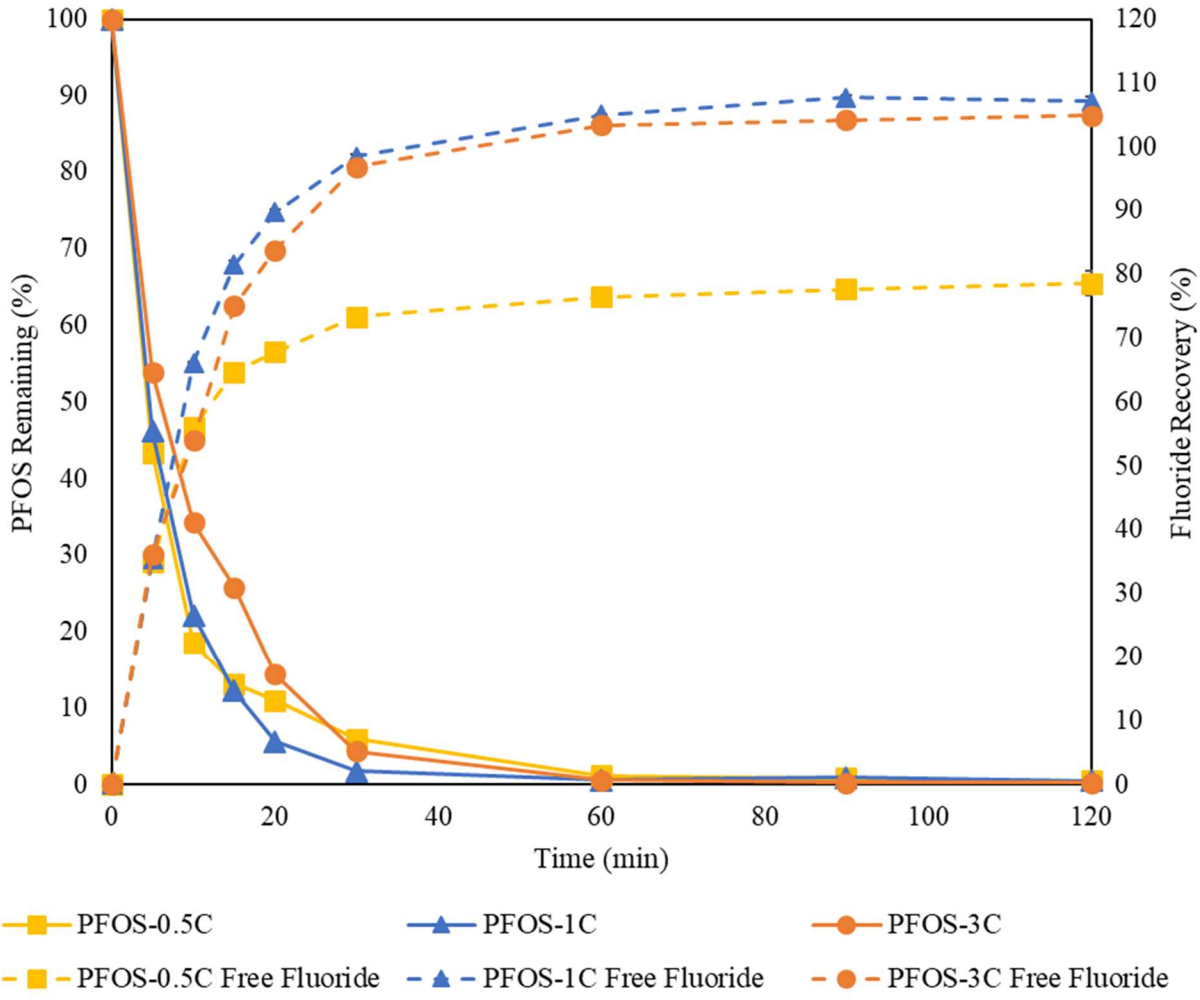

Figure 7. Degradation of PFOS in RADIANT cuvette system at three different initial concentrations: 0.4 mg/L (PFOS-0.5C), 1 mg/L (PFOS-1C), and 3 mg/L (PFOS-3C). Some error bars are obscured by markers.

Figure 7 depicts the degradation of PFOS and the generation of free fluoride as PFOS-spiked DI water is treated within the RADIANT system. The initial concentration of PFOS measured for PFOS-0.5C was 0.4 mg/L, while PFOS-1C and PFOS-3C were measured to have an initial concentration of 1 mg/L and 3 mg/L respectively. Pseudo-zero order and pseudo-first order rate constants were calculated for all trials, and can be found in Figure B10 in Appendix B. PFOS degradation was shown to follow a pseudo-first order reaction for the first 30 min of treatment. The rate of reaction was calculated based on the degradation of PFOS

from 0–30 min, and reaction rates were determined to be (0.9 ± 0.1) x 10^{-1} min^{-1} for the 0.4 mg/L trial, (1.34 ± 0.03) x 10^{-1} min^{-1} at 1 mg/L, and (1.00 ± 0.05) x 10^{-1} min^{-1} at 3 mg/L. While reaction rates were similar across all three levels of initial concentration, decreasing the initial concentration to 0.4 mg/L resulted in a reduction in fluoride recovery. Fluoride recovery was decreased from 105% and 107% for PFOS-1C and PFOS-3C respectively, to 79% when the initial concentration of PFOS was 0.4 mg/L. The reduction in fluoride recovery suggests that there may be a minimum concentration at which the RADIANT system is most effective, and is an area of investigation that could benefit from future work.

It should also be noted that PFOS-1C, the trial which demonstrated the highest reaction rate, was performed on a day where ambient temperatures were unusually high. Ambient temperatures in the laboratory are typically 20–25 °C, but the temperature of PFOS-1C was measured to be 28.7 °C prior to treatment. The temperature of PFOS-1C throughout the 2-hour treatment period is depicted in panel D of Figure 8. The high reaction rate observed for PFOS-1C may be attributed to the elevated temperatures measured on that day. The effect of temperature will be discussed in the following section, as experiments performed at the beaker scale have similarly noted increased reaction rates in response to high ambient temperatures.[21] Nonetheless, the aforementioned experiments can be interpreted to indicate that the effect of initial concentration on reaction rate is minimal. This enables the comparisons between beaker and cuvette set-ups in the following sections.

4.4.2 Comparison of Cuvette and Beaker Set-Up

This study provides a comparison of RADIANT system performance at the cuvette (1 mL) and beaker (800 mL) scale. The degradation of PFOS and PFBS was investigated with a 10 mM sulfite treatment, and degradation of PFOS was investigated in both DI water and groundwater. At the cuvette scale, initial PFOS concentrations were 3 mg/L and 2 mg/L in DI water (PFOS-3C) and groundwater (PFOS-GW) respectively. Initial PFOS concentrations in the beaker set-up were 1 mg/L in DI water (PFOS-1B) and 0.7 mg/L in groundwater (PFOS-GW). Initial PFBS concentrations were 3 mg/L at the cuvette scale, and 0.8 mg/L in the beaker set-up.

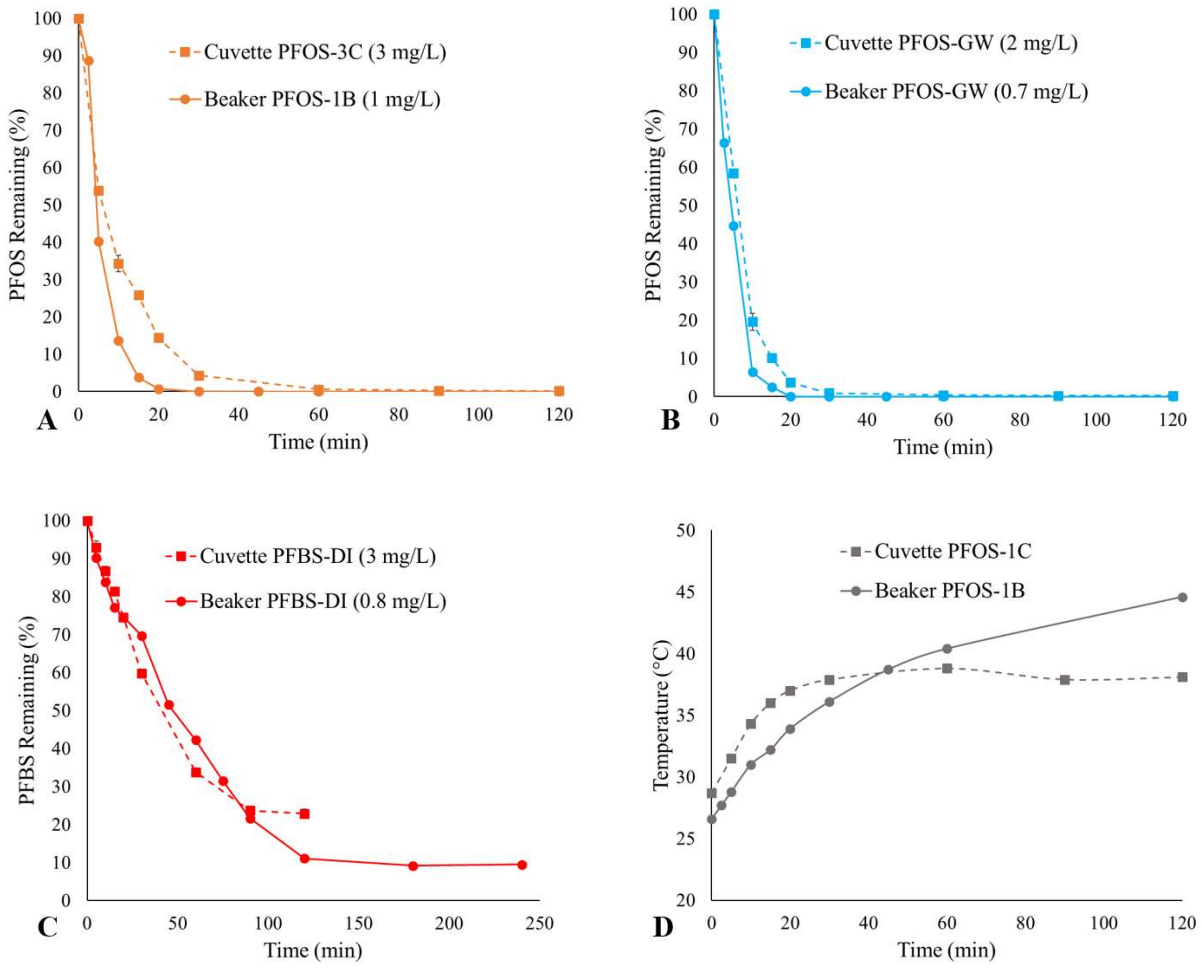

Figure 8. Comparison of beaker and cuvette set-up through (a) PFOS degradation in DI water, (b) PFOS degradation in groundwater, (c) PFBS degradation in DI water, (d) temperature of beaker and cuvette set-up during PFOS degradation. Starting concentrations are listed in the legends and tabulated with treatment conditions in Table 4.

Panels (A-C) in Figure 8 depict the decrease of PFOS and PFBS concentrations throughout the progression of treatment. Although not immediately visible from the figure, the extent of degradation was improved at the beaker scale. PFOS concentrations in DI water at the beaker scale reached non-detectable levels (<0.05 µg/L) after 45 minutes of treatment. In contrast, PFOS concentrations in the cuvette set-up plateaued after 90 minutes, reaching a final concentration of 12 µg/L after two hours of treatment in DI water. Although >99% degradation was achieved at both scales, PFOS concentrations in the cuvette did not go below the limit of detection. A plateau in treatment was also observed in the degradation of PFBS. As seen in panel (C) of Figure 8, PFBS treatment in the cuvette set-up plateaued at the 90-minute mark and remained at an elevated concentration for a total degradation efficiency of 77% by the end of a two-hour treatment. In contrast, PFBS concentrations at the beaker scale decreased steadily for the first two hours of treatment before plateauing, reaching 89%

degradation by the two-hour mark. The treatment of PFBS at both scales shows that the beaker set-up sustained a longer period of degradation compared to the cuvette set-up, which plateaued in degradation 30 min earlier than the beaker set-up.

The improved performance observed at the beaker scale is likely attributable to differences in the experimental set-up. While the cuvette system does not allow for mixing, the beaker set-up is equipped with a stir bar. The addition of mixing in the RADIANT system increases the probability of interaction between aqueous electron and PFAS, dispersing locally concentrated zones where reactants have been depleted. Mixing may also serve to prevent the formation of micelles and allow for increased availability of PFAS molecules for reaction. Additionally, the structure of the cuvette set-up may result in uneven irradiation of the solution, as the side which faces the lamp receives increased photon flux compared to the region of the cuvette furthest from the lamp. In the beaker set-up, this distance-dependent difference in photon flux may be overcome by mixing, which ensures that photosensitizers receive equal likelihood of reaction with photons. Experiments conducted by O'Connor et al. (2024) have also established that the photon flux of the beaker set-up is more than double that of the cuvette set-up, which was measured at 3.01 J s^{-1} L^{-1} compared to 7.26 J s^{-1} L^{-1} in the beaker set-up. The increase in photon flux is likely a large contributor to the improved performance observed at the beaker scale.

The increased temperature of the beaker set-up, as noted in Table 5, is also likely to increase the energy in the system. Although the difference in temperature between scales is not large, panel (D) of Figure 8 shows how temperature increases differently in the two set-ups. The temperature at the 0-minute mark, prior to treatment, is the room temperature at which the experiment was performed, and any subsequent increase in temperature is attributed to the heat generated by the UV lamp. The temperature at the cuvette scale rose until the 30-minute mark, after which increases in temperature were minimal. In contrast, no plateau in temperature was observed for the time frame measured at the beaker scale. Despite starting at a slightly lower temperature, the beaker set-up reached a final temperature of 44.6 °C, while the highest temperature measured at the cuvette scale was 38.1 °C. The cuvette set-up is shown to average a lower temperature than the beaker set-up due to the submersion of the lamp, and appears to be consistent with the maximum temperatures tabulated in Table 5, where the maximum value in the beaker set-up is 7 °C higher than that of the cuvette set-up. Experiments performed at the beaker scale have also noted increased reaction rates between replicate studies, wherein all experimental conditions were constant except for the higher ambient temperature of that day.[21] As such, improved performance at the beaker scale may be attributed in part to the higher average temperature of the beaker set-up.

Submersion of the lamp in the beaker set-up may also serve to promote a more direct interaction between the photons and the photosensitizer, increasing the generation of aqueous electrons. Improved RADIANT system performance at the beaker scale is also evident when comparing the rate of reactions calculated for experiments conducted in both set-ups, as depicted in Figure 9.

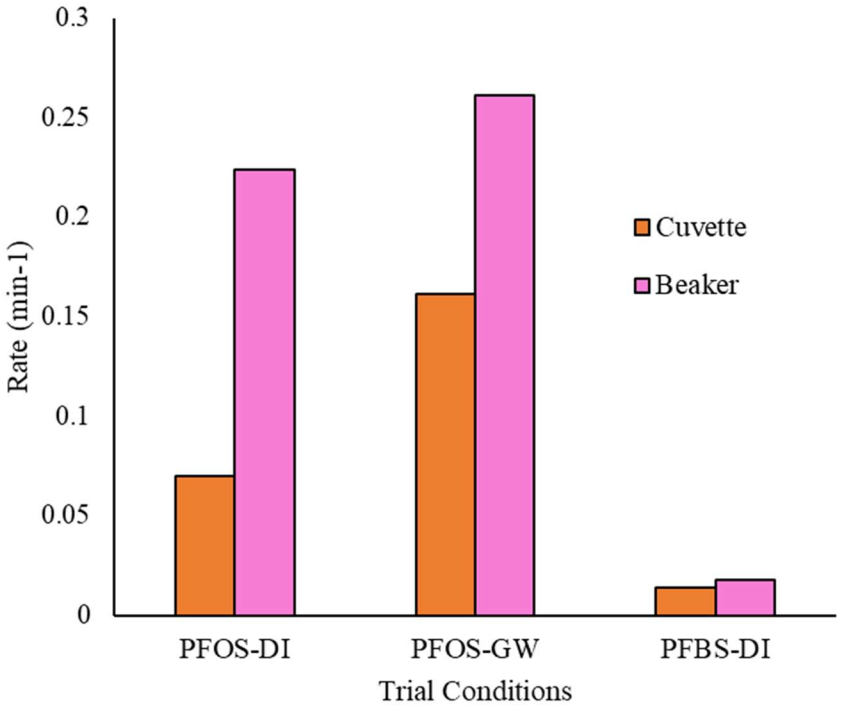

Figure 9. Comparison of reaction rates between cuvette (1 mL) and beaker (800 mL) set-up. PFOS-DI and PFOS-GW refer to the two-hour treatment of PFOS in deionized water and groundwater, respectively. PFBS degradation was carried out in DI water.

As demonstrated in Figure 9, an increase in reaction rate was observed when RADIANT was performed at the 800 mL scale. The rate of reaction for the degradation of PFOS in DI water at the cuvette scale was calculated to be 1.0×10^{-1} min^{-1}. The rate of reaction for the same experimental conditions at the beaker scale was more than two times larger at 2.2×10^{-1} min^{-1}.[21] Similarly, the rate of reaction at the beaker scale for the treatment of PFOS in groundwater was also much larger than that of the cuvette scale, at 2.6×10^{-1} min^{-1} compared to 1.6×10^{-1} min^{-1}. The difference between reaction rates was much smaller for PFBS trials. PFBS degradation at the cuvette scale was calculated to be 1.7×10^{-2} min^{-1}, while the beaker set-up produced a reaction rate of 1.8×10^{-2} min^{-1}.

The rate of reaction associated with the degradation of PFOS in the cuvette set-up more than doubled when treatment was performed in groundwater instead of DI water. In the beaker set-up, treatment in groundwater resulted in a far less dramatic 16% increase in reaction rate. This could simply be because the cuvette set-up has more room for improvement. As discussed in Chapter 3, groundwater may improve PFAS degradation due to its increased ionic strength, which can reduce the electrostatic repulsion between the anionic PFAS and aqueous electron. This promotes degradation by increasing the interaction between PFAS and aqueous electron, something that is already accomplished in the beaker set-up by the addition of mixing and increased temperatures.

At the cuvette scale, the rate of reaction associated with PFBS degradation was 83% lower than the rate of reaction for PFOS degradation. Similarly, the beaker set-up showed a 92% reduction in reaction rate between PFOS and PFBS. PFBS degradation progressed at a much slower rate than degradation of PFOS at both scales, but the difference in reaction rate was smaller at the cuvette scale than at the beaker scale. This suggests that the barrier to full PFBS degradation is inherent to the treatment protocol, and is addressed by the adapted treatment protocol, that is, sulfite additions every two hours, described in Chapter 3. The aforementioned adapted treatment protocol has also been applied at the beaker scale, and has been shown to be effective in achieving >99% degradation of PFBS.[21]

While the rate of reaction is different between the two scales, the relationships remain consistent across the cuvette and beaker set-ups. Both cuvette and beaker set-ups show an increased rate of reaction when the treatment is performed in groundwater, and a decrease in reaction rate from PFOS to PFBS. Additionally, treatment of PFAS contaminated groundwater sampled from a variety of impacted sites (landfill, AFFF-impacted groundwater, etc.) at the beaker scale has noted increasing lag times with increasing dissolved organic carbon (DOC) concentrations.[21] While this decrease in treatment efficiency cannot be directly attributed to DOC due to the presence of co-contaminants and other complexities in the matrix, the delayed reduction in PFAS concentrations observed at the beaker scale in the presence of DOC is similar to the effect of humic acid observed at the cuvette scale. As such, there is indication that the relationships and trends elucidated at the cuvette scale can be applied across RADIANT set-ups.

4.5 Conclusions and Future Work

Trials conducted at the beaker scale were capable of degrading PFAS to non-detectable levels (<0.05 µg/L), consistently achieving lower final concentrations than the cuvette set-up at a faster rate. In short, RADIANT system performance was significantly improved by the beaker set-up. These improvements are attributed largely to the mixing, increased temperatures, and direct application of UV light to solution. Therefore, parameters such as the rate of mixing and the temperature of operation have been identified as highly influential to the success of the RADIANT system, and would benefit from future investigation and optimization. Treatment of PFAS mixtures in complex matrices by the RADIANT system is the subject of ongoing research within the group. Future work could also benefit from exploring a wider range of PFAS, encompassing ultra-short chain PFAS that remain presently under-studied compared to their longer chain counterparts. Additionally, preliminary experiments at the cuvette scale indicate that lower initial concentrations may result in decreasing fluoride recoveries and reduced treatment rates. While the beaker set-up was shown to effectively degrade lower concentrations that would have likely impeded treatment within the cuvette set-up, future work would greatly benefit from exploring a wider range of concentrations at the beaker scale.

Experimental conditions that lead to improved performance in the cuvette set-up resulted in improved performance at the beaker scale. The groundwater matrix was shown to improve PFOS degradation at both scales in this study. Experiments performed at the

beaker scale on PFAS-contaminated groundwater, while not shown in this study, have been reported to show decreased degradation with increasing DOC levels,[21] similar to the effect of humic acid that was observed at the cuvette scale. The consistency between the two set-ups in response to changing conditions allow for findings at the cuvette scale to be soundly utilized at the beaker scale. Overall, the improved RADIANT system performance observed at the larger scale indicates a strong potential for future scale-up operations.

4.5 References

(1) Zhang, H.; Xu, H.; Qin, B.; Fu, Y.; Yao, Y.; Zhao, Y.; Qin, C. Review on the Sources, Distribution and Treatment of per- and Polyfluoroalkyl Substances in Global Groundwater. *Environ Res* **2025**, *275*, 121387. https://doi.org/10.1016/j.envres.2025.121387.

(2) Roy, J. W.; Weber, K. Per- and Polyfluoroalkyl Substances (PFASs) Contamination of Groundwater in Canada: A (Too) Short Review. *Canadian Water Resources Journal / Revue canadienne des ressources hydriques* **2025**, *50* (3), 236–249. https://doi.org/10.1080/07011784.2025.2519134.

(3) Fang, S.; Sha, B.; Yin, H.; Bian, Y.; Yuan, B.; Cousins, I. T. Environment Occurrence of Perfluoroalkyl Acids and Associated Human Health Risks near a Major Fluorochemical Manufacturing Park in Southwest of China. *Journal of Hazardous Materials* **2020**, *396*, 122617. https://doi.org/10.1016/j.jhazmat.2020.122617.

(4) *PFAS National Primary Drinking Water Regulation*. Federal Register. https://www.federalregister.gov/documents/2024/04/26/2024-07773/pfas-national-primary-drinking-water-regulation (accessed 2026-08-05).

(5) *Minister's Annual Report on Drinking Water (2024) | ontario.ca*. http://www.ontario.ca/page/ministers-annual-report-drinking-water-2024 (accessed 2026-08-04).

(6) Merino, N.; Qu, Y.; Deeb, R. A.; Hawley, E. L.; Hoffmann, M. R.; Mahendra, S. Degradation and Removal Methods for Perfluoroalkyl and Polyfluoroalkyl Substances in Water. *Environmental Engineering Science* **2016**, *33* (9), 615–649. https://doi.org/10.1089/ees.2016.0233.

(7) Duchesne, A. L.; Brown, J. K.; Patch, D. J.; Major, D.; Weber, K. P.; Gerhard, J. I. Remediation of PFAS-Contaminated Soil and Granular Activated Carbon by Smoldering Combustion. *Environ. Sci. Technol.* **2020**, *54* (19), 12631–12640. https://doi.org/10.1021/acs.est.0c03058.

(8) Blotevogel, J.; Thagard, S. M.; Mahendra, S. Scaling up Water Treatment Technologies for PFAS Destruction: Current Status and Potential for Fit-for-Purpose Application. *Current Opinion in Chemical Engineering* **2023**, *41*, 100944. https://doi.org/10.1016/j.coche.2023.100944.

(9) Harrison, B. G.; Major, D. W.; Kinsman, L. L.; Brown, J. K.; Gabayet, J. L. D.; Gerhard, J. I.; Patch, D. J.; Weber, K. P.; Chernysheva, L.; Brown, G. M.; Doudrick, K.; Abarca-Perez, A.; Peaslee, G. F.; Pennell, K. D.; Manz, K. E. Smoldering Treatment of PFAS: Investigation of Mass Balance and Volumetric Scale Up for Field Implementation. *ACS Omega* **2025**, *10* (28), 30489–30500. https://doi.org/10.1021/acsomega.5c02257.

(10) Rosansky, S.; Al-Dirani, S. M.; Scheitlin, C. G.; Dasu, K.; Dzurnak, M.; Xia, X.; Orth, C.; McCauley, M.; Mullins, L. Field Demonstration of PFAS Destruction in Various

Alcohol-Resistant AFFFs Using Supercritical Water Oxidation (SCWO). *ACS EST Water* **2024**, *4* (10), 4486–4496. https://doi.org/10.1021/acsestwater.4c00499.
(11) Scheitlin, C. G.; Dasu, K.; Rosansky, S.; Dejarme, L. E.; Siriwardena, D.; Thorn, J.; Mullins, L.; Haggerty, I.; Shqau, K.; Stowe, J. Application of Supercritical Water Oxidation to Effectively Destroy Per- and Polyfluoroalkyl Substances in Aqueous Matrices. *ACS EST Water* **2023**, *3* (8), 2053–2062. https://doi.org/10.1021/acsestwater.2c00548.
(12) Hao, S.; Reardon, P. N.; Choi, Y. J.; Zhang, C.; Sanchez, J. M.; Higgins, C. P.; Strathmann, T. J. Hydrothermal Alkaline Treatment (HALT) of Foam Fractionation Concentrate Derived from PFAS-Contaminated Groundwater. *Environ. Sci. Technol.* **2023**, *57* (44), 17154–17165. https://doi.org/10.1021/acs.est.3c05140.
(13) Pinkard, B.; Smith, S. M.; Vorarath, P.; Smrz, T.; Schmick, S.; Dressel, L.; Bryan, C.; Czerski, M.; De Marne, A.; Halevi, A.; Thomsen, C.; Woodruff, C. Degradation and Defluorination of Ultra Short-, Short-, and Long-Chain PFASs in High Total Dissolved Solids Solutions by Hydrothermal Alkaline Treatment─Closing the Fluorine Mass Balance. *ACS EST Eng.* **2024**, *4* (11), 2810–2818. https://doi.org/10.1021/acsestengg.4c00378.
(14) Patch, D.; O'Connor, N.; Koch, I.; Cresswell, T.; Hughes, C.; Davies, J. B.; Scott, J.; O'Carroll, D.; Weber, K. Elucidating Degradation Mechanisms for a Range of Per- and Polyfluoroalkyl Substances (PFAS) via Controlled Irradiation Studies. *Science of The Total Environment* **2022**, *832*, 154941. https://doi.org/10.1016/j.scitotenv.2022.154941.
(15) O'Connor, N.; Patch, D.; Noble, D.; Scott, J.; Koch, I.; Mumford, K. G.; Weber, K. Forever No More: Complete Mineralization of per- and Polyfluoroalkyl Substances (PFAS) Using an Optimized UV/Sulfite/Iodide System. *Science of The Total Environment* **2023**, *888*, 164137. https://doi.org/10.1016/j.scitotenv.2023.164137.
(16) Liu, C. J.; McKay, G.; Jiang, D.; Tenorio, R.; Cath, J. T.; Amador, C.; Murray, C. C.; Brown, J. B.; Wright, H. B.; Schaefer, C.; Higgins, C. P.; Bellona, C.; Strathmann, T. J. Pilot-Scale Field Demonstration of a Hybrid Nanofiltration and UV-Sulfite Treatment Train for Groundwater Contaminated by per- and Polyfluoroalkyl Substances (PFASs). *Water Research* **2021**, *205*, 117677. https://doi.org/10.1016/j.watres.2021.117677.
(17) Maldonado, V. Y.; Becker, M. F.; Nickelsen, M. G.; Witt, S. E. Laboratory and Semi-Pilot Scale Study on the Electrochemical Treatment of Perfluoroalkyl Acids from Ion Exchange Still Bottoms. *Water* **2021**, *13* (20), 2873. https://doi.org/10.3390/w13202873.
(18) Hopkins, Z. R.; Knappe, D. R. U. Predicting Per- and Polyfluoroalkyl Substances Removal in Pilot-Scale Granular Activated Carbon Adsorbers from Rapid Small-Scale Column Tests. *AWWA Water Science* **2024**, *6* (2), e1369. https://doi.org/10.1002/aws2.1369.
(19) Cheng, L.; Knappe, D. R. U. Removal of Per- and Polyfluoroalkyl Substances by Anion Exchange Resins: Scale-up of Rapid Small-Scale Column Test Data. *Water Research* **2024**, *249*, 120956. https://doi.org/10.1016/j.watres.2023.120956.
(20) Sörengård, M.; Gago-Ferrero, P.; B. Kleja, D.; Ahrens, L. Laboratory-Scale and Pilot-Scale Stabilization and Solidification (S/S) Remediation of Soil Contaminated with per- and Polyfluoroalkyl Substances (PFASs). *Journal of Hazardous Materials* **2021**, *402*, 123453. https://doi.org/10.1016/j.jhazmat.2020.123453.
(21) Phillips, S. Department of Civil Engineering, Queen's University, Kingston, ON. Personal communication, 2026.

5. Conclusions and Future Work

The overarching objective of this work was to assess the feasibility of applying the RADIANT system to treat PFAS-contaminated groundwater. To that end, the conclusions and future work are organized in the sections that follow.

5.1 Effects of Humic Acid and Nitrate

Humic acid and nitrate were identified as common groundwater components that were highly likely to interfere with RADIANT system efficiency due to their strong electron scavenging capacity. To explore their effects, a series of experiments was performed in deionized (DI) water that examined the individual and combined effects of these potential interferents under two treatment conditions (10 and 50 mM sulfite). Humic acid was found to result in a 30-minute delay in the reduction of PFOS concentrations, producing a prolonged period of elevated concentrations termed as a "lag time" at the beginning of treatment. Treatment performed in the presence of humic acid led to higher final concentrations, and the presence of humic acid reduced the efficiency of the 10 mM sulfite treatment from >99% to 96%. Increasing sulfite concentrations were hypothesized to overcome this inhibitory effect, but treatment at increased sulfite concentrations (50 mM) resulted in a further reduction in PFOS degradation to 86%.

All nitrate-spiked experiments achieved >99% PFOS degradation. The addition of nitrate was shown to increase initial reaction rates during the 10 mM sulfite treatment, but fluoride recovery was observed to decrease by approximately 30%. However, full fluoride recovery in the presence of nitrate was observed with the 50 mM sulfite treatment. The combination of humic acid and nitrate resulted in inhibitory effects comparable to the results of the humic acid spiked trials, in that a similar lag time was observed at the beginning of treatment. Although nitrate has been reported to be beneficial to PFAS degradation in UV-ARP systems due to the generation of reactive nitrogen species, this effect was not observed to counteract the inhibitory effects of humic acid.

As such, humic acid was identified as an influential interferent in the degradation of PFOS by the RADIANT system. Future work could benefit from exploring humic acid's effect on a wider range of PFAS compounds, and expanding the range of humic acid concentrations to higher concentrations that may be present in highly concentrated/contaminated streams.

5.2 Effect of Groundwater

Potable groundwater was spiked with PFOS and treated by RADIANT using the 10 mM and 50 mM sulfite treatment conditions. Both treatment conditions resulted in >99% degradation and lower final concentrations, compared to DI water, were achieved overall when RADIANT was applied to a groundwater matrix. The positive effect of the groundwater matrix was theorized to be the result of the increased hardness of groundwater. Synthetic hard water

was prepared at two levels of hardness (160 mg/L and 1300 mg/L) and treatment of PFBS using an adapted intermittent sulfite addition protocol was performed. PFBS degradation was observed to improve with increasing water hardness, with >99% PFBS degradation reported at the highest level of water hardness. This effect was theorized to be the result of the increased ionic strength of hard water. However, treatment of PFPrS with the same adapted protocol showed decreased treatment efficacy in groundwater. PFPrS degradation was reduced from 95% in DI water to 92% in groundwater.

Humic acid and nitrate experiments were replicated in groundwater to simulate the effect of complex matrices on the degradation of PFOS in the RADIANT system. Nitrate resulted in increased initial reaction rates for both treatment conditions investigated (10 and 50 mM sulfite). Additionally, the inhibitory effect of humic acid appeared to be mitigated when treatment was performed in groundwater. PFOS degradation in the presence of humic acid was increased from 96% and 86% in DI water, for the 10 and 50 mM sulfite treatments respectively, to 99% in groundwater across both treatment conditions. The initial lag in treatment observed when humic acid was present in DI water was not present when humic acid spiked trials were replicated in groundwater. Overall, >99% PFOS degradation was observed across all experimental conditions when the RADIANT system was applied to groundwater.

Although the groundwater matrix appeared to improve the degradation of PFOS in the presence of humic acid and nitrate, the decreased treatment efficiency of PFPrS in groundwater indicates that this effect may not be transferrable to all PFAS compounds. Groundwater experiments should be replicated for a wider range of PFAS, and ongoing work focuses on the degradation of PFAS mixtures in complex matrices. Future work may also benefit from replicating PFPrS trials in synthetic hard water, to determine if the decreased degradation observed in groundwater is a result of water hardness or other groundwater components present in the potable groundwater.

5.3 Treatment of Short and Ultra-Short Chain PFAS

The degradation of PFPeA, TFA, PFPrS, and PFBS was investigated under two treatment conditions (10 and 50 mM sulfite). The short and ultra-short chain PFCAs studied in this work were shown to degrade readily in the RADIANT system, reaching >99% degradation by the 10-minute mark for both treatment conditions. Short and ultra-short chain PFSAs proved to be more problematic. The 10 mM sulfite treatment condition resulted in 43% PFPrS degradation, and 60% PFPrS degradation was observed under the 50 mM treatment after two hours. PFBS degradation was reported to be 62% and 77% for the 10 and 50 mM treatment conditions respectively. Application of an adapted intermittent sulfite addition treatment protocol resulted in >99% degradation of PFBS, and was further improved when performed in hard water. Degradation of PFPrS with intermittent sulfite addition reached 95% after 8 hours.

Future work may involve further adapting the intermittent sulfite addition protocol to address ultra-short chain PFSAs like PFPrS. This may include increasing treatment times, or experimenting with higher sulfite concentrations due to the improved performance of the

50 mM sulfite treatment for PFPrS. As the primary source of aqueous electrons, future work could also greatly benefit from investigating varying concentrations of iodide, or considering different sulfite-to-iodide ratios.

5.4 Implications for Future Scale-Up

The performance of the RADIANT system was assessed at the cuvette (1 mL) scale and beaker (800 mL) scale. Reaction rates were noted to increase at the beaker scale, and the beaker set-up consistently achieved higher degradation efficiencies. The improved performance observed at the beaker scale was attributed to key differences in the different experimental set-ups. The addition of mixing was thought to be a significant contributor to the success of the beaker system, in addition to the increased temperatures observed at the beaker scale. As such, optimization of parameters such as mixing and temperature would be highly beneficial to future work in scale-up.

Additionally, the effect of initial PFAS concentration on RADIANT system performance was investigated. A 2 hour 10 mM sulfite treatment was performed on PFOS with initial concentrations of 0.4 mg/L, 1 mg/L and 3 mg/L. It was noted that the lowest initial concentration studied, 0.4 mg/L, resulted in an approximately 10-20% decrease in reaction rate in addition to a decrease in fluoride recovery. Although the beaker set-up achieved higher reaction rates and degradation efficiencies at lower concentrations than the cuvette scale, findings at the cuvette scale indicate that there may be a minimum concentration at which treatment efficacy begins to decrease for each set-up. This is an especially pertinent question if RADIANT is to be applied as part of a treatment train, and may guide the development of pre-treatment concentrating steps. Future work would benefit from exploring beaker set-up performance at low concentrations, to determine if this limitation is specific to the cuvette set-up. Further scale-up of the RADIANT system may also explore a variety of reactor types. While the cuvette and beaker set-ups have demonstrated effective PFAS degradation in batch reactors, ongoing work at the research group includes the adaptation of the RADIANT system within a flow-through cell. Changes in system performance within different reactor types, as well as the exploration of RADIANT in semi-batch or continuous stirred tank reactors (CSTR), may be an area for future research.

Appendix A

A.1 Treatment of PFAS in RADIANT System

All chemicals and reagents were purchased from the sources tabulated in Table A6.

Table A6: Chemicals and their sources

Chemical	Source
Na_2SO_3	VWR Life Sciences
KI	Fluka
$NaHCO_3$	Fisher Scientific
NaOH	EMD
Humic Acid (50-60%)	Acros Organics
Nitrate KNO_3	VWR Chemicals
Acetic acid	VWR Chemicals
Total Ionic Strength Adjustment Buffer (TISAB)	Hach
Methanol	Fisher Scientific
PFOS	Synquest
PFBS	
PFPrS	
PFPeA	
TFA	

Reagents tabulated in Table A6 were combined in the quantities listed in Table A7. Initial PFAS concentrations for all experiments listed in Table A7 were approximately 3 mg/L.

Table A7: Reagent concentrations used in all experiments in Chapter 3

PFAS	Sulfite (mM)	Remaining Reagent Concentrations	Matrix	Humic acid (mg/L)	Nitrate (mg/L)	Treatment Time (h)
PFOS	10	10 mM KI	DI water	0	0	2
PFBS	10	10 mM $NaHCO_3$	DI water	0	0	2
PFPrS	10	150 mM NaOH	DI water	0	0	2
PFPeA	10		DI water	0	0	2
TFA	10		DI water	0	0	2
PFOS	50		DI water	0	0	2
PFBS	50		DI water	0	0	2
PFPrS	50		DI water	0	0	2
PFPeA	50		DI water	0	0	2
TFA	50		DI water	0	0	2
PFOS	10		DI water	20	0	2
PFOS	10		DI water	0	10	2
PFOS	10		DI water	20	10	2
PFOS	50		DI water	20	0	2
PFOS	50		DI water	0	10	2
PFOS	50		DI water	20	10	2
PFOS	10		Groundwater	0	0	2
PFOS	10		Groundwater	20	0	2
PFOS	10		Groundwater	0	10	2
PFOS	10		Groundwater	20	10	2
PFOS	50		Groundwater	0	0	2
PFOS	50		Groundwater	20	0	2
PFOS	50		Groundwater	0	10	2
PFOS	50		Groundwater	20	10	2

PFBS	20 (+10 mM / 2h)		DI water	0	0	8
PFBS	20 (+10 mM / 2h)		Hard water (160 mg/L)	0	0	8
PFBS	20 (+10 mM / 2h)		Hard water (1300 mg/L)	0	0	8
PFPrS	20 (+10 mM / 2h)		DI water	0	0	8
PFPrS	20 (+10 mM / 2h)		Groundwater	0	0	8

The deionized (DI) water used in this experiment was from a Milli-Q system, with a resistivity of 16.8 MΩcm. The groundwater (GW) used in this study was sampled from an unimpacted residential site, bypassing any treatment systems. Basic water quality parameters of the groundwater are listed in Table A8. Groundwater was also tested for PFAS using the procedures described in section A.2, and was found to not contain any of the targeted PFAS compounds.

Table A8: Groundwater chemistry

Parameter	Concentration
Conductivity	349 µS/cm
Hardness	199 mg/L
pH	7.0
Chloride	4.3 mg/L
Sulfate	8.0 mg/L
DOC	2.3 mg/L
Dissolved sodium	4.3 mg/L
Nitrate	< 0.20 mg/L

A.2 PFAS Analysis

All samples were analyzed for PFAS using an Agilent 1260 high performance liquid chromatograph coupled to an Agilent 6460 Triple Quadrupole mass spectrometer in negative electrospray ionization mode using a 50mm x 2.1mm x 3.0 µm ACME C18 analytical column paired with a guard column. Mobile phases consisted of 0.3 mM ammonium acetate in deionized water (A) and acetonitrile (B). The elution profile started at 90% A / 10% B, transitioning to 10% A / 90% B, holding for 4 minutes, then equilibrating at starting conditions for 3 minutes, using a flow rate of 0.4 mL/min. PFAS was quantified with an external calibration curve (PFAC-24PAR and PFPrS from Wellington Labs, Pierce TFA from Thermo Scientific) ranging from 0.1 µg/kg MeOH:H_2O to 25 µg/kg MeOH:H_2O. Detection limits were set to the lowest concentration of each calibration curve (0.05 µg/L). The mass spectrometer conditions can be seen in Table A9, with multiple reaction monitoring (MRM) transitions for targeted PFAS listed in Table A10.

Table A9: Mass spectrometer conditions

Parameter	Value
Gas Temp (°C)	325
Gas Flow (L/m)	9
Nebulizer (PSI)	30
Sheath Gas (°C)	250
Sheath Gas Flow (L/m)	12
Capillary (L/m)	12
Nozzle Voltage (V)	0

Table A10: MRM Transitions for Targeted PFAS

Compound Name	Precursor Ion (m/z)	Product Ion (m/z)	Fragmentor (V)	Collision Energy (V)	Cell Accelerator (V)	Ret Time (min)	Ret Window	Polarity
10-2 FTSA	627	606.9	208	34	4	8.5	3	Negative
10-2 FTSA	627	81	208	42	4	8.5	3	Negative
11Cl-PF3OUdS	630.8	450.9	150	36	2	8.958	3	Negative
11Cl-PF3OUdS	630.8	83	150	32	2	8.958	3	Negative

13C4-PFOS	503	99	148	50	2	7.7	3	Negative
13C4-PFOS	503	80	148	54	2	7.7	3	Negative
4-2 FTSA	327	307	150	20	2	5.65	3	Negative
4-2 FTSA	327	81	150	36	2	5.65	3	Negative
5_1_2FTB	432.1	58.1	150	41	4	6	3	Positive
5_3FTB	414.1	58.1	150	41	4	6	3	Positive
6_2FTSAB	571.1	439.9	150	29	4	7.2	2	Positive
6_2FTSAB	571.1	104.1	150	33	4	7.2	2	Positive
6_2FTSAB	571.1	58.1	150	57	4	7.2	2	Positive
6-2 FTSA	427	407	150	30	2	6.79	3	Negative
6-2 FTSA	427	81	150	32	2	6.79	3	Negative
8-2 FTSA	527	507	200	30	4	7.79	3	Negative
8-2 FTSA	527	81	200	46	4	7.79	3	Negative
9Cl-PF3ONS	530.9	350.9	150	28	3	8.106	3	Negative
9Cl-PF3ONS	530.9	83	150	32	3	8.106	3	Negative
DONA	377	251	50	9	5	6.511	3	Negative
DONA	377	85	50	33	5	6.511	3	Negative
HFPO-DA	285	185	50	20	5	5.9	2	Negative
HFPO-DA	285	169	50	4	5	5.9	2	Negative
HFPO-DA	285	119	50	32	5	5.9	2	Negative
M62FTSAB	574.1	439.9	150	29	4	7.2	3	Positive
M62FTSAB	574.1	107.1	150	33	4	7.2	3	Positive
N-EtFOSAA	584	526	100	20	2	8	5	Negative
N-EtFOSAA	584	419	100	20	2	8	5	Negative
NFDHA	295	201	120	4	5	5.6	3	Negative
NFDHA	295	85	120	32	5	5.6	3	Negative
NFDHA	201	135	70	8	5	5.6	3	Negative

NFDHA	201	85	70	15	5	5.6	3	Negative
N-MeFOSAA	570	482.9	150	16	2	8	5	Negative
N-MeFOSAA	570	419	150	20	2	8	5	Negative
PFBA	213	169	72	8	2	1.68	3	Negative
PFBS	298.9	99	154	34	2	5.74	3	Negative
PFBS	298.9	80	154	36	2	5.74	3	Negative
PFDA	513	469	72	12	2	8.05	3	Negative
PFDA	513	269	72	16	2	8.05	3	Negative
PFDoDA	613	569	100	8	2	8	3	Negative
PFDoDA	613	269	100	24	2	8	3	Negative
PFDoS	698.9	99	156	62	2	8	3	Negative
PFDoS	698.9	80	156	67	2	8	3	Negative
PFDS	598.9	99	148	56	2	8	3	Negative
PFDS	598.9	80	148	60	2	8	3	Negative
PFEESA	314.9	135	124	28	5	5.381	3	Negative
PFEESA	314.9	83	124	20	5	5.381	3	Negative
PFEESA	314.9	69	124	60	5	5.381	3	Negative
PFHpA	363	319	72	8	2	6.49	3	Negative
PFHpA	363	169	72	16	2	6.49	3	Negative
PFHpS	448.9	99	148	42	2	7.62	3	Negative
PFHpS	448.9	80	148	50	2	7.62	3	Negative
PFHxA	313	269	72	8	2	5.87	3	Negative
PFHxA	313	119	72	24	2	5.87	3	Negative
PFHxS	398.9	99	156	40	2	6.92	3	Negative
PFHxS	398.9	80	156	56	2	6.92	3	Negative
PFMBA	279	235	80	7	5	5.125	3	Negative
PFMBA	279	85	80	13	5	5.125	3	Negative
PFMPA	229	185	50	7	2	2.415	3	Negative
PFMPA	229	85	50	12	2	2.415	3	Negative
PFNA	463	419	72	8	2	7.53	3	Negative

PFNA	463	219	72	16	2	7.53	3	Negative
PFNS	548.9	99	148	52	2	8.68	3	Negative
PFNS	548.9	80	148	56	2	8.68	3	Negative
PFOA	413	369	72	8	2	7.02	3	Negative
PFOA	413	219	72	16	2	7.02	3	Negative
PFOS	498.9	99	148	50	2	7.97	3	Negative
PFOS	498.9	80	148	54	2	7.97	3	Negative
PFOSA	497.9	169	150	36	3	8	3	Negative
PFOSA	497.9	78	150	36	3	8	3	Negative
PFPeA	263	219	72	4	2	4	4	Negative
PFPeS	348.9	99	144	40	2	6.49	3	Negative
PFPeS	348.9	80	144	44	2	6.49	3	Negative
PFPrS	248.9	79.9	80	32	4	3.437	5	Negative
PFTDA	712.9	669	100	12	2	8.5	3	Negative
PFTDA	712.9	369	100	20	2	8.5	3	Negative
PFTrDA	663	619	100	12	2	8.2	3	Negative
PFTrDA	663	319	100	20	2	8.2	3	Negative
PFUnDA	563	519	100	12	2	8.57	3	Negative
PFUnDA	563	319	100	20	2	8.57	3	Negative
TFA	112.9	68.9	80	12	4	0.49	3	Negative

A.3 Fluoride Analysis

Samples were prepared for fluoride analysis by combining 850 µL of treated solution with 850 µL of total ionic strength adjustment buffer (TISAB) in a 1:1 ratio. The pH of the sample was amended with 10 µL glacial acetic acid to achieve an approximate pH of 5.5. Fluoride analysis was conducted using the ThermoFisher Orion Fluoride Ion Selective Electrode (FISE) probe, with a six-point matrix matched calibration curve (R^2 > 0.99). Figure A11 depicts a typical calibration curve for the deionized water matrix, wherein the concentration of the calibration standards used were 0.05, 0.1, 0.5, 1, 2.5, and 5 mg/L fluoride.

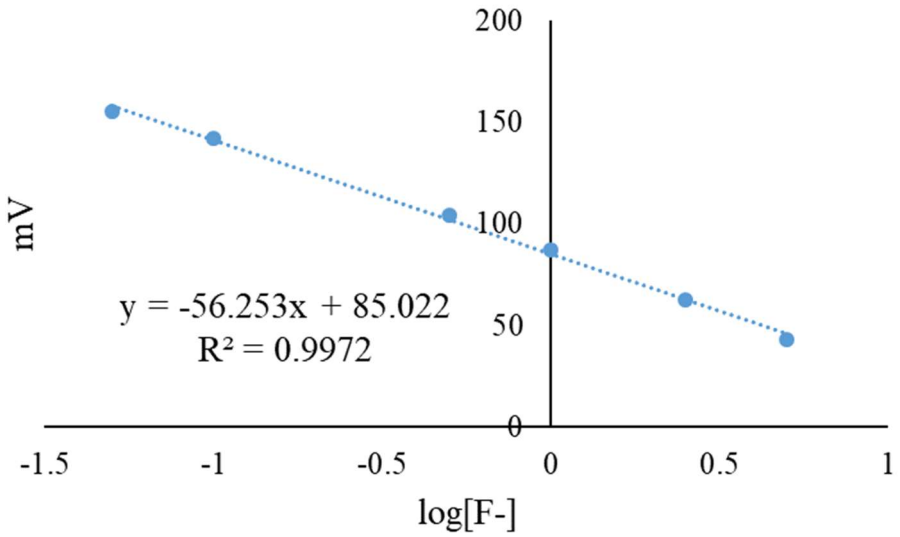

Figure A10. Fluoride calibration curve in deionized (DI) water.

Fluoride recovery can then be determined by comparing the measured free fluoride ion concentration in treated samples to the theoretical maximum fluoride concentration, as determined by the concentration of PFAS measured at T(0).

$$Fluoride\ Recovery = \frac{Fluoride\ Measured\ at\ T(x) - Fluoride\ Measured\ at\ T(0)}{Theoretical\ Maximum\ Fluoride} \times 100\%$$

The concentration of free fluoride measured at T(0) is treated as background, and subtracted from measured fluoride concentrations so that any fluoride measured after T(0) can be attributed to the defluorination of PFAS.

A.4 Calculation of Pseudo-First Order Reaction Rates

The rates of reaction associated with the degradation of PFPrS and PFBS using the intermittent sulfite addition protocol were extracted from the plots depicted in Figure A11.

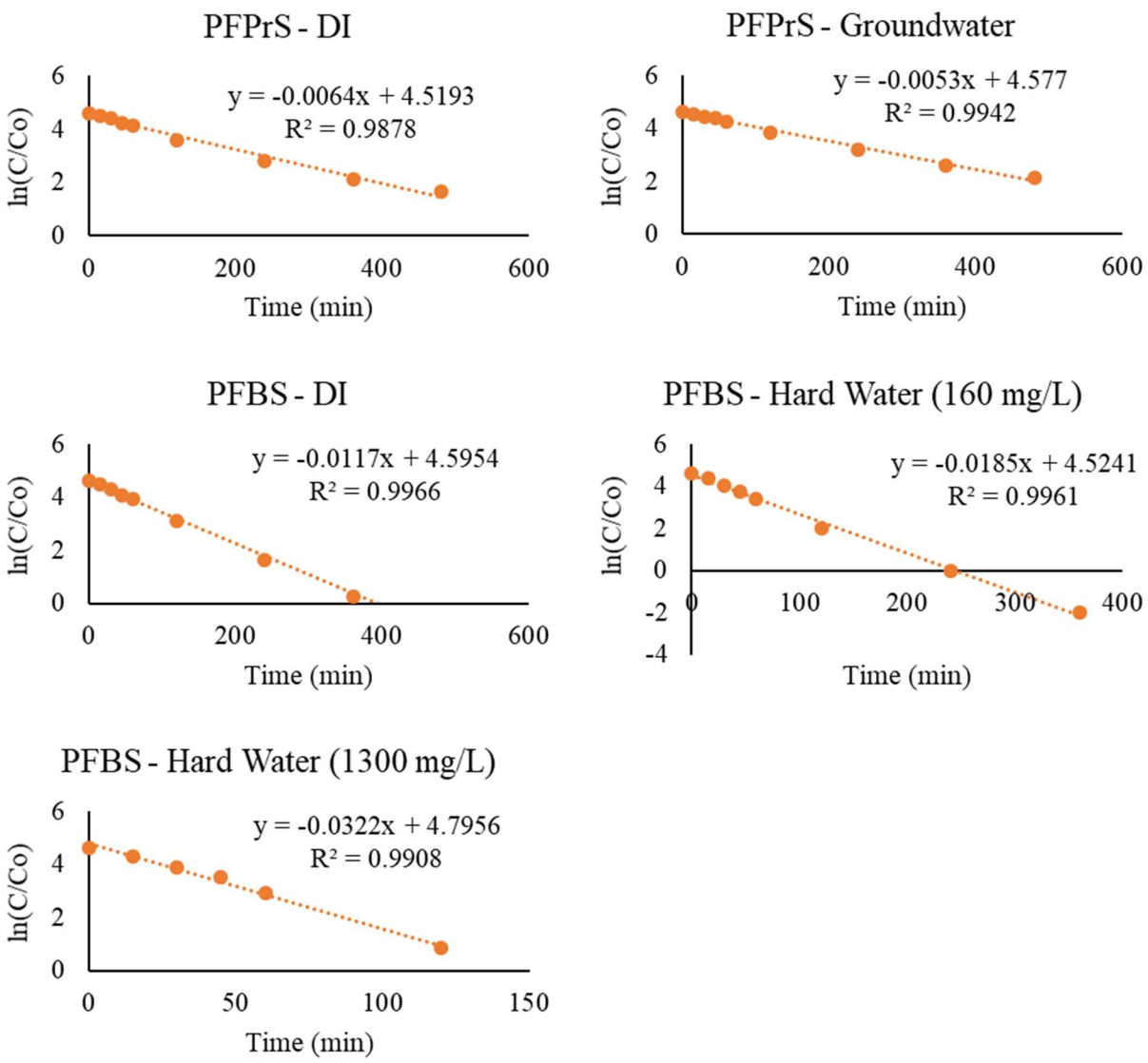

Figure A11. Pseudo-first order rate of reaction for degradation of PFPrS and PFBS with intermittent sulfite addition.

Appendix B

B.1 Rate of Reaction Calculations

The reaction rates reported in Chapter 4 were extracted from the pseudo-first order plots in Figure B12, with the exception of the reaction rate reported for PFOS-1B.

Pseudo-Zero Order	Pseudo-First Order
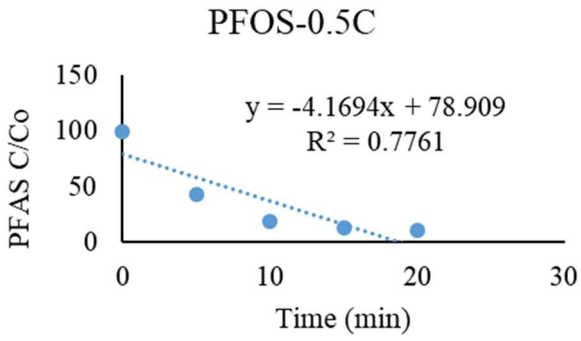	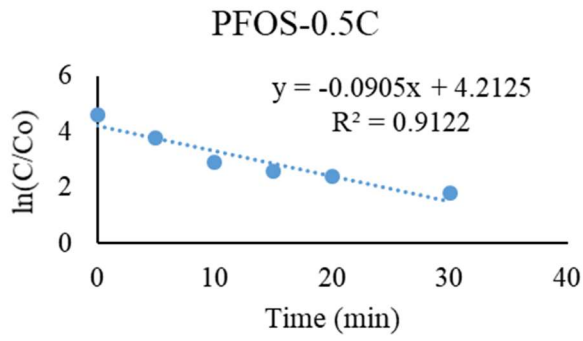
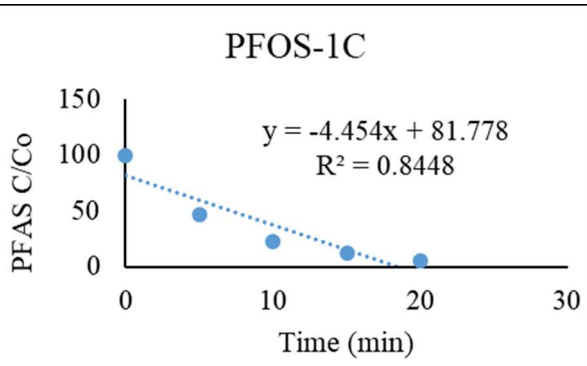	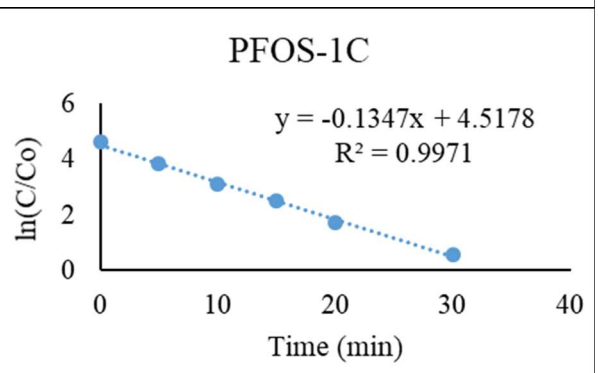
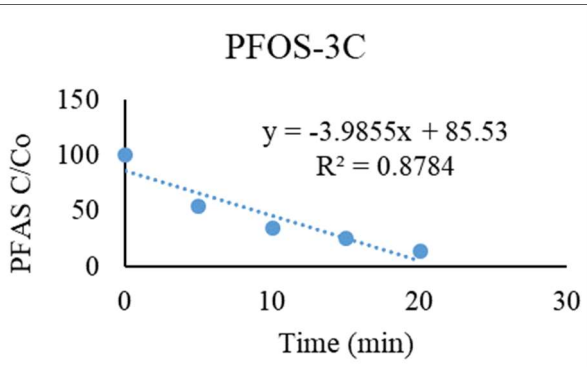	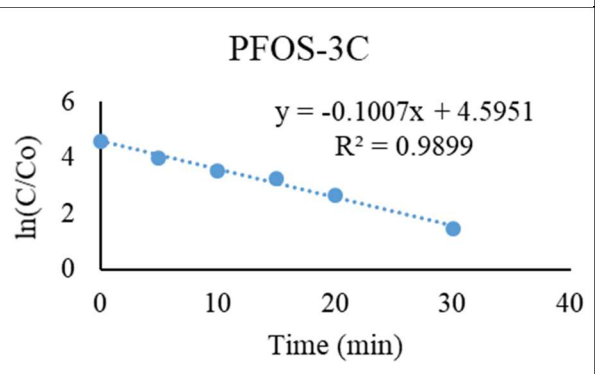

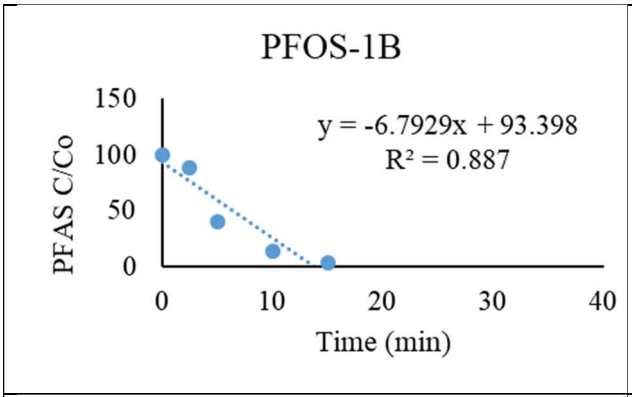
PFOS-1B
y = -6.7929x + 93.398
R² = 0.887
PFAS C/Co
Time (min)

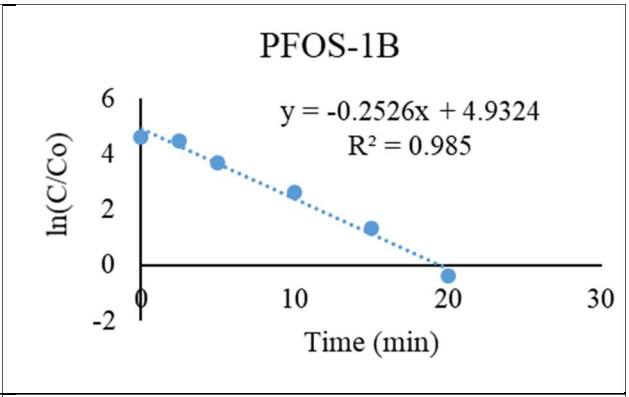
PFOS-1B
y = -0.2526x + 4.9324
R² = 0.985
ln(C/Co)
Time (min)

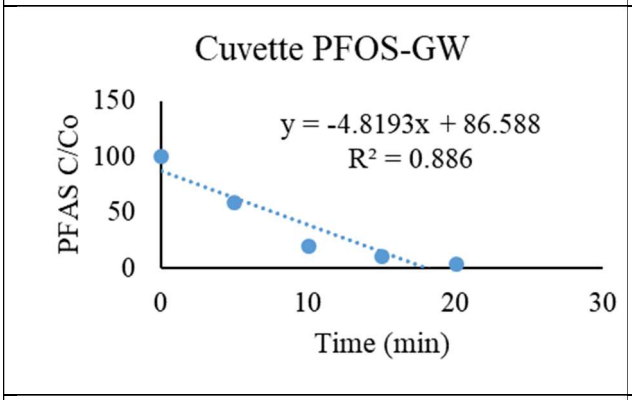
Cuvette PFOS-GW
y = -4.8193x + 86.588
R² = 0.886
PFAS C/Co
Time (min)

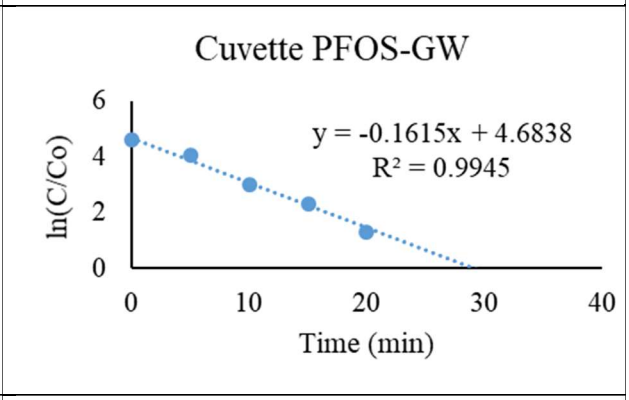
Cuvette PFOS-GW
y = -0.1615x + 4.6838
R² = 0.9945
ln(C/Co)
Time (min)

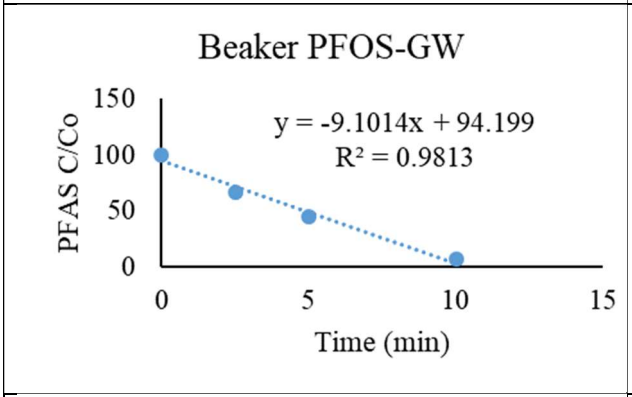
Beaker PFOS-GW
y = -9.1014x + 94.199
R² = 0.9813
PFAS C/Co
Time (min)

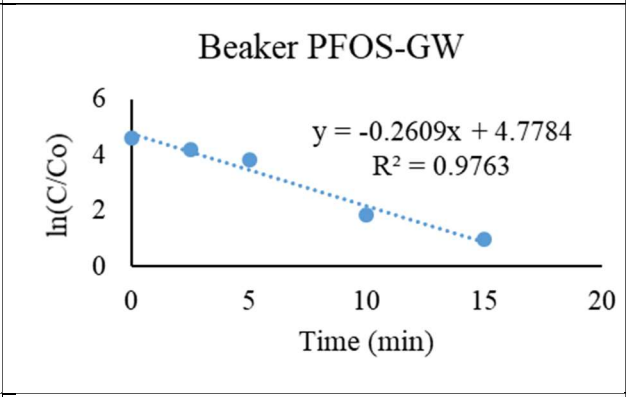
Beaker PFOS-GW
y = -0.2609x + 4.7784
R² = 0.9763
ln(C/Co)
Time (min)

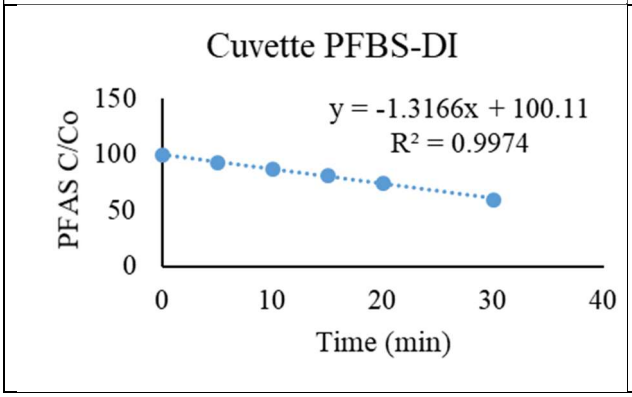
Cuvette PFBS-DI
y = -1.3166x + 100.11
R² = 0.9974
PFAS C/Co
Time (min)

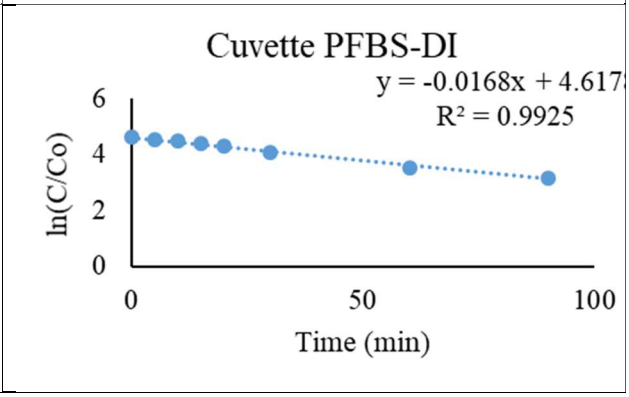
Cuvette PFBS-DI
y = -0.0168x + 4.617
R² = 0.9925
ln(C/Co)
Time (min)

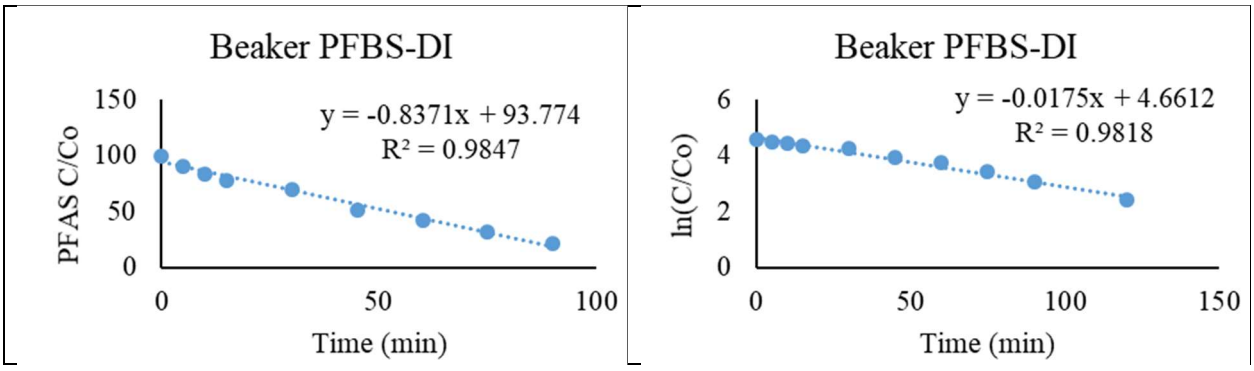

Figure B12. Pseudo-zero and pseudo-first order rate of reaction for all experiments discussed in Chapter 4.

B.2 Temperature of Cuvette and Beaker Set-Ups

Figure B13 shows the temperature of the cuvette and beaker set-ups during a 2-hour negative control (all reagents present except for PFAS).

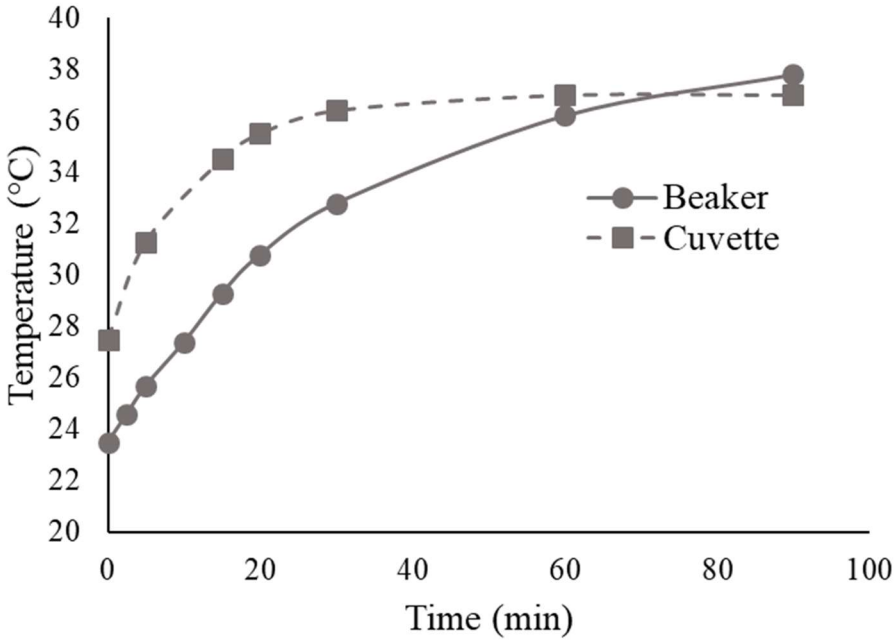

Figure B13. Temperature of cuvette and beaker set-up during negative control. Reagent concentrations were 10 mM sulfite, 10 mM iodide, 10 mM bicarbonate, and 150 mM hydroxide.